ASCE Manuals and Reports on Engineering Practice No. 67

Wind Tunnel Studies of Buildings and Structures

ASCE

AMERICAN SOCIETY OF CIVIL ENGINEERS

ASCE Manuals and Reports on Engineering Practice No. 67

Wind Tunnel Studies of Buildings and Structures

Task Committee on
Wind Tunnel Testing of Buildings and Structures
Aerodynamics Committee
Aerospace Division

Contributors:
J.E. Cermak, A.G. Davenport, F.H. Durgin,
P.A. Irwin, N. Isyumov, J.A. Peterka, S.R. Ramsay,
T.A. Reinhold R.H. Scanlan, T. Stathopoulos,
A.C. Steckley, H. Tieleman, and P.J. Vickery

Editor:
Nicholas Isyumov

Published by

ASCE American Society of Civil Engineers
1801 Alexander Bell Drive
Reston, Virginia 20191-4400

Abstract: This Manual of Practice provides guidelines to assist architects, building code officials, engineers, town planners, and others who become involved with the wind tunnel model testing of buildings and structures and/or the evaluation and use of information from such tests. Many Codes of Practice now permit such studies as alternative approaches for the design against wind action. Part 1 updates the Manual, which was first published in 1987, to reflect new developments in wind engineering and adds a chapter on atmospheric dispersion of exhausts and pollutants around buildings and in built-up areas. Part 2 is a Commentary which contains detailed information on specific methodologies of wind tunnel testing and the use of such data to predict the performance of full-scale buildings and structures. Rigorous model similitude requirements must be followed in order to assure that the findings of wind tunnel model studies are representative. A Glossary and an extensive list of references are included. This Manual has been prepared by a special Task group of the Aerodynamics Committee of the Aerospace Division and includes contributions from some of North America's leading wind engineering experts and laboratories.

Library of Congress Cataloging-in-Publication Data

Wind tunnel studies of buildings and structures / Aerospace Division of the American Society of Civil Engineers.
p. cm.—(ASCE manuals and reports on engineering practice ; no. 67)
Includes bibliographical references and index.
ISBN 0-7844-0319-8
1. Wind pressure. 2. Buildings—Aerodynamics—Testing. 3. Wind tunnels. I. American Society of Civil Engineers. Aerospace Division. II. Series.
IN PROCESS
624.1'75—dc21 98-44103
CIP

Library of Congress Catalog Card No: 98-44103
ISBN 0-7844-0319-8
Manufactured in the United States of America

MANUALS AND REPORTS ON ENGINEERING PRACTICE

(As developed by the ASCE Technical Procedures Committee, July 1930, and revised March 1935, February 1962, and April 1982)

A manual or report in this series consists of an orderly presentation of facts on a particular subject, supplemented by an analysis of limitations and applications of these facts. It contains information useful to the average engineer in his everyday work, rather than the findings that may be useful only occasionally or rarely. It is not in any sense a "standard," however; nor is it so elementary or so conclusive as to provide a "rule of thumb" for non-engineers.

Furthermore, material in this series, in distinction from a paper (which expressed only one person's observations or opinions), is the work of a committee or group selected to assemble and express informaton on a specific topic. As often as practicable the committee is under the direction of one or more of the Technical Divisions and Councils, and the product evolved has been subjected to review by the Executive Committee of the Division or Council. As a step in the process of this review, proposed manuscripts are often brought before the members of the Technical Divisions and Councils for comment, which may serve as the basis for improvement. When published, each work shows the names of the committees by which it was compiled and indicates clearly the several processes through which it has passed in review, in order that its merit may be definitely understood.

In February 1962 (and revised in April 1982) the Board of Direction voted to establish:

> A series entitled "Manuals and Reports on Engineering Practice," to include the Manuals published and authorized to date, future Manuals of Professional Practice, and Reports on Engineering Practice. All such Manual or Report material of the Society would have been refereed in a manner approved by the Board Committee on Publications and would be bound, with applicable discussion, in books similar to past Manuals. Numbering would be consecutive and would be a continuation of present Manual numbers. In some cases of reports of joint committees, bypassing of Journal publications may be authorized.

MANUALS AND REPORTS OF ENGINEERING PRACTICE

No.	Title
13	Filtering Materials for Sewage Treatment Plants
14	Accommodation of Utility Plant Within the Rights-of-Way of Urban Streets and Highways
34	Definitions of Surveying and Associated Terms
35	A List of Translations of Foreign Literature on Hydraulics
37	Design and Construction of Sanitary and Storm Sewers
40	Ground Water Management
41	Plastic Design in Steel: A Guide and Commentary
45	Consulting Engineering: A Guide for the Engagement of Engineering Services
46	Pipeline Route Selection for Rural and Cross-Country Pipelines
47	Selected Abstracts on Structural Applications of Plastics
49	Urban Planning Guide
50	Planning and Design Guidelines for Small Craft Harbors
51	Survey of Current Structural Research
52	Guide for the Design of Steel Transmission Towers
53	Criteria for Maintenance of Multilane Highways
54	Sedimentation Engineering
55	Guide to Employment Conditions for Civil Engineers
57	Management, Operation and Maintenance of Irrigation and Drainage Systems
59	Computer Pricing Practices
60	Gravity Sanitary Sewer Design and Construction
62	Existing Sewer Evaluation and Rehabilitation
63	Structural Plastics Design Manual
64	Manual on Engineering Surveying
65	Construction Cost Control
66	Structural Plastics Selection Manual
67	Wind Tunnel Studies of Buildings and Structures
68	Aeration: A Wastewater Treatment Process
69	Sulfide in Wastewater Collection and Treatment Systems
70	Evapotranspiration and Irrigation Water Requirements
71	Agricultural Salinity Assessment and Management
72	Design of Steel Transmission Pole Structures
73	Quality in the Constructed Project: A Guide for Owners, Designers, and Constructors
74	Guidelines for Electrical Transmission Line Structural Loading
75	Right-of-Way Surveying
76	Design of Municipal Wastewater Treatment Plants
77	Design and Construction of Urban Stormwater Management Systems
78	Structural Fire Protection
79	Steel Penstocks
80	Ship Channel Design
81	Guidelines for Cloud Seeding to Augment Precipitation
82	Odor Control in Wastewater Treatment Plants
83	Environmental Site Investigation
84	Mechanical Connections in Wood Structures
85	Quality of Ground Water
86	Operation and Maintenance of Ground Water Facilities
87	Urban Runoff Quality Manual
88	Management of Water Treatment Plant Residuals
89	Pipeline Crossings
90	Guide to Structural Optimization
91	Design of Guyed Electrical Transmission Structures
92	Manhole Inspection and Rehabilitation
93	Crane Safety on Construction Sites
94	Inland Navigation: Locks, Dams, and Channels
95	Urban Subsurface Drainage
96	Guide to Improved Earthquake Performance of Electric Power Systems
97	Hydraulic Modeling: Concepts and Practice

FOREWORD

The first edition of the *Manual of Practice for Wind Tunnel Studies of Buildings and Structures* was published in 1987. The wind engineering field continues to evolve, and this update of that manual emphasizes the circumstances under which tests might be needed, the types of tests that might be performed and the physical principles that need to be followed to ensure meaningful results.

This edition of the Manual has two parts. Part 1 is an updated version of *ASCE Manual 67* with an added section on Atmospheric Dispersion Around Buildings. Part 2 is a Commentary, which provides supporting information on the methodologies needed and examples of typical tests. It also includes a bibliography.

This Manual has been prepared by a Task Committee formed under the auspices of the Aerodynamics Committee of the Aerospace Division of the ASCE. Members of this Task Committee, who have contributed to the preparation of this Manual are:

Frank H. Durgin, Chairman
Wright Brothers Wind Tunnel
M.I.T., Building 17-110
Cambridge, Massachusetts, U.S.A. 02139
Tel: (617) 253-2270
FAX: (617) 258-7566

Nicholas Isyumov, Vice-Chair and Editor
Boundary Layer Wind Tunnel Laboratory
The University of Western Ontario
London, Ontario N6A 5B9, Canada
Tel: (519) 661-3338
FAX: (519) 661-3339

Jack E. Cermak
Fluid Dynamics and Diffusion Laboratory
Colorado State University
Fort Collins, Colorado, U.S.A. 805243
Tel: (970) 221-3371
FAX: (970) 221-3124

Alan G. Davenport
Boundary Layer Wind Tunnel Laboratory
The University of Western Ontario
London, Ontario N6A 5B9, Canada
Tel: (519) 661-3338
FAX: (519) 661-3339

Peter A. Irwin
Rowan Williams Davies & Irwin Inc.
650 Woodlawn Road West
Guelph, Ontario N1K 1B8, Canada
Tel: (519) 823-1311
FAX: (519) 823-1316

Jon A. Peterka
Cermak Peterka Petersen Inc.
1415 Blue Spruce Drive
Fort Collins, Colorado, U.S.A. 80524
Tel: (970) 221-3371
FAX: (970) 221-3124

Stephen R. Ramsay
U.S. Filter
1370-885 W. Georgia Street
Vancouver, British Columbia V6C 3E8, Canada
Tel: (604) 669-4422
FAX: (604) 669-5951

Timothy A. Reinhold
Department of Civil Engineering
Clemson University
110 Lowry Hall
Clemson, South Carolina, U.S.A. 29631
Tel: (864) 656-3326
FAX: (864) 656-2670

Robert H. Scanlan
Dept. of Civil Engineering
G.W.C. Whiting School of Engineering
202 Latrobe Hall
The Johns Hopkins University
Homewood Campus
Baltimore, Maryland, U.S.A. 21218-2686
Tel: (410) 516-7138
FAX: (410) 516-7473

Theodore Stathopoulos
Centre for Building Studies
Concordia University
1455 De Maisonneuve Blvd. West
Montreal, Quebec H3G 1M8, Canada
Tel: (514) 848-3186
FAX: (514) 848-7965

Andrew C. Steckley
QuantumLynx
202 Michael Grove Avenue
Bozeman, Montana, U.S.A. 59718
Tel: (406) 582-9745
FAX: (406) 582-9745

Henry Tieleman
Department of Engineering Science and Mechanics
Virginia Polytechnical Institute and State University
Blacksburg, Virginia, U.S.A. 24061
Tel: (540) 231-6651
FAX: (540) 231-4574

Peter J. Vickery
Applied Research Associates
811 Spring Forest Road, Suite 100
Raleigh, North Carolina, U.S.A. 27609
Tel: (919) 876-0018
FAX: (919) 878-3672

ACKNOWLEDGMENTS

The Task Committee for the Manual has received many valuable suggestions and comments over the past several years. Many came from other members of the Aerodynamics Committee of the Aerospace Division of the ASCE. Others came as a result of presentations of the Manual at ASCE Conferences, and its circulation to members of the wind engineering and wind tunnel testing communities and to interested engineers and architects. The contributions received are too numerous to permit specific mention. The Committee would therefore like to take this opportunity to extend its thanks and appreciation to all contributors.

Also acknowledged are the many valuable suggestions and comments by members of the ASCE Blue Ribbon Review Panel who reviewed this document and generously shared their experience and viewpoints with the Committee. These very much appreciated reviews and scrutiny have greatly improved this Manual.

Finally, the Committee and, in particular, the Editor of the Manual would like to acknowledge the contributions of Mrs. Tanya Spruyt of the Boundary Layer Wind Tunnel Laboratory of The University of Western Ontario, who typed the contributions from various Committee members and who helped to assemble the document. This involved several iterations over a number of years and included numerous cycles of corrections and improvements. Her patience and special effort are very much appreciated.

This page intentionally left blank

CONTENTS

COMMENTARY ON WIND TUNNEL STUDIES OF BUILDINGS AND STRUCTURES

This page intentionally left blank

Part 1

WIND TUNNEL STUDIES OF BUILDINGS AND STRUCTURES

This page intentionally left blank

Chapter 1
INTRODUCTION

1.1 OBJECTIVES

This Manual of practice provides guidelines intended to assist architects and engineers who may become involved with the wind tunnel model testing of buildings and structures. Included are procedures required to provide representative information on wind effects experienced during particular wind conditions, and methods for using such information to provide statistical predictions of full-scale behavior. ASCE Standard 7 (Formerly ANSI A58.1) and many other codes of practice now permit or require wind tunnel model studies for the design of buildings and structures against the action of wind. In some situations, such studies may be desirable in order to improve the reliability of performance, economy of design, or both.

The first *ASCE Manual of Practice for Wind Tunnel Model Studies of Buildings and Structures* was printed in 1987. Part 1 of this updated Manual reflects new developments in the wind engineering field. The Commentary in Part 2 contains detailed information on specific methodology and specific aspects of wind tunnel testing. Added to the Manual is a section dealing with wind tunnel studies of the dispersion of pollutants around buildings and in urban environments. If in doubt, the reader should seek the assistance of an established wind tunnel testing laboratory or a recognized wind engineering specialist. Finally, approval of the use of wind tunnel model data for design may rest with local code authorities. Appropriate inquiries about any special requirements or limitations would therefore be prudent.

The testing of prototype buildings and components and mock-ups of curtain-wall systems are outside the scope of this Manual. Model studies of the effects of wind on the deposition and drifting of snow on roofs and around buildings and structures also are not covered.

1.2 AREAS OF APPLICATION

Although wind tunnel model testing has gained wide acceptance, it is important to stress that the action of wind in many cases is adequately dealt with in existing building codes. It is therefore important to identify situations in which wind tunnel studies are desirable or necessary. The primary reasons for carrying out such studies are to improve the reliability of structural performance and to achieve cost effectiveness—both of the final structure and during the period of construction. Wind tunnel derived wind loads can, in many circumstances, fall below code prescribed values. Wind tunnel model studies, therefore, frequently lead to cost savings.

Other candidates for wind tunnel tests are buildings and structures that have an unusual sensitivity to the action of wind or that fall outside existing experience. This is particularly true when a significant part of the wind-induced response is dynamic. Examples are tall, slender, and flexible buildings, observation towers, masts and chimneys, intermediate and long-span bridges, pedestrian bridges, transmission line systems, and various special structures, such as large-span flexible roofs, cooling towers, large cranes, etc. Buildings and structures of unusual aerodynamic shape, which may experience large wind-induced overall forces or local pressures, also warrant special attention. Other areas of potential concern include the presence of unusual terrain and surroundings, and close proximity to major buildings and structures or prominent topographic features. In all situations, buildings and structures located in areas of high incidence of significant wind speeds are more likely to be in need of wind tunnel testing than those constructed in areas where winds are generally benign.

Wind tunnel tests are not always prompted by concerns for structural integrity. Such tests can also provide information on serviceability related questions, such as wind-induced drift or horizontal accelerations which, if excessive, may adversely affect occupant comfort. The effects of wind on pedestrians and the environment of built-up urban areas, including the dispersion of pollutants and the resulting air quality, are other questions that wind tunnel model studies can address. Such tests are particularly valuable if they are carried out at an early stage when design adjustments can still be made.

1.3 COMMON TECHNIQUES

Procedures used in wind tunnel model studies vary widely, depending on particular objectives and available resources. The more commonly used tests are listed in Table 1-1.

The modeling requirements for the wind tunnel tests, listed in Table 1-1, and for other tests are presented in Chapters 2 to 7. In many situations, it

Table 1-1. Common Wind Tunnel Model Tests and Their Uses.

Type of Test	Typical Information Provided
Local Pressures	
Tests of local pressures using scaled static models instrumented with pressure taps.	• Mean and fluctuating local exterior pressures on curtainwall, cladding, and roof components. • Estimates of wind-induced interior pressures, including fluctuations in the presence of significant openings. • Estimates of differential pressures on components of exterior envelope.
Area and Overall Wind Loads	
Tests of wind loads on specific tributary areas, using pressure models and spatial or time averaging of simultaneously acting local pressures.	• Mean and fluctuating wind loads on particular tributary areas due to external or internal pressures, or both. • Measures of the dynamic structural loads and actions as a result of spatially averaged wind loads on particular tributary areas. • Overall loads on buildings, long span bridges, and other structures, including the generalized wind forces associated with particular modes of vibration. • Simultaneously measured pressures on exterior surfaces of a building can be used to determine the generalized wind forces for various modes of vibration. Estimates of the corresponding wind-induced response, including building deflections and accelerations, are made analytically.
High Frequency Force Balance	
Direct measurements of overall wind loads on scaled static models, including high frequency base balance tests for tall buildings.	• Aerodynamic coefficients, which can be used with analytical methods to estimate the peak response assuming linear or nonlinear structural action. • Wind force spectra from which the resonant dynamic response can be obtained. • High-frequency base balance tests are commonly used to evaluate loads associated with the fundamental sway and torsional modes of tall buildings. • Estimates of the wind-induced responses, including building drift and accelerations, are made analytically after the forces are determined.
Section Model Tests	
Section model tests using dynamically mounted models. Usually for bridges, but also for other structures.	• Overall mean and dynamic wind-induced forces and responses. • Aerodynamic derivatives as required in analytical models.

Continued on next page

Table 1-1. Common Wind Tunnel Model Tests and Their Uses—*Continued.*

Type of Test	Typical Information Provided
Aeroelastic Studies	
Aeroelastic tests using dynamically scaled models of buildings, bridges, and structures.	• Aeroelastic model tests provide information on the wind-induced responses of buildings and structures due to all wind-induced forces, including those which are experienced by objects that move relative to the wind flow. These motion-dependent or "aeroelastic" forces are not experienced by pressure, overall load, and other stationary models, which do not move relative to the flow. • Direct measures of the overall mean and dynamic loads and responses of buildings and structures, including displacements, rotations, and accelerations. • Influence of pressurization on behavior of air-supported structures. • Effectiveness of active and passive systems to control dynamic motion. • Interaction of wind loads and direct indications of maximum combined force effects.
Pedestrian Winds	
Evaluations of pedestrian level winds using scaled static models of buildings or structures.	• Character of flow around buildings and structures. • Measures of local wind speeds and directions required for environmental assessments. • Selection, evaluation, and fine tuning of remedial measures. • Evaluation of helipad operations. •
Air Quality	
Tests to evaluate the dispersion of pollutants and determine the resulting air quality around buildings and in urban areas.	• Plume trajectories to indicate possible impingement and/or reingestion into fresh air intakes. • Concentrations of exhausted pollutants, expressed as a ratio of their source concentration. • Evaluation of potential for air quality exceedances. • Wind-induced ventilation rates in open areas.
Terrain and Topographic Studies	
Small-scale topographic model tests using flow visualization, hot-wire anemometry, or both.	• Character of flow over complex terrain, including the assessment of terrain roughness. • Correlations of flows at different locations and heights as required in the calibration of anemometer stations. • Assessments of the wind energy potential of particular sites.

becomes necessary to simplify or even to disregard some specific requirements of strict similarity theory. In fact, some problems (i.e., pedestrian level wind conditions and their amelioration) can sometimes be effectively examined with relatively approximate modeling methods.

It is important to be aware of the limitations of all tests made in wind or water tunnels or water flumes, particularly in situations in which partial or approximate models are used. Important measures of the practical value of all model test data are their relation to full-scale experience.

This page intentionally left blank

Chapter 2
MODELING THE WIND

2.1 WIND AND ITS ORIGIN

Temperature differences in the atmosphere are the primary cause for the existence of regions of low and high pressure. The forces caused by the horizontal pressure and temperature gradients, together with centrifugal forces and the effects of the earth's rotation (Coriolis force), govern atmospheric motions in the free atmosphere at altitudes above approximately 1000 to 2000 m. At lower elevations, in the atmospheric boundary layer, the influences of frictional and drag forces at the surface become increasingly important, while both the Coriolis and the centrifugal forces decrease in importance.

Furthermore, steep vertical temperature and moisture gradients near the surface create buoyancy forces that can strongly influence the development of circulations with vertical motions, such as hurricanes (also called typhoons and cyclones), and on a smaller scale, tornadoes, downbursts, and thunderstorms with powerful downdrafts and squalls. Vertical temperature gradients can also have an appreciable effect on the small-scale motions (turbulence) that are strengthened for unstable thermal conditions and are weakened for stable thermal conditions. Other factors that influence both small and intermediate (meso) scale wind characteristics near the surface are geographic features, human-made obstacles, and terrain roughness.

2.2 WIND TUNNEL SIMULATION OF THE ATMOSPHERIC BOUNDARY LAYER (ABL)

Quantitative wind-effect data for the design of buildings and structures, as well as for control of local air-pollutant transport, can be obtained through wind-tunnel studies using small-scale models. The wind tunnel must have

capabilities for creating flows that simulate the basic characteristics of natural wind at a site in order to obtain wind-effect data representative of full-scale conditions. Natural wind at the site is composed of characteristics associated with flow approaching the site (approach flow) and characteristics resulting from flow over nearby buildings, structures, and significant topographic features (near-field flow modifications). For most wind-engineering purposes, the approach flow is modeled to be representative of locally stationary ABL conditions.

For purposes of designing buildings and structures, strong wind, which is not significantly influenced by thermal stratification, is of primary concern. Therefore, the approach flow is usually an isothermal boundary layer that models a thermally neutral ABL. Wind tunnels designed to develop this type of flow are classified as boundary-layer wind tunnels (BLWT). Typically, such tunnels are 2 to 5 m wide, have long working sections (15 to 30 m), and use air at atmospheric pressure. Maximum operating speeds are usually in the range of 10 to 50 m/s. Alternatively, short-test-section wind tunnels are used with various devices (spires, vortex generators, and fences) placed at the entrance to the test section to generate acceptable mean and turbulent flow conditions. Devices of this type are also used to increase boundary-layer depth in long-test-section tunnels and to create partial-height, boundary-layer simulations for study of wind effects on low-rise structures. Acceptable ABL simulations in short test sections and for low-rise structures are more difficult to achieve.

A distinct gap exists in the power spectrum of wind-speed fluctuations at periods of about one hour. This conveniently separates atmospheric motion into micrometeorological variations or turbulence and a quasisteady mean wind that changes relatively slowly as a result of diurnal, synoptic, and seasonal variations. In wind-tunnel simulations, it is common to approximate natural wind during particular weather conditions with a turbulent boundary-layer flow with locally stationary mean and turbulent speed properties. Changes in the mean wind speed are achieved when needed by adjusting the wind-tunnel flow speed. Changes in wind direction are made by rotating the turntable on which the model is mounted.

2.3 APPROACH WIND

A BLWT should be capable of developing flows representative of natural wind over different types of full-scale terrain. The *minimum requirements* are:

1. vertical distributions of the mean wind speed and the intensity of the longitudinal turbulence component shall be modeled;
2. important properties of atmospheric turbulence, in particular the relevant length scales of the longitudinal turbulence component, shall be

modeled to approximately the same scale as that used to model buildings or structures; and

3. the longitudinal pressure gradient in the wind-tunnel test section should be sufficiently small as not to significantly affect the results.

These requirements can be satisfied for a range of model scales by reproducing most of the atmospheric boundary layer. For low-rise structures, it is usually sufficient to simulate the lower part of the ABL only. For these applications reproduction of the flow properties in the atmospheric surface layer (depth $z_s \cong 100$ m or lowest 10% of the ABL) is recommended. Typically, over flat terrain with uniform roughness, the turbulent stresses in this layer should vary no more than 10 to 25% of values at $z = 0$. For many wind-tunnel model tests, a more complete simulation of all aspects of the turbulent ABL flow is necessary. For example, simulation of the vertical component of turbulence is important in some wind-tunnel model studies of long-span bridges.

For air-pollution studies, in which turbulent diffusion is important relative to advective transport, thermal stratification of the ABL (particularly the atmospheric surface layer) can have significant consequences. An additional modeling requirement for thermally stratified ABL flows is that the bulk Richardson number, which represents the ratio of buoyancy forces to inertial forces, shall be equal for the full- and model-scale approach flows. An alternative modeling criterion is that z_g/L_{mo}, where L_{mo} is the Monin–Obukhov stability length, be equal for model and prototype.

2.4 TOPOGRAPHIC MODELS

Information on the characteristics of the full-scale wind applicable to the specific site may not be available in situations of complex topography or terrain. In such situations small-scale topographic models, constructed at scales in the range of 1:1000 to 1:5000, can be effective for estimating the full-scale mean flow field. Such data can form the basis for the subsequent modeling of the wind at a larger scale, as required for studying wind effects on buildings and structures. If a meteorological station exists within the bounds of the topographical model, wind data measured at this location on the model can be used to correlate the station wind data with wind characteristics at the site of the building.

2.5 NEAR FIELD

Nearby significant buildings, structures, and topographic features collectively modify the approach flow and should be included as part of the

model for simulations of wind at a particular location. In urban settings, the modeling of this near field typically requires the scaled reproduction of all major buildings and structures within about 300 to 800 m from the site and usually covers the entire turntable of the wind tunnel. The degree of model detail, used in these near-field or proximity models, can be reduced with distance from the site, and block outline representations of buildings are usually acceptable.

2.6 INFLUENCE OF SPECIFIC STRUCTURES

Inclusion of specific nearby structures in the proximity model ensures that their effects on local wind characteristics are properly accounted for in the wind-tunnel simulation. In some situations, it becomes important also to include possible aerodynamic influences of major buildings or structures beyond the proximity model on the turntable with a diameter that normally is equal to the wind-tunnel test-section width. Such buildings or structures should be placed upwind of the proximity model for appropriate wind directions.

The possible adverse influence of future adjacent buildings or structures is often considered in wind-tunnel tests. In the absence of precise information, approximate massing models are used to examine the sensitivity of various wind effects to possible future construction. Adverse effects are more likely in areas of new development, as there is a greater possibility for aerodynamic interference between isolated buildings or groups of buildings surrounded by lower structures or open terrain. The influence of specific new construction in built-up cities, with many other buildings of comparable size, is usually less pronounced.

In some situations, the scope of a wind-tunnel study is expanded to examine the influence of the building under study on wind effects for existing nearby buildings and structures. This extended examination usually includes measurements on the existing buildings and structures with and without the building under study in place.

2.7 SELECTION OF GEOMETRIC SCALE

2.7.1 Consistent Modeling of All Lengths

The geometric scale of the model of a building or structure should be chosen to maintain, as closely as possible, equality of model and prototype ratios of overall building dimensions to the important meteorological lengths of the modeled approach wind. Depending on the structure studied, the length-scale selection is based on an attempt to satisfy the following equalities:

$$\left(\frac{L_b}{z_0}\right)_m = \left(\frac{L_b}{z_0}\right)_p, \text{ the Jensen number equality,}$$

$$\left(\frac{L_b}{z_g}\right)_m = \left(\frac{L_b}{z_g}\right)_p, \text{ and}$$

$$\left(\frac{L_b}{L_t}\right)_m = \left(\frac{L_b}{L_t}\right)_p$$

in which L_b, z_0, z_g, and L_t are respectively, a characteristic dimension of the building or structure, the aerodynamic roughness length of the terrain, the gradient wind height of the boundary-layer, and the scale of turbulence. The subscripts m and p refer to model and prototype, respectively. Values of z_0 for various surface roughnesses are given in Tables C2.1 and C2.2.

For most modeling applications, the ratio L_b/L_t is the parameter that is matched to full scale and L_t is selected as the integral scale of the longitudinal component of turbulence ${}^xL_u$. However, in some instances it is advantageous, in the interests of maintaining a larger model scale for better geometric accuracy and avoidance of low Reynolds number effects, to relax the requirement to match L_b/L_t and, instead, to ensure only that the kinetic energy of the small-scale turbulence is correctly represented as a fraction of the kinetic energy of the mean flow. In these circumstances, the important scales of turbulence are those of dimensions similar to the widths of the shear layers at the edges of regions of flow separation and reattachment. Such a simulation may be termed a partial simulation of wind turbulence.

For low-rise buildings, a good simulation of all mean and turbulence characteristics can be achieved over a limited height above ground by omiting the gradient wind height and matching only the Jensen number L_b/z_0 and L_b/L_t. The height of this matched region should be several times the height of the tallest building of interest. For some studies, such as sectional model tests of bridges, where the ground surface is not specifically included in the model set-up, the roughness length is no longer a useful parameter for modeling purposes. In these instances, correct modeling of the small-scale turbulence can be achieved by matching the model nondimensional power spectrum nS_u/V^2 to the corresponding full-scale spectrum for values of nd/V of order unity and greater. Here n = frequency, S_u = power spectral density of the longitudinal component of turbulence, V = mean wind velocity at bridge deck height, and d = depth of bridge deck structure.

When partial simulations of wind turbulence are employed, the wind-tunnel results need to be combined with additional interpretation or analy-

sis to arrive at useful predictions of full-scale behavior, because the effects of the large-scale turbulence are missing from the tests.

Typical geometric scales used in studies of wind effects on large buildings and structures range between approximately 1:300 to 1:600. Larger scales, typically approximately 1:100 and larger, are used in studies of smaller buildings and structures in which the emphasis of the flow simulation is on the atmospheric surface layer or on the small-scale turbulence. For small buildings, the geometric scale is commonly chosen to maintain equality of the Jensen number L_b/z_0, the ratio of the characteristic dimension of the building to the depth of the atmospheric surface layer, denoted as L_b/z_s or the normalized power spectra, as described in the foregoing paragraph for sectional model testing of bridges.

2.7.2 Blockage Considerations

In selecting the model scale it is important to minimize the influence of wind-tunnel walls and excessive blockage of the test section. Models cause a blockage of the wind tunnel, as their size becomes significant relative to the cross-section of the wind tunnel. This blockage speeds up and distorts the flow over and around the model. This speed-up can be determined with wind-speed measurements made in the plane of the model. Correcting for the effects of the distortion of the flow is more difficult. For a blockage ratio of 5% and less (ratio of the frontal area of the model building or structure, including an allowance for the proximity model, relative to the cross-sectional area at the wind tunnel test section), distortion effects are negligible and a correction for the speed-up of the flow at the model is sufficient. For blockage ratios between 5 and 10%, distortion effects become significant and must be considered. For blockage ratios greater than 10%, the validity of the data must be ascertained through additional tests at a smaller scale.

2.8 SELECTION OF VELOCITY SCALE

The selection of wind speed in the wind tunnel to represent full-scale conditions at a particular full-scale velocity varies with the problem at hand. In studies of the flow field, including the pedestrian-level wind environment and aerodynamic forces on particular local areas or entire buildings and structures, the choice of the velocity scale is relatively arbitrary as long as the model and full-scale flows remain aerodynamically similar (i.e., independent of Reynolds number). In such situations, the velocity scale is largely determined by considerations of convenience and limitations of the instrumentation. For other types of tests, such as aeroelastic tests or dispersion tests in thermally stratified approach flows, appropriate similarity criteria to establish velocity scales are given in Chapters 6 and 7, respectively.

2.9 REYNOLDS NUMBER SCALING

Strict scaling of the mean wind and the turbulence Reynolds number for the approach flow is generally not possible for wind-tunnel model studies of buildings and structures. Usually this is not a serious limitation. Reynolds number independence of the approach flow over aerodynamically rough upwind fetches is assured if $u_* z_0/\nu > 2.5$. The friction velocity u_* is equal to $(\tau_0/\rho)^{1/2}$ where τ_0 is the surface shear stress, ρ is the mass density of air, and z_0 is the aerodynamic roughness length.

Flow corrections for differences between model and full-scale building Reynolds numbers $Re_b = V_h L_b/\nu$ (V_h = reference wind speed at building location) are sometimes required for rounded shapes. To improve local flow similarity, curved surfaces of models are sometimes roughened. In studies of aerodynamic forces on sharp-edged bodies, it is important to attain a minimum value of Re_b for the model in order to minimize local viscous effects. Nevertheless, the frequency range of turbulence spectra is Re dependent, and attention to the practical importance of model spectra distortion is appropriate. Distortion of the flow and the resulting variation in pressure distributions are considered negligible for Reynolds numbers Re_b in excess of 10^4. The consequences of insufficiently high values of Re_b on model pressures and other wind effects can be evaluated through comparisons with full-scale data, selected tests using a larger scale model, or tests conducted over a range of wind speeds, V_h.

This page intentionally left blank

Chapter 3
PEDESTRIAN LEVEL WINDS

Model studies can provide reliable estimates of pedestrian level wind conditions in outdoor areas of buildings and building complexes. Such estimates serve as inputs to the assessment of the suitability of such areas for assorted pedestrian uses, based on considerations of both comfort and safety. Most current suitability criteria are based strictly on the mechanical effects of the wind. Information is emerging on how the effects of wind, temperature, solar radiation, precipitation, humidity, and so on influence human comfort.

Such studies require geometrically scaled models that include aerodynamically significant details in all areas of interest. Models and flow conditions used should meet the requirements set forth in Chapter 2. The effects of the near field are of major importance. For instance, arcades, vertical or horizontal facade setbacks or outcrops, canopies, trees, and so on can be particularly important near a measurement station.

For initial estimates, it is possible to accept more approximate simulations of the approach flow than those suggested in Chapter 2.

The measurement technique used should provide good estimates of dynamic wind speeds at pedestrian level. Depending on the experimental procedure, such tests may also estimate local wind directions. Alternatively, flow directions can be obtained through flow visualization. Indications of local flow direction are helpful for indentifying local flow phenomena and in the selection of ameliorating measures.

Evaluations of the wind environment should be carried out for a full range of wind directions at 10 or 22.5 degree intervals, unless there are clear indications of symmetry or the local wind climate is highly directional. Such tests are normally performed at a single wind speed, and the results are presented as wind speed coefficients, or ratios of wind speed at pedestrian level to a reference wind speed. These ratios are then used with an appropriate

statistical description of the local wind climate to obtain estimates of the frequency of occurrence of winds of a specified level at each station of interest.

Typical experimental methods include:

1. various flow visualization techniques, such as smoke, tufts, or oil streaks, to provide qualitative information;
2. the scouring of sand or other particles to provide semiquantitative data; and
3. various devices to provide quantitative information, including those that directly measure wind speed (hot-wire or hot-film anemometers) and others that measure pressure (special surface probes) and force (elastically mounted devices that measure forces or indicate deformation), from which the wind speed and possibly direction can be estimated.

Measurements of the wind field are sometimes used to infer the drifting of snow and its accumulation both on the ground and on roofs.

For quantitative studies the instrumentation used should have sufficient frequency response to measure the equivalent of full-scale 3-second gusts. Wind tunnel wind speed data should include the average, the root mean square of the variation about the average (rms), and a measured and/or estimated peak over the equivalent of one hour full-scale for each station and wind direction.

Chapter 4
LOCAL AND PANEL WIND LOADS

4.1 GENERAL

Local wind loads refer to wind forces acting on small areas, such as individual windows or fasteners. Panel loads refer to forces on larger portions of a structure, such as parts of walls supported by the structural frame or a portion of a roof, supported by a single truss. The two load types grade continuously from one to the other and are distinguished by the effects of area averaging of wind pressure and by the possible inclusion of resonance of the member. Locally acting peak pressure may not be felt across the entire area, and spatial averaging results in lower effective peak pressures. The presence of resonance is indicated by a sharp increase in response amplitude and may be experienced in situations where natural frequencies are lower than several Hz.

The action of wind on parts and portions of the exterior envelope on which loads are to be determined, such as components of the curtainwall and roof cladding systems, can in many situations be treated as quasistatic. A quasistatic load implies that the internal stresses in the portion under investigation are in direct proportion to the applied force and that the part is not in significant resonant motion at one or more of its natural frequencies. The reason for the quasistatic response is that the frequencies of vibration of such components are usually well above those at which there is appreciable energy in the turbulent flow field. Portions with natural frequencies above approximately 1 to 2 Hz are likely to respond quasistatically. Maximum load effects on such components are therefore caused by short duration peak wind-induced pressures acting with little or no dynamic magnification by the component. In these cases, it is usually sufficient to test at a single wind tunnel speed and to express the results as a peak pressure acting as a static load. Clearly, there are exceptions, and it is prudent to examine the possibility of resonant vibrations in unusual situations such as cladding or roof panels that span larger than typical distances, that have natural frequencies lower than 1 to 2 Hz, or that may

be subject to fluctuating loads of high intensity at frequencies matching the natural frequency of a panel or a component.

Wind load codes usually assume a quasisteady wind load; that is, the peak load can be determined by a mean load coefficient combined with a peak gust wind speed. Although this approach may work in some cases, it fails in others, because it does not account for wind pressures generated by the direct interaction of the flow and the structure. For example, the peak pressures in areas of flow separation and vortex generation cannot be predicted with a quasisteady approach. For this reason, use of measured peak pressures or forces are usually preferable to measuring the mean load and calculating the peak load by multiplication by a gust factor. There are many cases in which the gust factor is not known without a test that measures the peak value, particularly when the mean load is small in the presence of large, fluctuating loads.

Some materials, such as wood and glass, have a higher capacity for resisting short-duration loads than longer-duration loads. Consequently there may be cases in which the effects of load duration need to be determined for use with appropriate resistance factors for a particular material.

In the design of roofing, cladding, and glazing elements and their fasteners, and for loosely laid roofing systems, it is important to recognize that the action of wind causes fluctuating loads with possible stress reversal. Hence, there is a potential for fatigue failure or the loosening of connections, or both. Fatigue failures frequently occur in hurricanes, during which high winds can persist for hours.

Wind tunnel evaluations of local wind loads acting on individual components or panels of a structure or building involve measurements of both mean and instantaneously acting exterior peak local and area pressures. This evaluation generally includes measurements or estimates of wind-induced internal pressures. Pressure measurements must be made in flow conditions which representatively simulate the natural wind (see Chapter 2). Buildings and structures are usually simulated with geometrically scaled static models that satisfy the criteria in Chapter 2.

The measuring instrumentation should have sufficient accuracy and frequency response, including both amplitude and phase relationships, to reliably evaluate the mean pressure and all fluctuations, which significantly contribute to the time-varying component of the peak pressures (see Chapters 8 and C8).

4.2 EXTERNAL PRESSURES

4.2.1 Local Pressures

Measurements of local, exterior pressures are made primarily to evaluate wind loads on components of the curtainwall and cladding systems. Care

must be taken to assure that measurements are taken in all areas of significance to the designer, with particular attention to areas of high local pressure or potential aerodynamic "hot spots." Pressures should be measured at a sufficient number of locations and wind directions so that no significant aerodynamic events are missed. For a major building this may involve measurements at some 300 to 1000 or more locations, depending on the complexity of the exterior geometry. Typically, measurements are made at azimuth increments of 10°, with finer steps, if necessary, in aerodynamically significant regions. Measurements of peak pressure magnitudes should account for the statistical variability in individual samples of the peak. Representative information for low-rise or less wind-sensitive buildings can be obtained with a more modest pressure tap coverage. In addition to exterior pressures, estimates of component wind loads must allow for internal pressures (see Section 4.3).

Pressures at various locations on the exterior surface are sometimes measured independently and sometimes measured simultaneously at a large number of pressure taps. The measured peak values at the various measuring points may not be coincident in time or may not be sufficient in number to be combined to estimate instantaneous overall forces. Where time coincidence and a sufficient pressure tap coverage of the surface permit, then instantaneous overall panel forces can be determined (see Section 4.2.2). In addition, mean values of local pressures can be integrated over exterior surfaces of a building or structure to determine the mean or static components of the overall wind loading. This offers an important opportunity to verify the results of direct overall wind load measurements (see Chapters 5 and 6).

4.2.2 Panel Wind Loads

Peak short-duration wind loads, effective over a panel or the tributary area of a structural member, can be evaluated by means of real-time spatial averaging of local pressures over the area of interest. Applications include such varied geometries as loads on cladding assemblies of more than about 100 square feet (smaller areas where load gradients are high), purlin loads on roofs, loads on building appendages, and differential pressures on canopies and solar collectors.

Area average pressures can be achieved either by on-line algebraic addition in the data acquisition computer of pressures measured simultaneously at a number of locations, or by pneumatic averaging using a single pressure transducer connected by a manifold to multiple taps. The averaging can be uniform, with all individual pressures considered equally, or weighted, so that some parts of the panel or tributary area are given greater importance. For example, in the case of the wind load on the tributary area of a beam or purlin, the pressures on individual parts of this area can be weighted so that the spatial average gives a direct measure of the mid-span bending moment.

Estimates of the instantaneous correlated peak wind pressures on a particular panel or some tributary area can be obtained with time averaging achieved by measuring the surface pressure or pressures through a low-pass filter. The time constant is selected so that the measured peak pressure can be taken to be correlated over the area of interest. This technique for evaluating the magnitudes of equivalent statically acting gusts is used in Great Britain, but has not been used much in North America. Selection of the time constant must be made carefully to avoid underestimates of loads.

Some panels may experience wind pressures on both sides. Differential pressures across such panels may be important. Examples include canopies, signs, solar collectors, free-standing walls, and some parapets. These differential pressures can be obtained by simultaneously measuring the area-average pressure on each side and algebraically evaluating the difference.

Internal pressures, acting on the back or underside of panels and tributary areas, must be included in estimates of panel loads (see Section 4.3).

4.3 INTERNAL PRESSURES

Internal pressures contribute to the differential pressure across the building skin, increasing or decreasing the pressure applied by the external wind load. Wind-induced internal pressures depend on: (1) the exterior pressure distribution; (2) the size and distribution of small unavoidable cracks and leakage paths; (3) the size and distribution of large orifices, such as doors or windows that are open by tenant operation, or by wind-induced breakage; and (4) in some situations, on the flexibility of the skin and the dynamic properties of the skin and the enclosed air volume. For buildings controlled by (1) and (2), the internal pressure is determined by leakage (infiltration) and the air ventilation system. Where large openings can occur during high winds, for example, truck doors or tenant operable doors and windows in office or residential units, or glass breakage, the influence of these openings can have a significant effect on net skin pressures and on structural frame loads (see Chapter 5). The specification of which openings are to be included for internal pressure analysis is not standard, even by wind load provisions of model building codes or in the national wind load standard American Society of Civil Engineers (ASCE) 7-95. Special care should be taken in the evaluation of mean and dynamic internal pressures. The significance of internal pressures has often been neglected and this has contributed to building failures.

Wind can induce pressures within other partially sealed volumes, such as spaces under loosely laid roofing material and ballast pavers, and in cavities behind vented exterior wall panels. These internal or cavity pressures must be allowed for in situations where they can add to the wind pressures on

surfaces behind the porous surface. For roof systems with impermeable layers and for rain-screen type curtainwalls, the venting of cavities behind exterior components can reduce the wind pressures acting on exterior surfaces by transferring a portion of the load to the underlying surface. Wind tunnel tests, including a representative simulation of the permeability of the exterior envelope, are required to ascertain the degree of pressure equalization. In the presence of a vented exterior surface, it becomes important also to examine the action of the cavity or back pressures on interior walls and components of the roof. In some cases, in which small changes in geometry of the exterior vented panel can significantly affect the level of cavity pressure, such as for roof pavers or some vented curtainwalls, model tests are in the developmental stages and are not always considered routine (see Section 4.4). In some cases, full-scale tests may be required.

Although the subject of wind-induced internal pressures is still an active research area, two limiting cases can be evaluated. The first is that of a relatively tight exterior envelope with approximately uniformly distributed leakage, as typically found in most major buildings. The second is that of a building with dominant openings which govern the inflow, and hence the internal pressure. Both cases can be experimentally studied using static pressure models. The internal volume in such cases can be modeled geometrically and may include dynamic (not constant) pressures. This case may also require that the pressure differential across internal partitions be evaluated. Analytical methods, using exterior pressure data, can also be effective for the evaluation of the wind-induced internal pressures.

4.4 ROOF PRESSURES

Roof pressure tests are similar to cladding tests except for special cases such as paver design, gravel ballast blowoff, standing seam metal roof differential pressures, or single membrane uplift. These cases are difficult to model at scales of 1:200 to 1:600, which are typically used to evaluate building wind loads, because of the small size of leakage paths that can provide internal pressures or underpaver pressures and to the small size of ballast. Research on small buildings at scales of 1:10 to 1:100, now in progress, may eventually yield more effective and economic tests than are now possible. A combination of model test and analysis may yield useful results.

In some cases, the largest local peak uplift pressures are the result of the action of roof corner vortices. The location of the largest uplift may be difficult to determine and may change with additional parapets or other geometric variables.

Where gravel ballast is used to hold a roof in place, for example, a single membrane, winds may scour the gravel clearing the ballast from an area.

This may permit "ballooning" of the membrane, and subsequent failure. Some guidance for gravel size to prevent scour is given in Kind and Wardlaw (1976). For other types of ballast, manufacturers literature should be consulted to determine adequacy. Wind-tunnel tests can sometimes help to determine adequate design, but these tests are specialized and general guidance is limited.

Chapter 5

OVERALL WIND LOADS AND WIND-INDUCED RESPONSES

5.1 GENERAL

Overall wind loads are external loads that act on a structure as a whole or are effective on large portions that can be treated as structural subsystems. An example of the latter would be the tributary area associated with a main roof truss or girder, in which adjacent primary members are structurally independent. These wind loads are composed of both mean and time-varying components. In cases in which aeroelastic effects, such as aerodynamic damping, are uncertain and can be neither neglected nor estimated, then full aeroelastic simulations are desirable. Such situations are considered in Chapter 6. On structures or elements where aeroelastic effects are not important, the overall external wind loads can be studied using static models with geometrically scaled external features.

The scaling of such models and of the natural wind should be in accordance with the guidelines in Chapter 2. A first approximation of the mean overall loads can be obtained if the mean velocity profile of the approach flow is modeled correctly. More accurate measurements of mean loads require a simulation of the turbulence characteristics, as defined in Chapter 2. Accurate measurements of both the mean and the dynamic components of the overall wind loads are obtained if both the approach flow and the near field are properly simulated (see Chapter 2).

Tests at a single wind speed are sufficient to determine the coefficients of mean and time-varying forces and, when applicable, spectra of the generalized or modal forces. A complete range of wind directions must be examined unless there are symmetries of shape and surroundings. Typically tests are carried out for winds at 10° azimuthal increments (36 for a full 360° range).

5.2 MEASUREMENT TECHNIQUES

5.2.1 Pressure Averaging

Averaging local pressures acting on the surface of the wind tunnel model may be done pneumatically, digitally on-line, or by some combination of these two. In many cases, weightings are introduced in the averaging process that combines the pressures acting on various tributary areas to form direct real-time measurements of particular structural actions, such as bending moments, member forces, or stresses in the primary structural system. It is important that the number of tributary measurements be sufficient to capture the significant spatial variations for the structural action of interest. The weightings used in such procedures employ influence coefficients obtained from an analysis of the structural system. Generalized forces associated with particular modes of vibration can also be evaluated in this way.

In some situations, it may be more convenient to carry out all or part of the averaging process in a "post-test" mode, that is after simultaneously measuring and recording time histories of individual point pressures or tributary loads. The determination of overall mean loads can be performed by straightforward combination of measured mean tributary loads. These mean aerodynamic data may be increased by appropriate gust effect factors to provide estimates of dynamic wind action. In some situations, this procedure can result in underestimates of the peak wind loads and should therefore be used with caution. For example, a building located in a built-up area may experience reduced mean wind loads, while the dynamic loads may be quite high.

Instantaneously measured local pressures can be integrated over the exterior surfaces of a building or structure to determine the corresponding overall forces, including the generalized forces for particular modes of vibration. This approach can provide aerodynamic data, which are comparable to those obtained from the High Frequency Force Balance Model Technique (see Section 5.2.3), but without any mode shape restrictions. The pressure tap coverage over the exterior surfaces must have adequate resolution to capture the spatial variations of the exterior pressures in the frequency range of interest.

5.2.2 Direct Load Measurements

Wind loads acting on models of whole buildings and structures or components thereof can be measured directly with force balances or load transducers which are capable of providing accurate information on both mean and time-varying effects. Such data are usually used with analytical methods to develop descriptions of overall wind-induced loads and structural responses.

It is important in direct load techniques that the measured loads represent the applied aerodynamic loads only, and that the model itself does not introduce dynamic amplification of the wind loads. (The exception, of course, is an aeroelastic simulation in which the model has been specifically designed to simulate the particular dynamic response of the prototype; these tests are covered in the next chapter.)

The next section describes a specific application of direct load measurements used for high-rise structures.

5.2.3 High-Frequency Force Balance Technique

For many high-rise structures, the lowest sway modes may be approximated as varying linearly with height, in which case measurements of the base overturning moment may be used to represent the generalized or modal wind-induced force. In this procedure, a stiff geometric replica of the structure is mounted on a highly sensitive and stiff force balance that measures the base moments and also the base torque. The frequency of the model and balance system must be sufficiently high to avoid distortions of the dynamic wind loads in the frequency range that affects the resonant response of the full-scale structure.

The frequency of the dynamic loading in the wind tunnel, which corresponds to the full-scale excitation at the natural frequency of the structure, f_{0_p}, and a full-scale wind speed of V_p is

$$f_{0_m} = f_{0_p} \frac{(L_b)_p}{(L_b)_m} \frac{V_m}{V_p}$$

in which V_m = the corresponding model wind speed, L_b = characteristic dimension of the structure, and m and p respectively denote model and full-scale values.

The measured base torque may be used to provide an estimate of the generalized torque, which is the integral of the torque per unit height weighted by the mode shape taken over the height of the building. In this case, however, an empirical adjustment must be applied. Corrections to the generalized sway forces can be made in situations in which the fundamental sway mode shapes do not vary linearly with height. The loads in the two sway directions and the torque can be combined for dynamic systems, which have three-dimensional modes of vibration. Analytical methods are used to evaluate the dynamic structural response once the generalized forces and the generalized torque are determined.

The highest model frequency for which wind loading data are needed is determined by the lowest full-scale wind speed for which response information is required. This highest frequency can be reduced by lowering the

wind tunnel test speed, providing that the balance sensitivity is sufficient to provide reliable dynamic load measurements and that the model value of Re_b remains acceptable (see Section 2.9).

5.3 ANALYSIS METHODS

The mean and dynamic wind-induced aerodynamic loads may be obtained by any of the methods discussed above and, in some cases, these may be the final quantities of interest. More often, however, what is required is the wind-induced responses of the structure to those loads, for example resisting forces and moments, accelerations, or deflections. These responses must then be calculated taking into account both the static response, because of the mean loads, and the time-varying response, which must include any dynamic amplification effects of the structural system. The calculation of response may be carried out in the time domain using stored time histories of the aerodynamic loads, but more commonly, the calculation is performed in the frequency domain using power spectral densities of the applied modal wind loads and assuming steady-state conditions.

The high-frequency force-balance technique has become widely accepted in studies of tall buildings. Recent advances in solid-state pressure scanning, which allow large numbers of simultaneous pressure measurements, have made the integrated pressure technique a viable alternative. It provides more information on the distribution of aerodynamic loads. Aeroelastic simulations are valuable in situations where aeroelastic effects or motion-induced forces become important. These are considered in Chapter 6.

Chapter 6
AEROELASTIC SIMULATIONS

6.1 GENERAL

Aeroelastic simulations are capable of providing information on the overall wind-induced mean and dynamic loads and responses of a structure. Such tests are important for slender, flexible, and dynamically sensitive structures that experience aeroelastic effects—namely, in which the body motion may add to or modify the aerodynamic forces or in which the dynamic modes of vibration are strongly three-dimensional and the aerodynamic modal forces are difficult to evaluate. To be representative, such tests must model the properties of natural wind and the aerodynamically significant features of the exterior geometry, as detailed in Chapter 2. Furthermore, it is also necessary to correctly simulate the stiffness, mass, and damping properties of the structural system. Properly scaled aeroelastic tests of sharp-edged structures can provide reliable direct estimates of the effective wind loads and the elastic responses of a prototype structure. For Reynolds number sensitive shapes (circular or rounded) and in the case of partial models, such as section model tests, adjustments based on full-scale data, theoretical considerations, or both, may be necessary.

Aeroelastic measurements should be carried out at several speeds, selected to simulate a representative range of full-scale wind speeds. A full range of wind directions should be examined unless there are symmetries of shape, structural properties, and surroundings, or unless the important directions of wind can be ascertained at the outset, as in the case of most bridges, or be determined from other studies.

6.2 DETAILED REQUIREMENTS

Additional similarity requirements arise for aeroelastic models which can provide direct information on the response of a structure to wind action. These are given in the subsections that follow.

6.2.1 Mass Modeling

The modeling of the mass of the structure is determined by the requirement that the inertia forces of the structure and those of the flow be scaled consistently. Similarity of inertia forces is achieved by maintaining a constant ratio of the effective bulk density of the building or structure to the density of air. An equation to express density scaling is

$$\left(\frac{\rho_s}{\rho}\right)_m = \left(\frac{\rho_s}{\rho}\right)_p$$

in which ρ_s and ρ = structural bulk density and air density, respectively.

The modeling of the generalized mass and the generalized mass moment of inertia of particular modes of vibration then becomes, for mass scaling

$$\frac{M_m}{M_p} = \frac{\rho_m}{\rho_p}\frac{L_m^3}{L_p^3}$$

and for mass moment of inertia scaling

$$\frac{I_{M_m}}{I_{M_p}} = \frac{\rho_m}{\rho_p}\frac{L_m^5}{L_p^5}$$

6.2.2 Damping

Similarity of dissipative or damping forces is maintained by requiring that ζ, the critical damping ratio for a particular mode of vibration, is the same in model and in full scale. The modeling of the structural damping is important in situations in which the dynamic response has a significant resonant component, and in which the aerodynamic damping is likely to be small or negative.

6.2.3 Stiffness Scaling

The forces which resist the deformation of a structure must be scaled consistently with scaling of inertia forces. Having satisified the scaling of mass (see Section 6.2.1), the approach taken is largely determined by the requirement for simulating the primary source or sources of structural stiffness.

In situations where the resistance to deformation is predominantly the result of the action of elastic forces, and essentially independent of gravity effects or self-weight, consistent scaling of stiffness and flow-induced forces

is achieved by maintaining the Cauchy Number, *Ca*, constant in model and in full scale. This requires that

$$\left(\frac{E_{eff}}{\rho V^2}\right) = \text{constant}$$

where, depending on the structural action to be modeled, the effective modulus E_{eff} is taken as E for replica models and $E\tau/L$, EA/L^2 or EI/L^4 for various equivalent models, which respectively simulate the action of membrane forces, axial forces, and flexure or torsion. Here E, ρ, V, τ, A, I, and L are the Young's modulus, the air density, a characteristic wind speed, the wall thickness of a tube or membrane, the cross-sectional area, the moment of inertia or torsional constant, and a characteristic overall dimension.

Correspondingly, the ratio of model and full-scale flow velocities becomes

$$\frac{V_m}{V_p} = \left(\frac{E_{eff_m}}{E_{eff_p}} \times \frac{\rho_p}{\rho_m}\right)^{1/2}$$

This approach is satisfactory for most free-standing or unguyed structures, including tall buildings, chimneys, and observation towers; shells, truss, arch and girder bridges, and roof systems; and all structures in which the stiffness of the prototype can be approximated by elastic action in the model.

For structures in which the resistance to deformation is influenced by the action of gravity, such as suspension bridges or guyed structures, it also becomes necessary to maintain Froude number equality. This requires that

$$\left(\frac{V^2}{gL}\right) = \text{constant}$$

The acceleration of gravity, g, is essentially equal in model and in full scale, and the wind speed scale becomes the square root of the length scale. This is an important practical constraint for small-scale models, because the wind tunnel must be operated at low speeds and Reynolds number independence may be a concern.

In some situations, such as suspension bridges, both elastic and gravity forces contribute to the stiffness. In such cases, the velocity scale is determined by Froude number similarity and becomes the square root of the length scale. The scaling of elastic forces, based on *Ca* equality, then becomes

$$\frac{E_{eff_m}}{E_{eff_p}} = \frac{(\rho L)_m}{(\rho L)_p}$$

For particular modes of vibration of properly scaled aeroelastic models the relationship between length, time, and velocity is based on the equality of the reduced frequency in model and in full scale, and can be expressed as

$$\left(\frac{f_0 L}{V}\right) = \text{constant}$$

in which f_0 = natural frequency of a mode of vibration.

6.3 TYPES OF AEROELASTIC MODELS

Aeroelastic models of buildings and structures are designed to simulate the dynamic properties for modes of vibration that contribute significantly to the wind-induced response. Such models may represent the structure in full or in part. Aeroelastic models normally only scale elastic structural behavior. This information is usually then extrapolated, analytically or with numerical methods, to examine the behavior of the structure as it approaches its maximum capacity because of material failure, instability, or fatigue.

Aeroelastic modeling techniques include replica, equivalent, and section models, which are described in the following subsections.

6.3.1 Replica Models

These are full-scale aeroelastic models in which the geometric scaling of all dimensions results in a scaled reproduction of elastic properties. Replica models are practical for structures in which the elastic properties are concentrated along the exterior geometry, for example in the case of slender chimneys, cooling towers, tubular structures, and so on. Such models result in full dynamic similitude and provide direct measures of the wind induced response if the flow conditions and geometric scaling are in accordance with the guidelines in Chapter 2.

6.3.2 Equivalent Models

Most equivalent aeroelastic models simulate the full structure using some mechanical analog to represent certain selected aspects of the dynamic characteristics of the prototype structure. Usually, such models use a nonstruc-

tural "skin" to maintain similarity of the overall geometry and the aerodynamic forces. An internal equivalent structural system is used to model the stiffness properties. Unlike replica models, which are in complete dynamic similitude with the full-scale structure, equivalent aeroelastic models are designed to simulate only particular structural behavior. Continuous equivalent or "spline" models are effective for structures in which flexural, torsional, or axial force effects predominate. For complicated structural systems, such as buildings, the full-scale structure can be represented by equivalent lumped parameter systems. The aeroelastic modeling in such cases requires the construction of a structural model system which correctly simulates the scaled mass and stiffness matrices of the prototype structure.

6.3.3 Section Models

Dynamically mounted rigid parts or sections of structures are used to evaluate wind forces acting on slender, line-like structures, such as long-span bridges, chimneys, towers, cables, and other structures in which the flow can be treated as two-dimensional. Examining only a part of the structure allows somewhat larger models to be used. Typical geometric scales range between 1:10 and 1:100. Section model tests can provide information on the aerodynamic stability of particular modes of vibration, or aerodynamic derivatives which are used in conjunction with theoretical methods. Section models can be "driven" with controlled amplitudes and frequencies to study the effects of body motion on the aerodynamic forces. Although such tests are traditionally carried out in uniform smooth flow, current methods often include tests in partial simulations of atmospheric turbulence using coarse grids or active turbulence generators.

6.4 TALL BUILDINGS

The wind-induced dynamic response of tall buildings is predominantly in the fundamental sway and torsional modes of vibration. The wind loads that excite these three (3) fundamental modes can be evaluated with a high-frequency force balance (see Section 5.2.3). Consequently, this technique has become the norm for wind tunnel studies of overall structural wind loads and responses of many tall buildings. Nevertheless, aeroelastic models continue to be used in situations in which aeroelastic effects and, in particular, the aerodynamic damping are of concern, or in which the structural system is unusually complex, resulting in unusual mode shapes.

Equivalent aeroelastic models with discrete or lumped-mass parameter systems are used to study the action of wind on tall buildings. A two-degree-of-freedom or "stick" model, which simulates the building response in its two fundamental sway modes of vibration, is effective for tall buildings of

compact cross-section, where the drag and across-wind responses are dominant. Multi-degree-of-freedom models are required when it becomes necessary also to examine the response of the building in its fundamental torsional mode and in higher modes of vibration. Depending on the complexity of the building, such models could comprise 4 to 7 lumped masses each, with two translational and one rotational (torsion) degrees of freedom. Tall buildings tend to have sharp-edged geometries, and the results of such tests can be readily transformed to full scale.

6.5 TOWERS, MASTS, AND CHIMNEYS

Theoretical methods for line-like structures are applicable to this category, because the flow tends to be two- rather than three-dimensional. Aerodynamic data required in such analytical approaches are commonly obtained from section model tests. The large model size, possible with sectional model tests, has advantages for towers and chimneys of circular and rounded geometry for which *Re* effects can be significant. For latticed towers with members of circular cross-sections, an improved simulation of individual member forces is achieved by scaling the product of the member diameter and its drag coefficient.

For structures with sharp-edged geometries, full aeroelastic models can provide results that are directly transferable to full scale. For cross-sections where *Re* corrections are necessary, full aeroelastic models provide valuable validations when used in conjunction with theoretical methods and section model data. Aeroelastic models are important in situations in which the flow is complex, as in unusual terrain or topography, or in which the structure is located on top of or near a building. Aerodynamic interference can be an important consideration for pairs or groups of closely spaced chimneys, masts, and electric power conductors.

6.6 COOLING TOWERS

Replica aeroelastic models can be used to study the wind-induced response of concrete hyperbolic cooling towers. For this application, it is important to use a model material that has a Young's modulus low enough to allow a significant range of full-scale velocities to be simulated in the wind tunnel. For strict replica models of shell structures, it becomes necessary also to maintain equality of the Poisson ratio. Cooling towers, because they are round, are somewhat sensitive to *Re* scaling and adjustments may be necessary in conversions to full scale.

6.7 FLEXIBLE ROOFS

Representative estimates of both static and dynamic wind loads for most roofs can be obtained using overall force measuring techniques, as described in Chapter 5. Nevertheless, aeroelastic models are valuable for some flexible roof systems, including roofs of unusual spans, cantilevered grandstand roofs, and various tensioned and air-supported structures. For girder, trussed, and cable-stayed spans, equivalent aeroelastic models can be used to simulate the full roof system or parts of the roof. The stiffness of these structures comes primarily from the action of elastic forces. Proper allowance for internal or underside pressures is important.

For tensioned and cable-supported fabric structures, the geometric stiffness tends to dominate, and the requirements for scaling elastic forces can be relaxed. Representative aeroelastic models of such structures are achieved by scaling the overall geometry and the fabric and cable tensions. The tensions are scaled in proportion to the dynamic velocity pressure. Internal or underside pressures can be important for such structures. The modeling of inertia forces requires the scaling of fabric and cable masses. In some situations, virtual mass effects can dominate, and some relaxation of the structural mass scaling may be permissible. Scaling the structural damping becomes less important for these lightweight structures because the aerodynamic damping tends to dominate.

Aeroelastic modeling requirements for pneumatic or air-supported structures are similar to those for tensioned fabric systems. The geometric stiffness tends to be more important in comparison with the elastic stiffness. An additional consideration is the action of the internal pressurization. The internal pressure is scaled in proportion to the dynamic velocity pressure. The action of gravity forces can be approximately allowed for by scaling the internal pressure minus the weight of the structure per unit area of the membrane rather than the internal pressure directly. The importance of modeling the pneumatic stiffness on volume displacing modes of vibration and the pneumatic damping must be examined in such simulations. As in the case of tensioned fabric structures, the scaling of mass and the structural damping can be approximate.

6.8 LONG-SPAN BRIDGES

The action of wind on slender, long-span bridges can be studied effectively with both section and full aeroelastic models. Models of all types require geometric similarity of the deck cross-section to that of the prototype. Model studies should be accompanied by an interpretation of the observed model response relative to that of the prototype. Model dynamics may differ from prototype dynamics. Section models have been tradition-

ally used to determine the aerodynamic stability characteristics of bridge sections and to provide aerodynamic data, as required in theoretical methods. Both smooth and turbulent flows are used in such tests.

Full-bridge aeroelastic models at geometric scales ranging from 1:100 to 1:500 are used to provide information on the wind-induced response of both suspension and cable-stayed bridges. Models can be designed to simulate both under-construction stages and the completed bridge. Such models can representatively allow for the interaction of the turbulence with the three-dimensional dynamic action of the bridge. Other advantages include the ability to examine skewed wind directions and the effects of topographic features. Froude number (*Fr*) scaling must be allowed for in full aeroelastic model studies of suspension bridges. This results in quite low wind tunnel speeds and there are increased concerns for *Re* scaling (see Section 2.9). In studies of cable-stayed bridges, it is usually possible to pretension the staying cables and thus avoid scaling *Fr*.

Single-span flexible models, including taut-strip or taut-tube models, are occasionally used as simplified versions of the full-bridge model. These can be constructed at geometric scales comparable to those of full aeroelastic models and tested in properly scaled turbulent boundary layer flows. Such modeling approaches may examine the effects of wind direction, terrain, and topographic features.

The present state of the art is such that model studies of any kind should be associated with a sound method for interpreting or extrapolating their results to the prediction of full-scale prototype behavior.

6.9 CABLES AND TRANSMISSION LINES

Section model tests are effective in studies of forces on cables and tower sections. For most cables, *Re* can be properly scaled in such tests. Section models can be effective in studies of the "galloping" or other dynamic behavior of iced cables or cables covered with water droplets or rivulets, which can lead to increased wind-induced vibrations during periods of rain. Full aeroelastic models can be used to study the interaction between different spans of transmission line systems.

Chapter 7
DISPERSION AROUND BUILDINGS

7.1 GENERAL

Many problems involving dispersion near buildings, or more correctly, dispersion within the region of the aerodynamic influence of the building, are amenable to wind tunnel modeling techniques. In fact, because of the complexity of these problems and the current limitations of computational methods, this may be the only practical method for investigation.

Buildings have a significant effect on the flow near them and, therefore, on the dispersion of pollutants released near the building or transported toward the building from upwind sources. The effect of the building on the flow can also extend for a considerable distance downstream, influencing the dispersion from releases located downwind from the building. The dispersion from sources near buildings is influenced both by the atmospheric boundary layer and the local effect of the building on the mean and turbulent flow. Whether either or both of these processes is important depends on the details of the particular problem, and, given the great diversity of possibilities and the inherent complexity of the problem, it is often difficult to say *a priori* which will be dominant.

We may arbitrarily divide dispersion problems into those concerned with the near field (i.e., the region near the building) and the far field (i.e., at some distance from the building) acknowledging that there may be significant interaction between these regions in some circumstances. Far field problems may be treated with success using numerical methods. However, physical modeling may be required to properly quantify the effects of buildings on the source term used in such analyses.

7.2 PROBLEM AREAS

In dispersion problems it is usually necessary to determine the concentration of a pollutant at points of interest. For example, it may be necessary to

determine the location and magnitude of the maximum ground level concentration or the concentration at the air intake location of a building. A difficulty not often recognized is the great range of concentrations involved in the problems for which the experimental investigation is undertaken. For example, flammability problems involve concentrations of the order of a few percent, toxicity problems involve concentrations of the order of parts per million (ppm) and odor problems involve concentrations of the order of parts per billion (ppb).

In all dispersion modeling, the atmospheric boundary layer needs to be modeled in a manner similar to that described in Chapter 2, with some additional complications introduced for dispersion. The main difficulty is that the usual assumption of a neutrally stratified boundary layer may not be appropriate for dispersion problems. It is possible that the worst case (maximum) concentrations will occur at low wind speeds, when the atmosphere is stable or in unstable flow situations which result in greater plume spread. This significantly complicates the modeling process. Generally the local effect of the building on the flow is dominant in the near-field region. However, in the far field, and in the transition between these regions, the effect of atmospheric stability could be important. Very few wind tunnel facilities are able to explicitly model this.

It is also necessary to model the characteristics of the source of the pollutant. The diversity of possible sources and the physical mechanisms involved in releases can complicate the modeling considerably. For example, sources may have both momentum and buoyancy fluxes (because of thermal effects), which must be correctly modeled.

Several classes (or types) of problem are common. These include releases from stacks and vents on a building or industrial plant, where there may be both momentum and buoyancy fluxes; entrainment of exhausts from the building or nearby buildings into air intakes; impingement of releases from upstream sources on the building surface; and releases from line or area sources which occur because of automobile traffic. Concerns include both toxicity and odor issues.

Another class of problems related to dispersion is concerned with the natural ventilation of buildings. In these problems, the concern is the movement of air *within* the building under the influence of external wind pressures. These problems may also require the modeling of natural wind at low wind speeds and the use of tracer gases to determine the air movement in the building.

The experimental methods used in these studies generally involve the release of a tracer from the modeled source, which is detected by smoke flow visualization or some other instrumental technique (hydrocarbon detector).

There can be many complicating factors related to the meteorology and the surface roughness and topography at the site. For example, in the imme-

diate vicinity of a shoreline, the structure of the boundary layer can be strongly influenced by the local conditions. This type of modeling requires a wind tunnel with a capability to model thermally stratified flows; however, isothermal model flow simulations can be used to address certain parts of the problem.

The far-field problems have attracted the attention of regulatory bodies, in particular the Environmental Protection Agency (EPA). The reader is referred to the relevant EPA documents for a description of the extensive test protocols that have been established for far-field applications.

7.3 SIMILARITY REQUIREMENTS

7.3.1 Boundary Layer Modeling

Wind tunnel simulations of dispersion require representative modeling of the characteristics of the atmospheric boundary layer, relevant structures and obstacles, and the dynamics and thermal properties of the source. Similarity requirements for wind tunnel simulations of natural wind during neutral stability are presented in Chapter 2. Most near-field diffusion problems, which are dominated by the aerodynamics of particular buildings, can be representatively studied in model flow fields which simulate the neutral atmospheric boundary layer. In some situations it is important to simulate stratified ABL flows (see Chapter 2).

7.3.2 Source Modeling

Because of the nature of dispersion problems, it is impossible to make absolutely general statements about the source modeling requirements. Often this is done in comparison with some equivalent plume.

Having established a representative simulation of the atmospheric boundary layer at a geometric scale of $\lambda_L = L_m/L_p$, where L is a characteristic length and the subscripts m and p refer to model and full scale (prototype) quantities respectively, the additional modeling requirements (for similar plume behavior) include:

Geometric similarity of stack $$\frac{L_m}{L_p} = \lambda_L$$

Froude number $$\left(\frac{V^2}{Lg}\right)_m = \left(\frac{V^2}{Lg}\right)_p$$

Density ratio $$\left(\frac{\rho_s}{\rho}\right)_m = \left(\frac{\rho_s}{\rho}\right)_p$$

Velocity scaling $$\left(\frac{W_s}{V}\right)_m = \left(\frac{W_s}{V}\right)_p$$

Stack Reynolds number $$\left(\frac{dW_s}{\nu_s}\right)_m \geq Re_{s_{\min}}$$

Building Reynolds number $$\left(\frac{L_b V}{\nu}\right)_m \geq Re_{b_{\min}}$$

where V, W_s, ρ, ρ_s, ν, ν_s, L_b, and d are a characteristic wind velocity, the average stack exit velocity, the air density, the stack gas density, the kinematic viscosity of air, the kinematic viscosity of the stack gas, a characteristic overall dimension of a building, and the internal stack diameter respectively. Note that $\rho_s/\rho = T/T_s$, where T and T_s are the ambient air and stack gas temperatures, respectively. Reynolds number similarity is important both for the internal (within the stack) and the external flows. The value of $Re_{b_{\min}}$ for external flows is usually assumed to be about 10,000. Above the minimum value it is assumed that Reynolds number independence exists for most typical building configurations. Note, however, that particularly for curved structures (e.g., circular cylinders) this criterion may not be adequate to ensure Reynolds number independence, and special treatment of these cases may be required. For flows within the stack, it is usually possible to achieve turbulent flow by tripping the flow and/or roughening the inside wall.

For hot, buoyant exhausts, the model velocities, scaled using Froude number similarity, tend to become very low. This complicates the requirement for modeling the ABL and the achievement of Reynolds number independence. In some cases, approximate models based on momentum scaling are used. Momentum scaling is achieved by requiring that

$$\left(\frac{\rho_s W_s^2}{\rho V^2}\right)_m = \left(\frac{\rho_s W_s^2}{\rho V^2}\right)_p$$

It is important to recognize the limitations of such approximate models.

Chapter 8
INSTRUMENTATION

The instrumentation used in wind tunnel model tests of all aforementioned wind effects should be capable of providing adequate measures of the mean and, where necessary, the dynamic or time-varying response over periods of time corresponding to about 1 hour in full scale. For quantitative measurements of time-varying pedestrian level wind speeds, local pressures, overall wind loads, and aeroelastic responses, the frequency response of the instrumentation system should be sufficiently high to permit meaningful measurements at all relevant frequencies without magnitude and phase distortions. Consideration of phase becomes important in spatial averaging procedures, in which simultaneous measurements of local pressures are combined to form dynamic loads on particular tributary areas or on the entire building or structure.

All measurements should be free of significant acoustic effects, electrical noise, mechanical vibrations, and spurious pressure fluctuations, including fluctuations of the ambient pressure within the wind tunnel caused by the operation of the fan, door openings, and the influence of atmospheric wind. Where necessary, corrections should be made for temperature drift.

Most current instrumentation systems are highly complex and include on-line data acquisition capabilities. There is a growing level of automation with computers used to control experiments. Nevertheless, in some situations it is still possible to provide useful information with more traditional techniques, including smoke flow visualization and surface-streaks and particle-erosion methods. Although difficult to perform in turbulent flow without proper photographic techniques, flow visualization remains a valuable tool for evaluating the overall flow regime and for providing qualitative information on pedestrian level winds, on air circulation and ventilation, and, in some situations, on the potential presence of particular aerodynamic loading mechanisms.

This page intentionally left blank

Chapter 9

QUALITY ASSURANCE OF WIND TUNNEL DATA

The reliability of all wind tunnel data must be addressed and should include considerations of both the accuracy of the overall simulation and the accuracy and the repeatability of the measurements. Checks should be devised where possible to assure the reliability of the results. These should include basic checkout procedures of the instrumentation, including its traceable calibration, the repeatability of particular measurements, and, where possible, comparisons with similar data obtained by different methods. For example, mean overall force or aeroelastic measurements, or both, can be compared with similar data obtained from the integration of mean local pressures. Also valuable are credibility checks with codes, and comparisons with full-scale data and existing experience.

Comparisons with full-scale data are particularly important to assure that experimental techniques and analysis procedures provide representative information. Unfortunately, such comparisons are not without difficulties. Both model and full-scale processes are stochastic and allowance must be made for their inherent variability. Also, long periods of time may be required before the full-scale monitoring program captures a significant event. Comparisons of full-scale and model data for a broad range of wind effects can be found in the literature. These include overall responses of wind-sensitive structures, including tall buildings, masts, towers, long-span bridges, and various specialty structures; local wind loads on components of both tall and low-rise buildings; wind conditions at pedestrian level; local winds and turbulence over complex terrain including hills, valleys, and ridges; and tracer concentrations downwind of point, line, and area sources. The picture that has emerged is an encouraging one and confirms that properly scaled wind tunnel tests are capable of providing representative information on the action of wind on buildings and structures.

This page intentionally left blank

Chapter 10

WIND CLIMATE AND PREDICTION OF FULL-SCALE BEHAVIOR

The end product of a wind tunnel simulation is usually the prediction of a load or response for a given recurrence interval or probability of exceedance. To obtain the predicted load or response, the data derived from the wind tunnel simulation for a range of wind speeds and directions are combined with statistical information on the local wind climate. A number of different methods for combining wind tunnel and climatological data are available, and the particular technique employed often depends on the form of available climatological data.

The simplest, and most conservative, method for predicting full-scale response is to combine the worst aerodynamic response, regardless of wind direction, with the design wind speed. This approach is typically used when the local climatological data are sparse, or of poor quality, and when a wind climate model that considers wind directionality cannot be developed.

In most instances there are enough historical records of wind speed and direction available that a statistical model of the local wind climate can be developed that considers wind direction. Such an approach provides more realistic predictions of the full-scale response than does the simple, direction-independent model. This approach also takes full advantage of wind tunnel results and may offer considerable reductions in the predicted responses when the worst aerodynamic response occurs for wind directions that are infrequent in full-scale.

In the United States, it is common to record surface-level winds (often taken at 10 m above ground) in the form of daily fastest mile wind speeds, 1- or 2-minute averages recorded either once per hour or once every three hours, and the daily peak gust speed (3-second average). The fastest mile data are no longer collected, but historical wind data are frequently available in this form. The wind direction is usually recorded in 45-degree or 22½-degree sectors in the case of the fastest mile data, and either 22½-degree or

10-degree increments in the case of the 1-minute average and 3-second gust data. In most cases surface anemometers are positioned at heights ranging between 3 and 20 m, and the measured windspeeds are adjusted to a 10 m value. At some locations in the United States, measurements of surface level wind speeds are supplemented by upper level (balloon measurements) taken one to four times per day.

The 1-minute average surface level data and the upper level data can be used to define a parent probability distribution of wind speed and direction. Then, response data obtained from the wind tunnel are combined with the parent probability distribution of mean hourly wind speed and direction and with information on the effective occurrence rate of independent storms to predict responses for various recurrence intervals. The parent distribution of wind speed and direction does not model the extreme wind events or extreme responses. The extremes can be derived analytically from the combination of the parent distribution and the effective occurrence rate, or extracted from recorded data.

The wind-climate models developed from the surface level and the upper-level data have both advantages and disadvantages. The major advantage of surface-level wind records is the large amount of data. This results in statistically more reliable estimates of the wind climate. The major disadvantage of the surface-level data is that the measured wind speeds and directions can be influenced by local terrain and topographic features, vegetation, and nearby structures. Furthermore, the surface-level winds usually must be adjusted to a reference height usually taken well above the building or structure or to the free stream above the boundary layer (gradient height) to facilitate use with wind tunnel data. These adjustments to a gradient height are a function of the upstream aerodynamic roughness lengths and fetch lengths and often vary with wind direction and season. The prime advantage of the upper-level (balloon) measurements is that they are direct measures of the gradient winds, free from the influence of local terrain features, and so on. Disadvantages of the upper-level measurements are their relative scarcity (one to four measurements per day), and the difficulties of releasing balloons in extreme winds.

The annual maximum fastest-mile and peak gust wind speeds as a function of direction can be extracted from the daily maxima. These annual maximum fastest-mile wind speeds and the annual maximum peak gusts represent direct measures of the extreme winds at a particular site. The extremes are converted to equivalent mean hourly values, and then combined with the wind tunnel measurements to produce predictions of the response as a function of recurrence interval. The fastest-mile and peak gust data, however, are surface-level measurements and are subject to the same terrain effects as the surface-level 1-minute averages.

In regions influenced by tropical cyclones, a sufficient number of direct measurements of wind speed and direction is not available, and indirect

methods for predicting wind speeds must be employed. The method most commonly used for predicting hurricane-induced wind speed is a Monte Carlo technique, in which statistical distributions of key parameters of a mathematical model of winds within a hurricane are sampled from the historical records of all tropical cyclones within the region of interest. Using a mathematical model of the hurricane windfield and the statistical distribution of key parameters in the model, thousands of years of hurricane storms are simulated and the wind speeds and directions generated at the site are recorded and combined with the wind tunnel data to obtain predictions of structural responses versus recurrence interval.

Wind loads associated with tornadoes are, in general, not considered for most structures. These are extremely rare events and do not influence predicted windspeeds for recurrence intervals of less than several hundred years. Only in cases of critical facilities, such as nuclear power plants, are tornadoes typically included in the estimates of extreme wind speeds. In cases in which wind speeds associated with tornadoes are required, analytical models are available based on regional tornado data or Monte Carlo simulation techniques similar to those employed to estimate hurricane-induced winds are used.

The wind climate model is a major source of uncertainty in the prediction of loads and responses. It is prudent, therefore, to consider wind data from all possible sources in the development of the climate model(s). Frequently this results in different statistical wind speed and directional models. In such cases it becomes important to "envelope" the response predictions to reflect a range of possible wind climates.

This page intentionally left blank

Part 2

COMMENTARY ON WIND TUNNEL STUDIES OF BUILDINGS AND STRUCTURES

This page intentionally left blank

Chapter C1
INTRODUCTION

Part 2 of the ASCE *Manual of Practice For Wind Tunnel Studies of Buildings and Structures* provides information to assist with the use of the Manual. It includes explanations of concepts, which are important in order to ensure representative modeling at a reduced geometric scale, provides examples of typical wind tunnel tests, and includes a bibliography.

It is important to realize the relatively rapid changes in testing methods made possible by advances in instrumentation and computer-based data acquisition. At the time of the writing of the first Manual, published in 1987, the high-frequency force-balance technique for evaluating the dynamic wind loads on buildings and other vertical structures became possible because of advances in strain gauge and quartz transducer technology. While it is still the most commonly used technique for determining the dynamic structural wind loads on tall buildings, it is now being complemented by developments in pressure instrumentation that allow simultaneous measurements of instantaneous pressures at many locations. These can be integrated in real time using appropriate influence coefficients to determine generalized forces for the lower modes of vibration, as well as information on the spatial distribution of nonresonant time-varying forces, which, up to now, have been difficult to measure.

It is important to be aware of this rapid change in technology and to realize that many of today's state-of-the-art procedures may be substantially altered or even replaced. An important new development in wind engineering is the use of computational fluid dynamics (CFD). While still largely a research tool, there is a growing confidence in CFD applications in such areas as the prediction of mean flow and pressure fields around simple buildings and in partially enclosed spaces. Other applications will no doubt follow as CFD techniques complement and extend current wind tunnel technology.

This page intentionally left blank

Chapter C2
MODELING THE WIND

C2.1 GENERAL

Physical modeling of wind effects on buildings and structures in wind tunnels has provided and continues to provide data for design, building code development, and research to establish relationships between wind and wind-effect variables. An essential requirement that must be met is to ensure that model data correctly predict wind effects for the prototype. A correct modeling of the wind is an important prerequisite in this process. Modeling of boundary-layer winds, the basic wind type used in wind-engineering practice, is highly developed, with the result that wind-effect data derived therefrom can be used with confidence for most applications providing that the modeling guidelines, given in Chapter 2, are adhered to. Wind simulations for the study of wind loads on low-rise structures are given special consideration. However, modeling of wind for extreme meteorological events—tornadoes, downbursts, within the eye walls of hurricanes, low-level jets, and mountain lee waves—is being developed through ongoing research and is not discussed herein.

Material in the following sections is focused on modeling of wind in atmospheric boundary layers (ABL) with neutral stability. This is of particular interest to engineers and architects engaged in the design of buildings and structures. For this application strong winds are of interest in which mixing by mechanically generated turbulence destroys any thermal stratification to give neutral stability (isothermal flow in the wind tunnel and an adiabatic lapse rate of –1 °C/100 m for the atmosphere). An overview of wind characteristics for this type of boundary layer, as determined by micrometeorological measurements and theoretical considerations, is presented in Section C2.2. This is followed by a discussion of modeling criteria in Section C2.3 and a state-of-the-art account of boundary-layer wind tunnels and characteristics of the modeled wind in Section C2.4. Flow characteristics pre-

sented for the modeled and natural wind reveal good agreement for essential features needed to model wind effects on buildings and structures. Additional requirements for modeling the ABL for studies of dispersion, in which thermal stratification is important, are discussed in publications by Cermak (1975) and Snyder (1981).

The information on flow in the lower atmosphere that follows is not intended to be a rigorous or comprehensive presentation of the physical processes involved. Emphasis is given to features of the ABL that can be satisfactorily approximated in wind tunnels to model wind effects for wind-engineering applications. Some comparisons of model and full-scale data that have provided confidence for the modeling techniques are presented by Chuang and Cermak (1966), Dalgliesh (1975), Meroney (1980) and Teunissen (1983).

C2.2 THE ABL

C2.2.1 Flat Uniformly Rough (FUR) Terrain

Vertical distributions of mean velocity V throughout the planetary boundary layer (PBL) have been measured for a FUR terrain near Jacksonville, Florida, which has a geostrophic level of approximately 750 m (Holton 1971). The height where forces caused by the Coriolis acceleration and pressure gradient are in equilibrium is designated as the geostrophic level z_{geo} and the mean wind speed by V_{geo}. The essential features of the PBL, when no upper-level thermal winds are present, are represented by a model developed by Lettau (1962). An illustrative PBL, computed in accordance with this model, is shown in Figure C2.1.

For middle latitudes and *neutral flow* over FUR terrain, Panofsky and Dutton (1983) give the following expression for estimating z_{geo}:

$$z_{geo} = 0.175 u_* / f_c \tag{C2.1}$$

where the Coriolis parameter $f_c = 2\omega\sin\phi$; ω is the angular velocity of the earth ($\omega = 7.27 \times 10^{-5}$ rad/s); and ϕ is the latitude. However, Panofsky and Dutton (1983) state that z_{geo} is actually often smaller than given by Eq. (C2.1).

For wind-engineering purposes, the assumed ABL height is commonly defined as the height where effects of surface shear stress become negligible and V becomes a maximum or remains constant with height. This height is designated as the gradient height, defined as $z = z_g$. The wind speed at this height is denoted as $V = V_g$.

The lower portion of the ABL, where turbulent fluxes vary within about 10% of surface values, is defined as the atmospheric surface layer (ASL) with

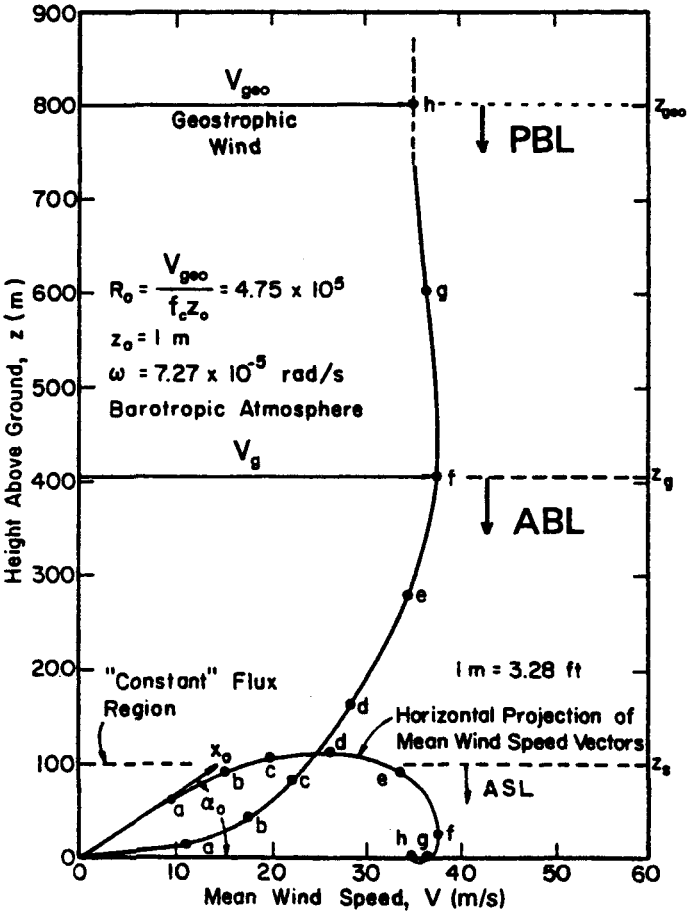

FIGURE C2.1. Planetary Boundary Layer Example According to Model of Lettau (1962).

a height z_s. Mean velocity profiles in the ASL are given by the well-established logarithmic distribution

$$V(z) = (u_*/\kappa)\ln(z/z_0) \tag{C2.2}$$

where κ, the von Kármán constant, is equal to 0.4, and z_0 is the aerodynamic surface-roughness length (the height where $V(z_0) = 0$). The friction velocity u_* is defined as $(\tau_0/\rho)^{1/2}$, where τ_0 is the mean surface shear stress and ρ is the density of air. Eq. (C2.2) is used to obtain values of u_* and z_0 for a particular location when measurements are made of V at several heights in the

TABLE C2.1. Aerodynamic Roughness Lengths for FUR Terrains.

Surface type	Roughness length (m) z_0
Sea, loose sand, and snow	~0.0002 (V-dependent)
Concrete, flat desert, tidal flat	0.0002–0.0005
Flat snow field	0.0001–0.0007
Rough ice field	0.001–0.012
Bare ground	0.001–0.004
Short grass and moss	0.008–0.03
Long grass and heather	0.02–0.06
Low mature agricultural crops	0.04–0.09
High mature crops (grain)	0.12–0.18
Continuous bushland	0.35–0.45
Pine forest	0.8–1.6
Dense low buildings (suburb)	0.4–0.7
Regularly built large town	0.7–1.5
Tropical forest	1.7–2.3

Source: adapted from Wieringa 1992.

ASL. Values of z_0 for a variety of surface types, according to Wieringa (1992), are given in Table C2.1. A long upstream fetch of uniform terrain roughness (typically 10 to 20 heights of interest) is needed to develop velocity profiles with these characteristics. Details on equilibrium boundary layer flows are provided by Wieringa (1993).

Various models of the vertical distribution of the mean velocity throughout the ABL have been put forward. Simplified models developed during the 1960s formed the basis for wind profiles given in current North American codes and standards and still provide acceptable results for most practical applications of wind engineering. However, it must be recognized that these simplified models are based mostly on data obtained near ground level, and there are indications that they may not be fully representative high above the ground surface. In particular there is evidence that they underestimate the true thickness of the ABL. Although this is not of consequence for the great majority of structures, which are confined to the lowest portion of the ABL, there can be some consequences for very tall structures extending into the higher regions of the ABL.

The following equation for vertical distributions of mean wind speed throughout the entire PBL, in the absence of thermal winds above the ABL, has been proposed by Harris and Deaves (1981):

$$\frac{V(z)}{u_*} = \frac{1}{\kappa}\left[\ln(z/z_0) + a_1(z/z_{geo}) + a_2(z/z_{geo})^2 + a_3(z/z_{geo})^3 + a_4(z/z_{geo})^4\right] \quad \text{(C2.3)}$$

where $a_1 = 5.75, a_2 = -1.875, a_3 = -1.33$, and $a_4 = 0.25$ are constants. Numerical models of the PBL by Estoque (1973) reveal that thermal winds can cause major variations of wind speed and direction above the ABL. Therefore, when the thermal wind and the geostrophic wind are in the same direction, Eq. (C2.3) will underestimate the wind speed.

A convenient empirical formulation often used for boundary layers in general (not just ABLs) is the "power law" proposed by Hellman (1916)

$$\frac{V(z)}{V(z_r)} = \left(\frac{z}{z_r}\right)^{1/\alpha} \tag{C2.4}$$

where z_r = a reference height. Applying Eq. (C2.4) to the ABL, Davenport (1960) chose z_r to be at the "top" of the boundary layer, which he called "gradient" height. Compared with present-day estimates of the true gradient height in strong winds the values given by Davenport tend to be low. Also they do not vary with wind speed as implied by more physically correct recent models. However, as discussed above, the "power law" type of model has the advantage of simplicity and is of sufficient accuracy for most wind-engineering applications. This type of model velocity profile may be written as

$$\frac{V(z)}{V(z_g)} = \left(\frac{z}{z_g}\right)^{1/\alpha} \tag{C2.5}$$

where z_g is the "gradient" height in the sense that it is the top of the assumed ABL and $1/\alpha$ is an empirical exponent. Tables of z_g, $1/\alpha$, and corresponding values of z_0, according to the Davenport model, are given in Table C2.2. Also tabulated are the terrain roughness categories implied by Exposures A, B, C, and D of ASCE 7-95. For wind-tunnel tests of most structures the power law with properties given in Table C2.2 gives adequate descriptions of the ABL. However, for very tall structures, of 300 m or higher, this simplified model of the ABL may not be adequate, and the simulated boundary layer should be made deeper to better represent the true ABL above 300 m.

Turbulence characteristics in the ABL for neutral FUR conditions strongly depend on the surface roughness. Turbulent flow velocities vary randomly in time and space; therefore, statistical descriptions are necessary. Statistics of primary interest for wind-engineering applications are the variances or the standard deviations σ_i, the power spectral densities S_i, and the integral scales ${}^jL_i$ for the ith velocity component and the jth coordinate direction.

Turbulence intensities $I_j(z) = \sigma_j(z)/V(z)$ in the ASL have been studied extensively by means of micrometeorological measurements—Kaimal et al. (1972), Busch (1973), and Panofsky and Dutton (1983). The turbulence intensities for neutral stability in the ASL can be expressed as

TABLE C2.2. ABL Characteristics

Class	Terrain Description	(z_0) (m)[a]	$(1/\alpha)$[b]	$I_u(\%)$[c]	Exposure[d]	z_g (m)[d]
1	Open sea, fetch at least 5 km	0.0002	0.10	9.2	D	215
2	Mud flats, snow; no vegetation, no obstacles	0.005	0.13	13.2		
3	Open flat terrain; grass, few isolated obstacles	0.03	0.15	17.2	C	275
4	Low crops; occasional large obstacles, $x'/h > 20$	0.10	0.18	21.7		
5	High crops; scattered obstacles, residential suburbs, $15 < x'/h < 20$	0.25	0.22	27.1	B	370
6	Parkland, bushes; numerous obstacles, $x'/h \sim 10$	0.5	0.29	33.4		
7	Regular large obstacle coverage (dense spacing of low buildings, forest)	1.0–2.0	0.33	43.4	A	460
8	City center with high- and low-rise buildings	≥ 2	0.40~ 0.67	—		

[a]Regional roughness lengths from Wieringa (1992).
[b]Power-law exponents from Davenport (1960).
[c]Turbulence intensities for FUR terrain ($z = 10$ m) according to (C2.6)
[d]Exposure categories and gradient heights from ASCE 7–95.

$$I_i = A_i/\ln(z/z_0) \tag{C2.6}$$

where $A_i = 0.4(\sigma_i/u_*) = 1.0$, 0.8, and 0.5 for $i = u$, v, and w, respectively. Values of I_u at $z = 10$ m are given in Table C2.2 for various terrain types. Harris and Deaves (1981) have proposed an estimation of σ_u/u_* throughout the entire PBL given by the following equation:

$$\sigma_u / u_* = 2.63(1-6f_c / u_*)[0.538+0.09\ln(z / z_o)]^{16(1-6f_c z/u_*)} \tag{C2.7}$$

The power spectral density for the longitudinal component (direction of mean velocity) of turbulence $S_u(z)$ has been investigated more thoroughly than for the other two components. This power spectral density is used extensively for analysis of along-wind building loads and motion (Simiu and Scanlan 1986). Widely used equations for power spectra were developed by von Kármán (1948) based on the theory of isotropic turbulence. Equations for the u and w components of turbulence are the following:

$$\frac{nS_u(z,n)}{\sigma_u^2} = \frac{4n^x L_u / V}{[1+70.8(n^x L_u / V)^2]^{5/6}} \tag{C2.8}$$

and

$$\frac{nS_w(z,n)}{\sigma_w^2} = \frac{4n^x L_w / V[1+755.2(n^x L_w / V)^2}{[1+283.1(n^x L_w / V)^2]^{11/6}} \tag{C2.9}$$

Based on Eqs. (C2.8) and (C2.9) and the theory of isotropic turbulence, Irwin (1979) has developed equations for the cross-spectra of u or w at two locations in terms of the separation distance.

Using a general nondimensional formulation of Olesen et al. (1984), Tieleman (1992a) developed spectral equations for u, v, and w over ideal and slightly perturbed FUR terrains. These equations for the longitudinal component u are as follows:

a. ideal FUR terrain—

$$\frac{nS_u(z,n)}{\sigma_u^2} = \frac{20.53f}{1+475.1f^{5/3}} \tag{C2.10}$$

b. perturbed FUR terrain—

$$\frac{nS_u(z,n)}{\sigma_u^2} = \frac{40.42f}{(1+60.62f)^{5/3}} \tag{C2.11}$$

where n is frequency in Hertz and f is the reduced frequency $nz/V(z)$. (Monin similarity parameter) Eq. (C2.10) is similar in form to the Kaimal et al. (1972) spectrum

$$\frac{nS_u(z,n)}{\sigma_u^2} = \frac{32.0f}{(1+50f)^{5/3}} \tag{C2.12}$$

when σ_u/u_* is set equal to its value of 2.5 in the ASL. Other forms for S_u are used extensively in wind-engineering practice. A spectrum proposed by Davenport (1961a), which does not provide for height dependence, is given by

$$\frac{nS(n)}{\sigma_u^2} = \frac{2}{3}\frac{x^2}{(1+x^2)^{4/3}} \tag{C2.13}$$

where $x = 1{,}200n/V(10)$ and $V(10)$ is the mean wind speed in m/s at $z = 10$ m. Eq. (C2.13) is used in the National Building Code of Canada, NBCC (1995). Extensive discussions of the basis for and the differences of the various power spectral density formulations are given by Simiu (1974), Simiu and Scanlan (1986), Tieleman (1992a and b) and Kaimal and Finnigan (1994).

Nine integral scales are defined by ${}^{j}L_i$; however, ${}^{x}L_u$ is a measure of the most energetic gust size used widely in wind-engineering practice. Other components of ${}^{j}L_i$ are significant, but ${}^{x}L_u$ has been the most accessible from the usual wind-speed measurements on instrumented towers. An estimate of ${}^{x}L_u$ in the ASL is given by the following equation:

$$ {}^{x}L_u = \frac{z}{2\pi f_m} \tag{C2.14} $$

where f_m is the reduced frequency for which $nS_u(n)$ is a maximum. The value of f_m for Eq. (C2.10), the ideal FUR terrain, is 0.032 and for Eq. (C2.11), the perturbed FUR terrain, f_m is 0.025. Analysis of various sets of atmospheric turbulence data by Counihan (1975) indicates that ${}^{x}L_u$ decreases with increasing surface roughness and that ${}^{y}L_u \cong 0.3\,{}^{x}L_u$ and ${}^{z}L_u \cong 0.5\,{}^{x}L_u$. Additional discussion on the dependence of ${}^{x}L_u$ on flow parameters is presented by Harris (1986).

C2.2.2 Non-FUR Terrain

Deviations of the flow from that described for a FUR terrain are caused by nonuniform surface roughness; low hills, patches of trees, and groups of buildings; and complex terrain. These non-FUR features and their effects on the ASL are discussed by Tieleman (1992b).

Only three of the simplest non-FUR features are characterized in building codes and data sets. These are a step change of surface roughness over flat terrain, a two-dimensional elevation change (escarpment or cliff), and a three-dimensional axisymmetrical isolated hill on flat terrain. Flow characteristics for more complicated terrain features, particularly for complex terrain, are usually determined for specific sites by wind-tunnel modeling (Britter 1982 and Cermak 1984). Design guidance for non-FUR terrains has been provided by Cook (1985, 1990).

Flow characteristics for a step change of surface roughness are given by ESDU (1993a). For this case an internal boundary layer develops downwind of the roughness change. The depth of this internal surface layer increases at an approximate rate of 1 m per 100 m and the transition layer between the upwind ASL and the internal ASL grows at an approximate rate of 1 m per 10 m. This results in slope discontinuities (kinks) for the downwind mean velocity profile.

Wind speeds are increased at hilltops and at the upper level of escarpments for flow approaching from the lower level. Speed-up factors developed by wind-tunnel modeling are reported by Lemelin, Surry and Davenport (1988). Mean wind speeds for a variety of topographic configurations, including irregular hill shapes, multiple hills, and valleys, are presented in ESDU (1993b). Topographic wind-speed factors for flow over isolated two-dimensional ridges, two-dimensional escarpments, and an axisymmetrical hill are given in ASCE 7-95.

C2.2.3 Non-Boundary Layer Atmospheric Flows

So far the presented material dealt primarily with the flow properties of the neutral ABL, conditions which usually occur on extremely windy days when a thick cloud cover is present. Non-neutral thermal conditions prevail during extreme wind storms, including thunderstorms, downbursts, tornadoes, and hurricane eye walls. These non-boundary layer flows are often the most hazardous and destructive storms for which at the present time basic understanding is lacking. Knowledge of the flow structure (mean and turbulence) of these storms near the earth's surface is limited to a few scant observations (Golden and Snow 1991). The height variation of these non-boundary layer storms will certainly affect the high-rise class of buildings and structures, but is less of a problem for low-rise structures. However, few data are available for the variation of the mean flow and turbulence structure with height. Statistical analysis of a limited amount of hurricane wind-speed data (anemometer heights 6.7 and 10 m) has led to the conclusion that peak gusts are larger than those observed in extratropical storms (Krayer and Marshall 1992). These results indicate that convective flow processes for hurricanes are sufficiently significant to lead to increased spectral densities at intermediate frequencies ($n \cong 0.5$ Hz) and therefore lead to increased turbulence intensities.

The jet stream circles the earth in a meandering pattern and is responsible for the formation and sustenance of extratropical cyclones. These cyclones are cold-core systems which are driven by tight isobars (high pressure gradients) and do not lose their intensity as far up as the altitude of the jet stream. The boundary layer winds created by these systems generally fall into the near-neutral category. On the contrary, hurricanes develop over warm ocean water and derive their energy from the latent heat release because of condensation of water vapor. The temperature at the center of the hurricane is higher than that of the surrounding regions. Consequently these storms are limited in height, as the influx of colder upper air weakens the intensity of the hurricanes aloft. Similarly, the mean wind and turbulence structure of tornadoes, downbursts, and microbursts vary with height in a way that is different from the neutral ABL wind model. Additional details of these meteorological events are presented in Chapter 10.

The effects of hurricane winds on buildings and structures can be satisfactorily studied by assuming that their flow structure is similar to that of ABL winds, albeit with mean velocity profiles taken to correspond to a somewhat more open terrain and increased turbulence intensities, particularly at greater heights above ground. No adequate experimental techniques are currently available to simulate the effects of severe thunderstorms, downbursts, and tornadoes.

C2.3 MODELING CRITERIA

Wind-tunnel simulation of ABL flow with neutral thermal stability requires dynamic similarity (equality of both the Reynolds number and the Rossby number), kinematic similarity of the incident flow, and geometric similarity of model and flow (Cermak 1975). However, similarity in an "exact" sense is not possible. Consequently, compromises must be made which, based on comparisons of model/full-scale data, have proven to be acceptable for wind-engineering applications.

C2.3.1 Dynamic and Kinematic Similarity

In general, wind tunnels are not equipped to model the turning of the mean wind direction with height by Coriolis forces as shown in Figure C2.1. Fortunately, this effect is negligibly small below about 300 m, which includes most engineering structures. Furthermore, excluding this effect is conservative in most wind-loading situations.

For most modeling applications of structures immersed in the ABL, an exact equality of the mean flow Reynolds number cannot be achieved. Fortunately, the equality of model and full-scale Reynolds number, based on the mean wind speed and a characteristic dimension of the structure L_b, is not necessary for sharp-edged structures, provided that the model Reynolds number $L_b V_h/v$ is not less than 10,000. Furthermore, Reynolds number equality for model and prototype mean velocity and turbulence of the approach flow cannot be satisfied. However, Reynolds number independence of these flow characteristics can be realized in long test-section wind tunnels for sufficiently rough surfaces; i.e., $u_* z_0/\nu > 2.5$. Figure C2.2 illustrates the fetch Reynolds number required to achieve Reynolds number independence when the test section entrance configuration includes only a simple sawtooth turbulence trip. When entrance configurations include devices such as spires or vortex generators, the effective fetch length is increased. In Figure C2.2, K_s is the equivalent sand roughness diameter taken as $K_s = 30\, z_0$.

Wind-tunnel simulations of thermally stratified ABLs require that additional similarity criteria be satisfied. The primary additional dimensionless

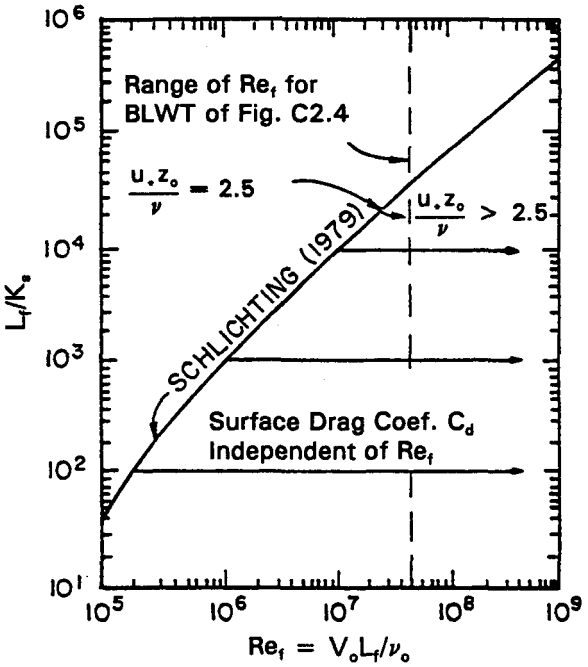

FIGURE C2.2. Reynolds Number Independence for Local Surface Shear Stress

Source: Cermak 1975; reprinted with permission, American Society of Mechanical Engineers.

parameter for a monotonic temperature variation with height is a bulk Richardson number of the following form:

$$Ri = (\Delta T_0/T_0)(L_0 g/V_0^2) \tag{C2.15}$$

where the subscript 0 indicates a reference value. If an elevated inversion exists, the height ratio z_{inv}/z_r should be made equal for model and prototype. These similarity criteria are of paramount importance when modeling dispersion in the atmospheric surface layer and are discussed further in Chapter C7.

C2.3.2 Geometric Similarity

Criteria for geometric similarity and the scaling of the neutral ABL flow are expressed as the ratios of three characteristic lengths of the flow (z_0, z_g, and ${}^xL_u$) and a representative building dimension L_b as follows: L_b/z_0, L_b/z_g, and $L_b/{}^xL_u$. When only the ASL is modeled for low-rise building investiga-

tions, the ratio L_b/z_g is replaced by L_b/z_s. For geometric similarity, each of the length ratios should be equal for the model and the prototype.

Parameters of the BLWT mean velocity profile presented in Figure C2.10(b) for which $z_0 = 0.35$ cm, $z_g = 100$ cm and $1/\alpha = 0.33$ together with parameters for Exposure A in Table C2.2 ($0.5 < z_0 < 2.0$ m, $z_g = 460$ m and $1/\alpha = 0.33$) determine the length scale for the modeled ABL. For this example, the similarity criteria result in the following equalities:

$$\frac{(L_b)_m}{(L_b)_p} = \frac{(z_g)_m}{(z_g)_p} = \frac{1}{460} \tag{C2.16}$$

and, with a reasonable value for $(z_0)_p$ of 1.5 m,

$$\frac{(L_b)_m}{(L_b)_p} = \frac{(z_0)_m}{(z_0)_p} = \frac{0.0035}{1.5} = \frac{1}{429} \tag{C2.17}$$

The foregoing result indicates that scaling of the large-scale motion (based on z_g) and the small-scale motion (based on z_0) are approximately equal when the power-law exponent is the same for both flows. This is true provided the wind-tunnel flow is fully developed and is in equilibrium with the surface roughness and the power spectral density $S_u(n,z)$ contains a substantial range of reduced frequencies in the inertial subrange, as seen in Figure C2.13. Furthermore the ratio of integral scales $({}^xL_u)_m/({}^xL_u)_p$ should be equal to $(L_b)_m/(L_b)_p$ or approximately 1/450. The value of $({}^xL_u)_m$, determined from the spectra shown in Figure C2.13 at $z = 5$ cm, is 0.20 m. Accordingly, the value of $({}^xL_u)_p$ would be 90 m at $z = 22.5$ m, if the modeled ABL properly simulates the Exposure A boundary layer. An estimate of ${}^xL_u$ for the prototype with $z_0 \cong 1.5$ m, using information given in ESDU (1991), results in a value of about 100 m. This is in reasonable agreement with the scaled value of 90 m.

C2.3.3 Modeling of Flow Over Complex Topography

Meteorological data for flow over complex topography reveal that mean velocity distributions and turbulence statistics (variances, integral scales, and spectra) are significantly different from those for flow over FUR terrain with the same surface roughness (Panofsky and Dutton 1983). Small-scale regional topographic models are helpful in providing wind data at sites located in or downwind from complex topography. Examination of time series of wind direction in flow over complex terrain show 50 to 100° variations in short time spans of about 1 second (Tieleman 1992b). Although walls of a BLWT tend to restrict lateral direction fluctuations, local flow character-

istics measured over topographic models with geometric scales in the range 1:1000 to 1:5000 compare well with corresponding field measurements for neutral thermal conditions (Cermak 1984). Studies by Meroney (1980) of flow over the Rakaia Gorge region of New Zealand, using a 1:5000 scale model, gave wind speed and direction data that were in good agreement with field measurements.

C2.4 BOUNDARY LAYER WIND TUNNELS (BLWTS) FOR MODELING THE WIND

For wind-engineering applications, the gradient wind speed V_g is usually taken to be the mean wind speed at a height z_g, where effects of the surface shear stress become negligible. At this height, V becomes a maximum and remains constant with increasing height Figure C2.1 shows the location of V_g at height z_g in an example ABL calculated using the model of Lettau (1962) for a specific roughness length z_0, latitude ϕ, and geostrophic wind speed V_{geo}. The ASL in the region $0 < z \leq z_s$ is also shown in Figure C2.1. Heights of "high-rise" buildings and structures are greater than z_s but usually less than z_g, while the heights of "low-rise" buildings and structures are less than z_s. The function of BLWTs is to model mean flow and turbulence properties of the ABL and ASL that are essential for modeling wind effects on buildings and structures.

C2.4.1 Characteristics of BLWTs

Basic features of a BLWT test section are illustrated by Figure C2.3 for flow without thermal stratification. Detailed discussions of the features summarized in the following paragraph are available in the wind-engineering literature (Davenport and Isyumov 1967; Cermak 1975; Cermak 1981).

The key feature of a BLWT is the test section length L. Fully developed boundary layers with scaled gradient heights z_g from 0.5 to 1.5 m are required for modeling of wind effects on high-rise building models in the common scale range 1:200 to 1:600. This requires that L be in the range of 15

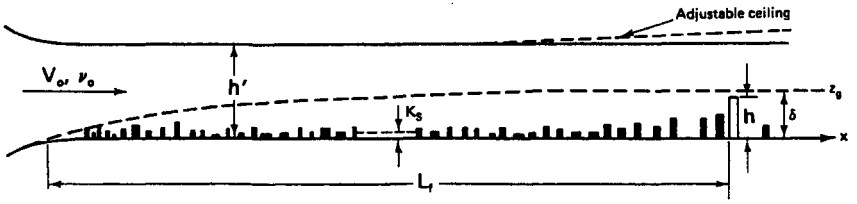

FIGURE C2.3. Definition of BLWT Test Section.

to 30 m when no boundary-layer augmentation devices are placed at the test-section entrance as discussed in Section C2.4.3 (Cermak 1958). Test-section lengths of about 15 m can develop satisfactory boundary layers when augmentation devices are installed. This is particularly true when the building under study is surrounded by other buildings that modify the approach flow by their wakes. The height and width of the test section are commonly in the range of 2 to 4 m. Flow resistance of the rough upwind fetch and model is substantial; therefore, height adjustment of the test-section ceiling is necessary to obtain a longitudinal pressure gradient $\partial p/\partial x$ equal to the desired value of zero. Wind speeds V_g required for a BLWT intended only for studies of wind pressures and overall wind loads on buildings and structures are modest compared to requirements for an aeronautical wind tunnel. A satisfactory range for V_g is 10 to 50 m/s. Acoustical noise in the test section caused by the fan, standing waves, and structural vibrations should have an rms value that does not exceed 3 to 5% of the wind-induced rms pressure fluctuations on a wind tunnel model. For investigations of air-pollutant dispersion, particularly in thermally stratified boundary layers, values of V_g as low as 0.5 m/s may be required to achieve Richardson number equality.

C2.4.2 Types of BLWTs

Two basic types of BLWTs are in common use. These are designated according to their configuration as a closed-circuit type or an open-circuit type.

An example of a closed-circuit BLWT is shown in Figure C2.4 (Cermak 1958, 1981). Width of the 27.4-m long test section increases uniformly with distance from the entrance (1.83 to 2.06 m). This design supplements pressure-gradient control provided by ceiling-height adjustment that can increase the height from 1.83 to 2.30 m. A heat-exchanger in the flow-return section provides the capability for maintaining constant air temperature during tests. This heat exchanger in combination with heating and/or cooling of the test-section floor enables modeling of a wide variety of thermally stratified flows. This capability is not required for the investigations of wind pressures and loads on buildings during strong winds, but is important for investigations of air-pollutant dispersion (see Chapter C7).

Open-circuit BLWTs, such as that shown in Figure C2.5, have been constructed in several laboratories. The 3.66-m wide and 2.13-m high test section permits larger and more extensive models to be studied without excessive blockage. An extensive list of BLWTs in various countries is given in a book on low-speed wind-tunnel testing by Rae and Pope (1984). Marshall (1984) gives an extensive review of BLWTs that have been constructed in Japan for wind-engineering applications. During the last decade large BLWTs have been constructed at The University of Western Ontario, Can-

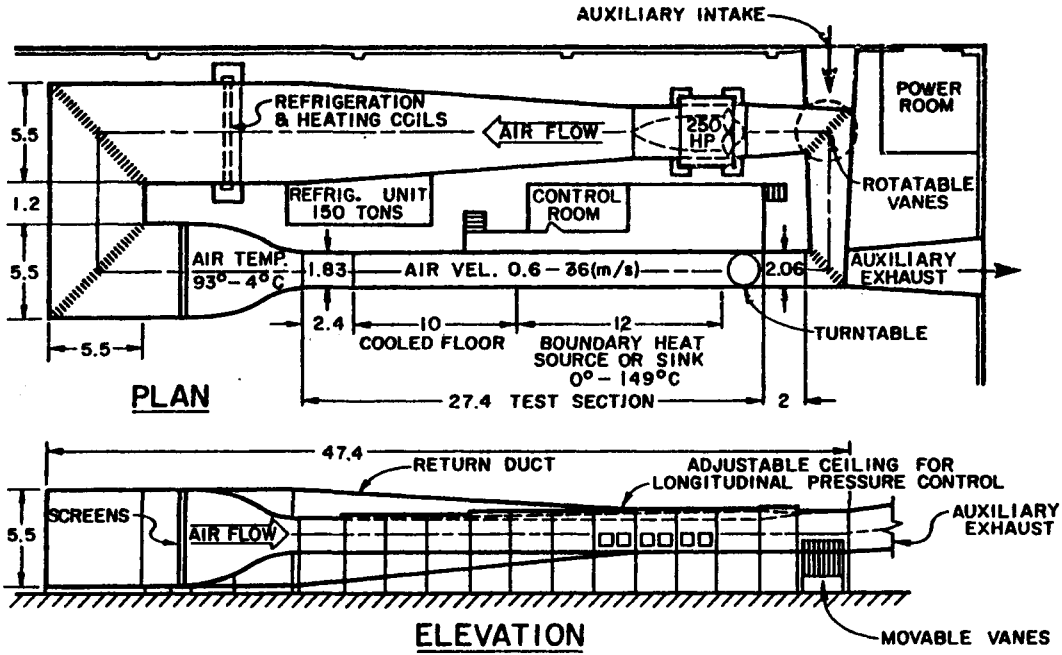

FIGURE C2.4. Example of a Closed-Circuit BLWT with Thermal Controls—Colorado State University Meteorological Wind Tunnel (MWT).

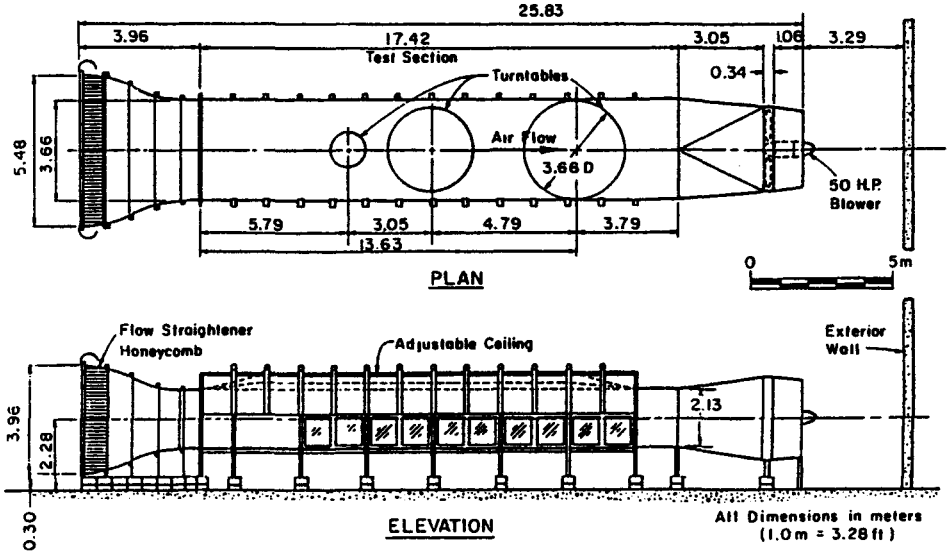

FIGURE C2.5. Example of an Open-Circuit BLWT—Colorado State University.

ada (Davenport et al. 1985); the Public Works Research Institute, Japan; Monash University, Australia; and the Danish Maritime Institute, Denmark (Cermak, 1995). Other BLWTs have recently been constructed at the University of Minnesota, Clemson University, and The University of Notre Dame.

Properly modeled boundary layers should satisfy the requirement of Reynolds number independence. Figure C2.2 gives the Reynolds number for which the surface drag coefficient, and consequently the local flow characteristics, become independent of Reynolds number for a given relative roughness (Cermak 1975). The Reynolds number independence curve of Figure C2.2 applies to flow with neutral thermal stratification, uniform roughness, and no boundary-layer augmentation devices at the test-section entrance.

A typical installation of upwind roughness, test-section entrance configuration, city (proximity) model, and new building model prepared for pressure and pedestrian-level wind measurements is shown in Figure C2.6. In this example, the upwind roughness represents a FUR terrain. The roughness elements are selected to develop a power-law exponent $1/a$ selected following an examination of the terrain surrounding the building site, with guidance from Table C2.2. For most sites the terrain characteristics are different for wind approaching from different wind directions. Therefore, the roughness shown in Figure C2.6 may require changes when modeling wind

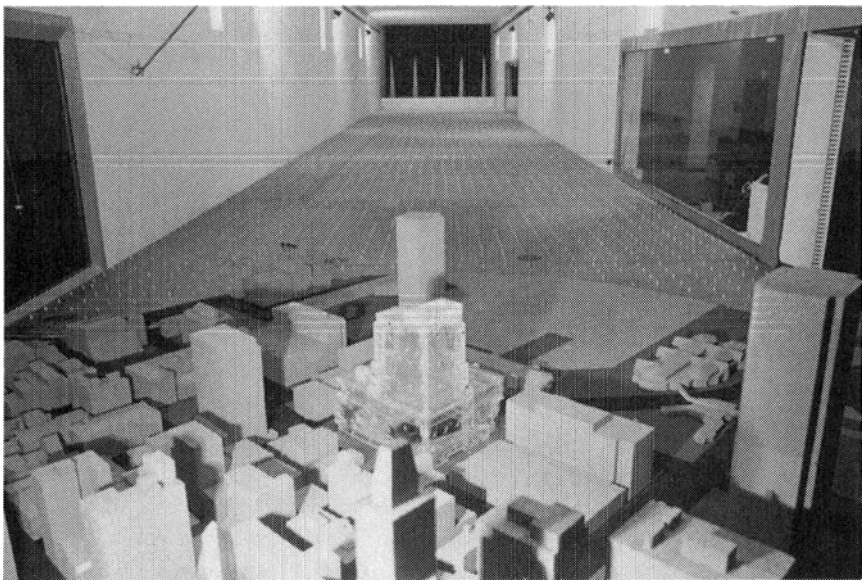

FIGURE C2.6. Test Section (3 × 2.5 × 21 m) with Roughness Elements and z_g Augmentation Devices to Model Approach Wind over FUR Terrain for Pressure Test of a 1:300 Scale Building Model.

from other directions. To facilitate these changes, roughness elements can be designed for computer-programmed height adjustment as the turntable is rotated (Davenport et al. 1985). For some directions wind over non-FUR terrain may need to be modeled. In such cases, modeled topographic features, buildings and/or nonuniform roughness would be required upwind of the city model. Devices for increasing the gradient height z_g are shown at the test-section entrance in Figure C2.6. These devices result in z_g being increased to 1.2 m at the upwind edge of the model city. Details of the boundary-layer thickening devices are presented in Section C2.4.3.

C2.4.3 Augmentation of Boundary-Layer Height z_g

Two types of devices, other than fence-like trips, used to increase the boundary-layer height z_g are a vortex-generator array (Counihan 1969) and a spire array (Standen 1972). Flow characteristics for these devices and several different lengths of upwind surface roughness have been reported by Cook (1978). A modified shape of the Standen spire, a simple triangle, has been studied by Irwin (1981a). Irwin presents equations for design of spire-roughness combinations, required for a desired value of z_g. An array of vortex generators and an array of spires are shown in Figures C2.7 and C2.8, respectively, as installed in the BLWT of Figure C2.4. These devices affect boundary-layer characteristics as flow proceeds through the test section. Effects of these devices are determined by comparing flow characteristics when augmentation devices are installed with flow developed "naturally" with only an initial sawtooth-roughness turbulence trip in place as described by Figure C2.9 (Cermak 1982).

For illustrative purposes flow comparisons are presented at two distances downwind from the test-section entrance, $x = 6.10$ m and $x = 18.3$ m, for a uniformly rough boundary with $z_0 = 0.35$ cm. Figures C2.10, C2.11, and C2.12 show vertical profiles of mean velocity, longitudinal turbulence intensity, and turbulent shear stress, respectively. The following observations are of significance for evaluating performance of boundary-layer augmentation devices:

1. boundary-layer characteristics with the devices deviate substantially from the "naturally" developed boundary layer at $x = 6.10$ m;
2. characteristics of the augmented boundary layer and the "natural" boundary layer are in good agreement at $x = 18.29$ m; and
3. the devices increase z_g by approximately 33% at $x = 18.29$ m.

Irwin (1981) suggests that spires should be about 6 or more the spire heights upwind of the model in order to achieve a boundary layer in equilibrium with the surface roughness.

Spectra of the longitudinal component of turbulence for the three entrance configurations are given in Figure C2.13. The spectra are measured

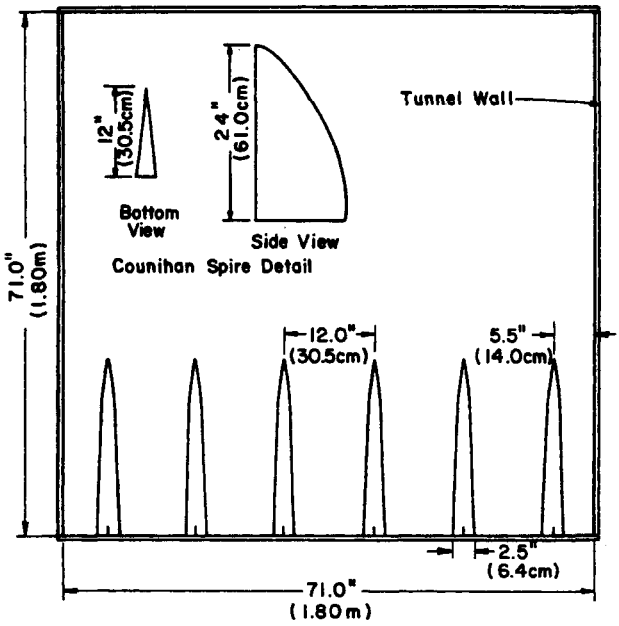

FIGURE C2.7. Vortex-Generator Array for Augmentation of z_g.

Source: Reprinted from J. Counihan (1969), "An Improved Method of Simulating an Atmospheric Boundary Layer in a Wind Tunnel," *Atmospheric Environment*, 3, 197–214, with permission from Elsevier Science.

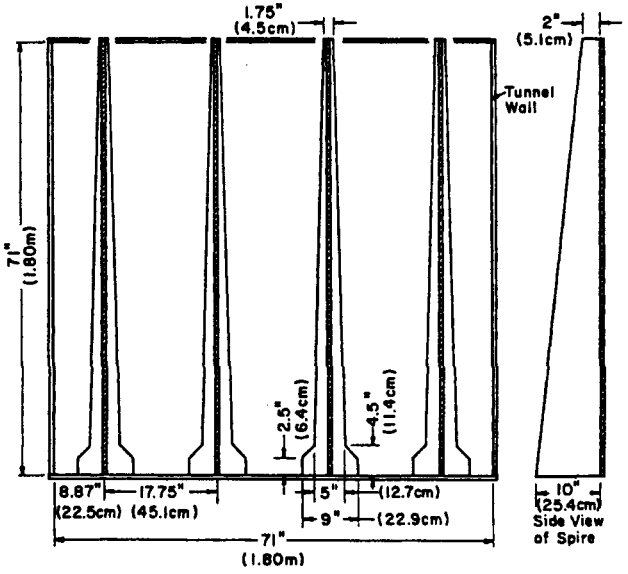

FIGURE C2.8. Spire Array for Augmentation of z_g *(Standen 1972).*

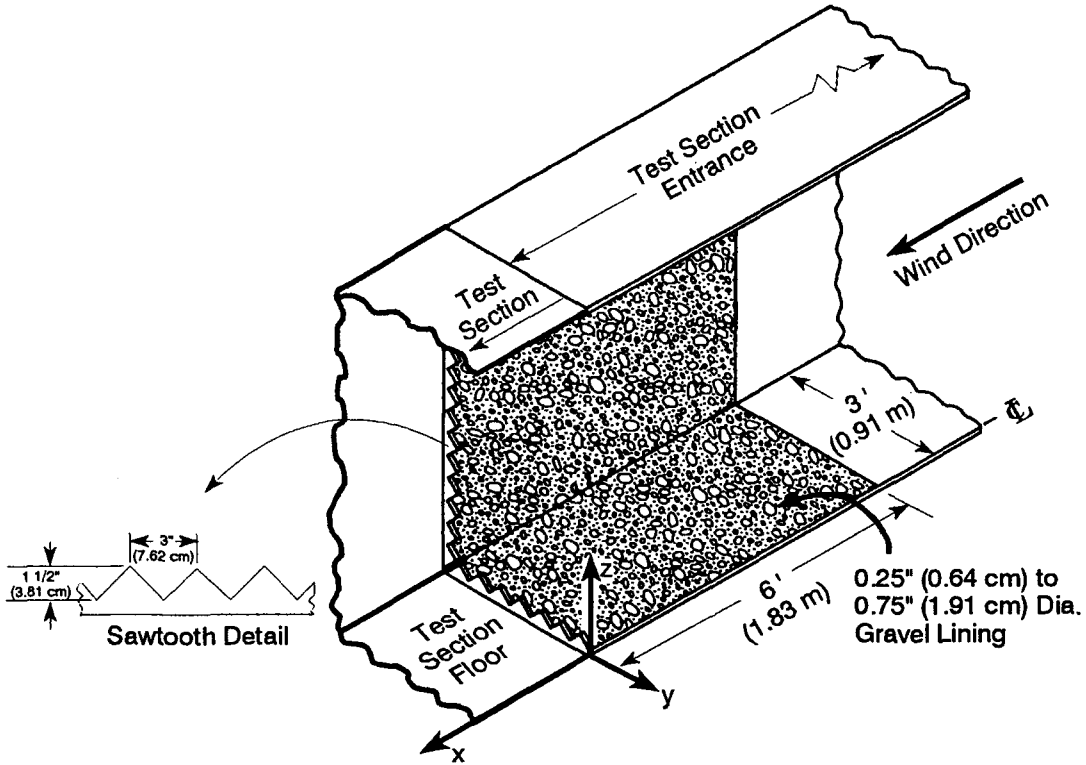

FIGURE C2.9. Sawtooth-Roughness Boundary-Layer Trip at Entrance to Test Section of BLWT in Figure C2.4.

Source: Cermak 1982; reprinted with permission of Cambridge University Press.

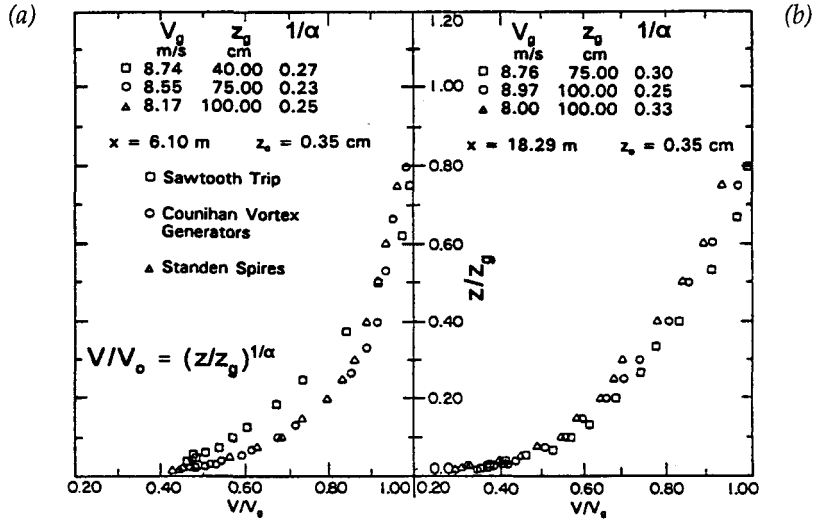

FIGURE C2.10. Mean Velocity Profiles at (a) x = 6.10 m and (b) x = 18.29 m for Test-Section Entrance Configurations Defined by Figures C2.7, C2.8, and C2.9.

Source: Cermak 1982; reprinted with permission of Cambridge University Press.

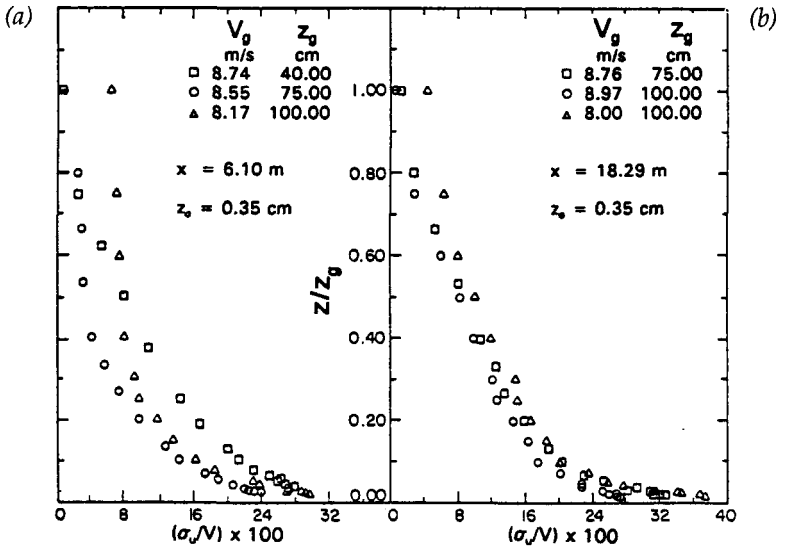

FIGURE C2.11. Longitudinal Turbulence Intensity Profiles at (a) x = 6.10 m and (b) x = 18.29 m for Test-Section Entrance Configurations Defined by Figures C2.7, C2.8, and C2.9.

Source: Cermak 1982; reprinted with permission of Cambridge University Press.

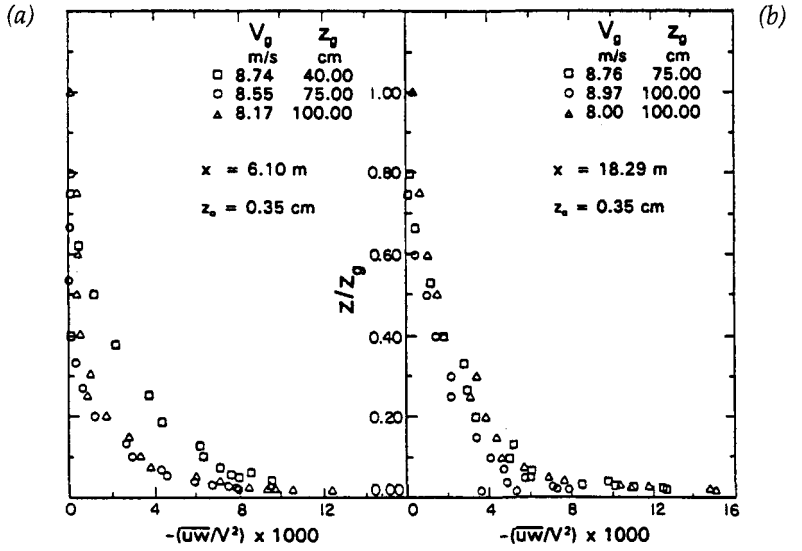

FIGURE C2.12. Turbulent Shear (Unit Mass Density) Profiles for (a) x = 6.10 m and (b) x = 18.29 m for Test-Section Entrance Configurations Defined by Figures C2.7, C2.8, and C2.9.

Source: Cermak 1982; reprinted with permission of Cambridge University Press.

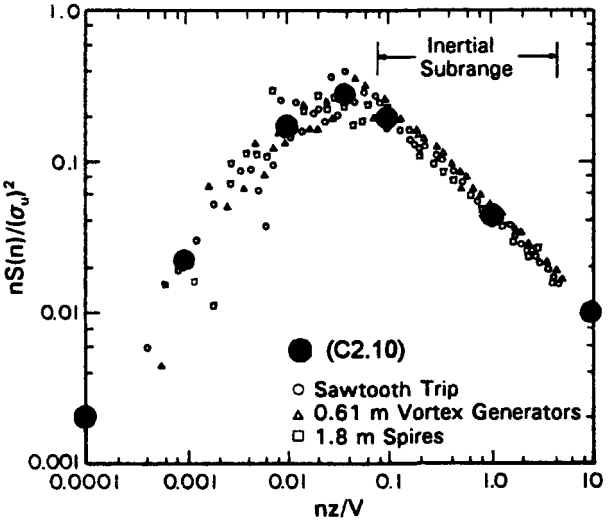

FIGURE C2.13. Spectrum of Longitudinal Turbulence: x = 18.29 m, z_o = 0.35 cm, V_g = 18 m/s, and z/z_g = 0.05. Spectrum given by (C2.10) is Indicated by Circles.

Source: Cermak 1982; reprinted with permission of Cambridge University Press.

at a height z equal to 0.05 z_g over the rough boundary (z_0 = 0.35 cm) at x equal to 18.29 m. The spectrum has over two decades of the reduced frequency nz/V in the inertial subrange. The entire spectrum of the modeled ABL is in excellent agreement with the atmospheric spectrum, as given by (C2.10) for neutral flow over FUR terrain.

C2.4.4 Augmentation of ASL Height z_s

Low-rise buildings are submerged in the ASL, as shown in Figure C2.1. A property of the ASL is approximate constancy of turbulent flux of heat and momentum as illustrated by the turbulent shear stress profiles for neutral flow given in Figure C2.14 measured over FUR terrain in a field study (Izumi 1971). This layer is only about 5 to 15% of z_g for boundary layers formed without augmentation devices over moderately rough surfaces; therefore, partial modeling of the ABL is desirable in which z_s is magnified and the upper region of the ABL is not modeled. Cook (1973) reported flow characteristics for the lower third of the ABL developed by insertion of the turbulence generation devices consisting of a grid, a fence, and an equivalent urban roughness. Augmentation of the ASL can be accomplished by the flow-conditioning system illustrated in Figure C2.15 (Cermak et al. 1993) which was developed to model the ASL at the Texas Tech University (TTU) field site (Chok 1988). The field site includes an experimental building (9.1 × 13.7 × 4.0 m) mounted on circular rails to permit rotation and an instrumented 50-m meteorological tower surrounded by near FUR terrain. The

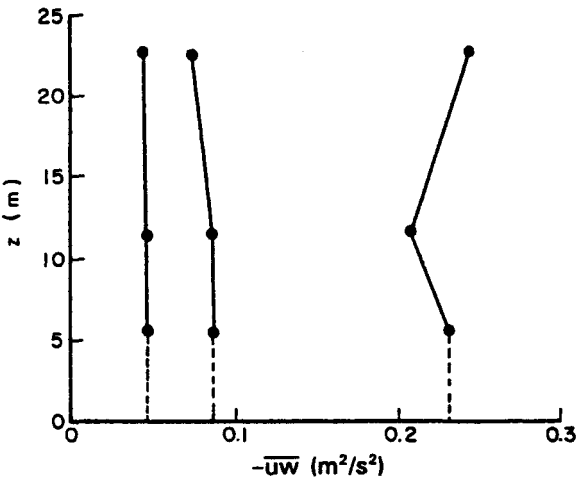

FIGURE C2.14. Shear Stress (Unit Mass Density) Profiles Measured in ASL for Near Neutral Flow during the 1968 Kansas Field Program.

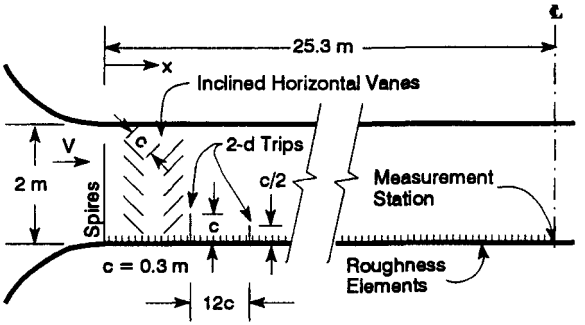

FIGURE C2.15. Flow-Conditioning System for Augmentation of ASL Height in BLWT of Figure C2.4.

Source: Reprinted from J.E. Cermak, L.S. Cochran, and R.D. Leffler (1993), "Wind Tunnel Modeling of the Atmospheric Surface Layer," *J. Wind Eng. & Ind. Aerodynamics*, 54/55, 505–513, with permission from Elsevier Science; Cochran 1992.

vertical distribution of shear stress at $x = 25.3$ m for the augmentation system (Figure C2.15) is shown by Figure C2.16 to be "constant." Accordingly, the value of z_s is increased to about 0.5 m. The shear-stress distribution varies with x and about 25 m are required to develop a constant vertical distribution. A length scale of 1:50 is used to relate wind-tunnel heights to measurement heights. This scaling is consistent with the similarity criterion of Jensen (1958).

$$\frac{(L_b)_m}{(L_b)_p} = \frac{(z_0)_m}{(z_0)_p} \tag{C2.18}$$

For these flows $(z_0)_m \cong 0.3$ cm and the average $(z_0)_p \cong 13.7$ cm. Therefore,

$$\frac{(L_b)_m}{(L_b)_p} \cong \frac{0.3}{13.7} \cong \frac{1}{46} \tag{C2.19}$$

Comparisons of mean velocity and turbulence intensity profiles for the wind-tunnel (configuration given by Figure C2.15) and full-scale TTU field site (Chok 1988) are presented in Figures C2.17 and C2.18. These data indicate that augmentation of the ASL height can be accomplished while maintaining satisfactory similarity of the mean flow and turbulence distributions.

Further validation of correct modeling of turbulence is provided by comparison of longitudinal turbulence spectra in the wind tunnel (Figure C2.15) and in the field (Thomas et al. 1993). These are shown in Figure C2.19. Spectra for both the modeled and field ASL are in good agreement, except at

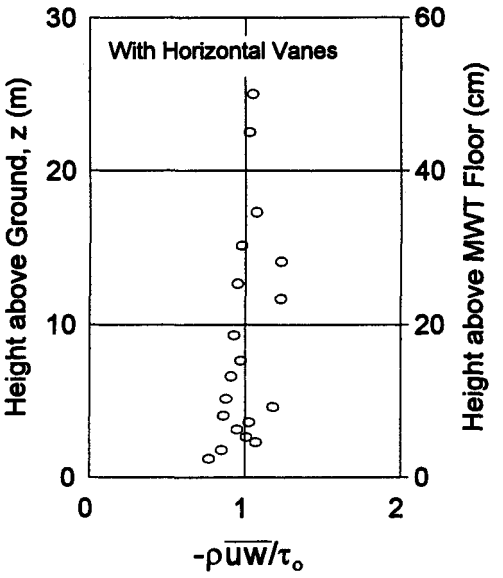

FIGURE C2.16. Vertical Profiles of Shear Stress at x = 18.29 m with Flow-Conditioning System Shown in Figure C2.15.

Source: Reprinted from J.E. Cermak, L.S. Cochran, and R.D. Leffler (1993), "Wind Tunnel Modeling of the Atmospheric Surface Layer," *J. Wind Eng. & Ind. Aerodynamics*, 54/55, 505–513, with permission from Elsevier Science.

high reduced frequencies, where slow response of the field instrumentation (UVW propeller anemometers) results in spectral values that are too low. Exploratory measurements with a sonic anemometer (Sarkar 1996) are in excellent agreement with the wind-tunnel spectrum. The longitudinal turbulence spectrum given by Eq. (C2.11) is shown in Figure C2.19. Agreement of the spectrum for the modeled ASL and Eq. (C2.11) for the universal velocity spectrum is excellent. The integral scales of longitudinal turbulence ${}^{x}L_{u}(z)$ for the wind-tunnel (Figure C2.15) and field (Chok 1988) are presented in Figure C2.20. Modeling of this integral scale is correct up to about 25 m and becomes deficient at higher elevations. For modeling of wind effects on low-rise buildings this is considered not to be a significant deficiency.

C2.5 WIND SIMULATIONS IN SHORT TEST SECTION WIND TUNNELS

Wind tunnels having long test sections of 15 to 30 m, described in Section C2.4, are classified as BLWTs. If the test-section length is less than about 15 m, the facility is classified as a short test-section wind tunnel.

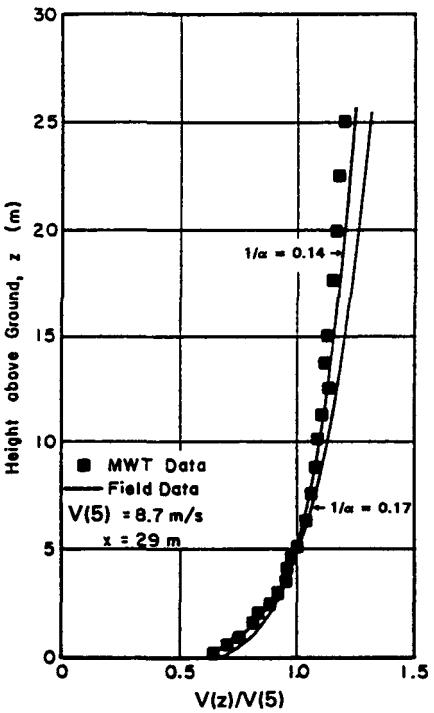

FIGURE C2.17. Vertical Profiles of Mean Velocity in MWT with Augmentation System of Figure C2.15 and Texas Tech Field Site Data.

Source: Reprinted from J.E. Cermak, L.S. Cochran, and R.D. Leffler (1993), "Wind Tunnel Modeling of the Atmospheric Surface Layer," *J. Wind Eng. & Ind. Aerodynamics*, 54/55, 505–513, with permission from Elsevier Science; Chok 1988.

The minimum requirements for the simulation of neutral ABLs stated in Section C2.3 can be achieved with acceptable approximation in a short test-section by insertion of various flow-conditioning devices at the test-section entrance. Commonly used devices are vortex generators (Figure C2.7), spires (Figure C2.8), and floor-mounted fences that can be seen in Figure C2.6. Flow generated over a rough boundary ($z_0 = 0.35$ cm) of 6.10 m length, with entrance vortex generators and with spires, are described by vertical profiles of mean velocity (Figure C2.10a), turbulence intensity (Figure C2.11a), and turbulent shear stress (Figure C2.12a). In this situation, the flow characteristics at 6.10 m do differ somewhat from those of the fully developed flow at 18.29 m. Nevertheless, the boundary-layer has a desirable depth z_g of about 1 m. For tests on a building surrounded by nearby buildings that perturb the approach flow by their wakes, the approach flow at 6.10 m would be acceptable. In summary, short test-section wind tunnels

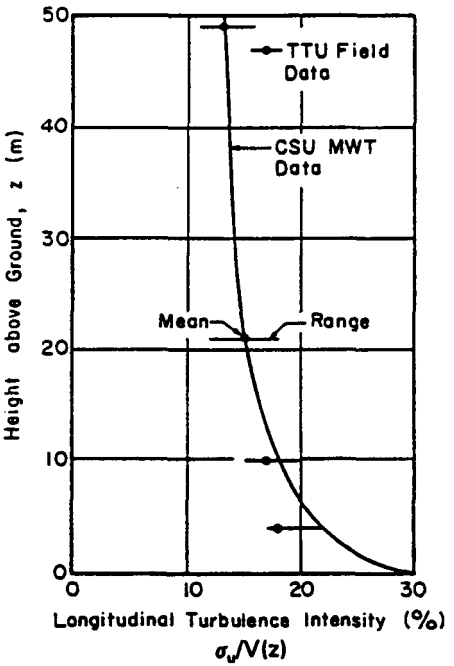

FIGURE C2.18. Vertical Profiles of Longitudinal Turbulence Intensity in MWT with Augmentation System of Figure C2.15 and Texas Tech Field Site Data.

Source: Reprinted from J.E. Cermak, L.S. Cochran, and R.D. Leffler (1993), "Wind Tunnel Modeling of the Atmospheric Surface Layer," *J. Wind Eng. & Ind. Aerodynamics*, 54/55, 505–513, with permission from Elsevier Science; Cochran, 1992; Chok 1988.

can provide acceptable approximations of the ABL for studies of the effects of wind on buildings and structures.

Short test-section wind tunnels can also be used effectively for section-model tests of long-span bridges (see Section C6.8.4) or masts, towers, antennae, and other high-aspect ratio structures. Flow for these tests is usually uniform nonturbulent (smooth) flow. For tests in turbulent flow turbulence can be developed by spanning the test-section entrance with a stationary grid or by an active generator such as an array of oscillating airfoils (Bienkiewicz et al. 1983).

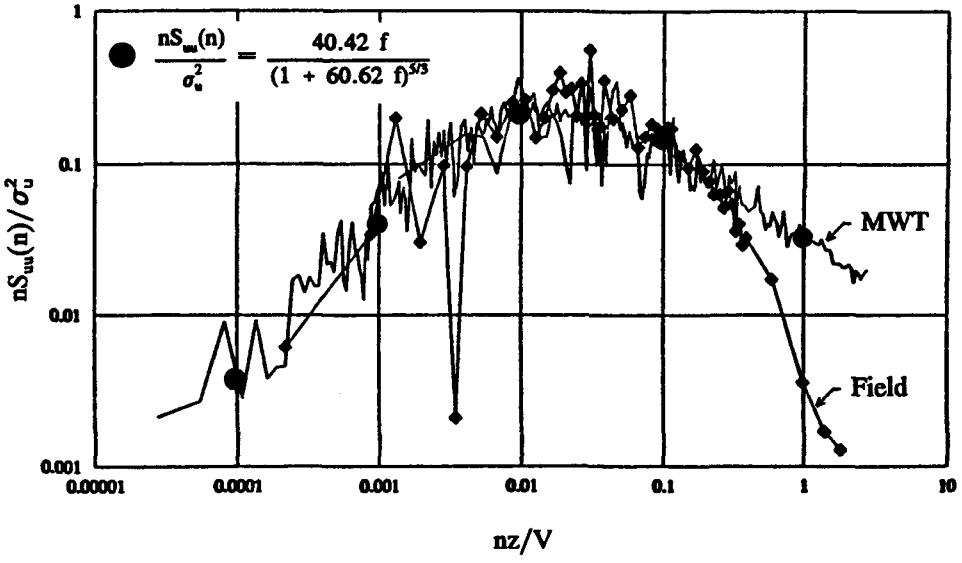

FIGURE C2.19. Longitudinal Turbulence Spectra at Roof Height (4 m) of TTU Building and in the MWT. Spectrum Given by Eq. (C2.11) Is Indicated by Circles.

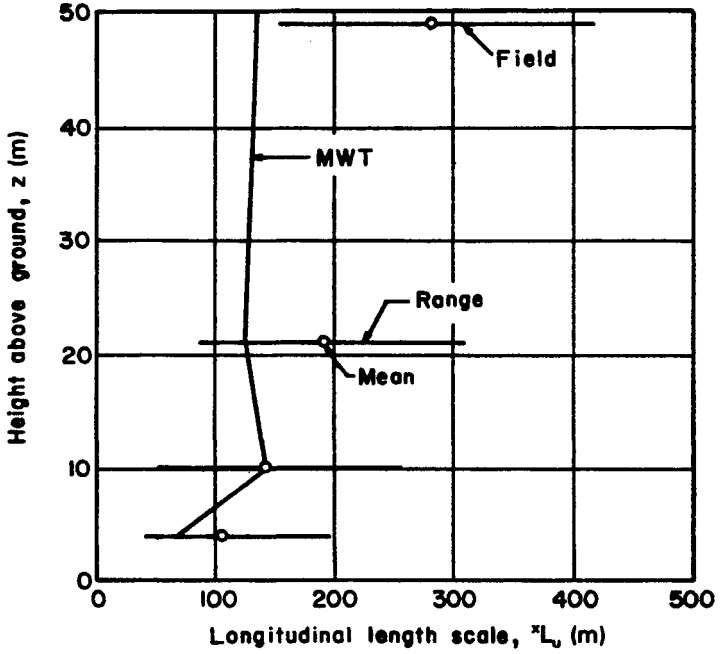

FIGURE C2.20. Comparison of Integral Scale for Longitudinal Turbulence in the MWT and Field.

Source: Reprinted from J.E. Cermak, L.S. Cochran, and R.D. Leffler (1993), "Wind Tunnel Modeling of the Atmospheric Surface Layer," *J. Wind Eng. & Ind. Aerodynamics*, 54/55, 505–513, with permission from Elsevier Science; Chok 1988.

This page intentionally left blank

Chapter C3
PEDESTRIAN LEVEL WINDS

C3.1 INTRODUCTION

In the introduction to Chapter 1 of this Manual, it was noted that "candidates for wind tunnel tests are buildings and structures that have unusual sensitivity to the action of wind or that fall outside existing experience." In the case of pedestrian level winds (PLWs), even ordinary buildings can experience problems and need to be tested. Some cities (Boston, Toronto, New York, San Francisco, for instance) now require such tests depending on building height or other factors (Durgin 1985, 1989). The determination of when wind tunnel tests may be called for in cases where they are not required by local ordinance can be made by a person experienced in PLWs and/or using some of the computational techniques currently available and being developed (Bottema 1992, Bottema et al. 1992, Stathopoulos et al. 1992, Wu and Stathopoulos 1993, Stathopoulos and Baskaran 1996).

C3.2 APPROACH FLOW, MODELING, AND SIMILARITY

Approach flow conditions and modeling should meet the requirements given in Chapter 2 and its commentary.

Winds affecting pedestrian comfort and safety may occur at times when wind conditions can be influenced by thermal stratification. The works of Murakami et al. (1979), Carpenter (1990), and Williams and Wardlaw (1992) found that, while on any given day the agreement between wind tunnel and full-scale data may be poor, when long-term averages are used, the agreement is much better. If only daytime winds are considered, even the long-term averages may not agree, because of heating of the ground by the sun.

PLW studies are frequently performed for existing and new building conditions on streets, pedestrian ways, and at entrances in the vicinity of the

new development. Accurately measured PLWs require detail modeling near the ground in the vicinity of all measurement stations. Thus in many cases, additional modeling at ground level may be needed, compared to that for pressure and force tests (Durgin 1985, Durgin 1989). At times, when less accuracy is needed, upstream modeling requirements can be relaxed.

Model and full-scale times are related through the equality of a non-dimensional time parameter:

$$\left(\frac{tV}{L_b}\right)_m = \left(\frac{tV}{L_b}\right)_p \tag{C3.1}$$

where:

t is a characteristic time;
V is a wind speed;
L_b is a characteristic length; and
subscripts m and p denote model and prototype values.

As noted in Chapter 2, the total sampling time should be the equivalent of about one hour full-scale because of the gap in the spectrum of the wind noted by Van Der Hoven (1967). Sometimes the data are filtered to eliminate gusts substantially shorter than 2 seconds full scale, since both Hunt et al. (1976) and Murakami et al. (1979a) have shown that high frequency gusts do not affect the balance of a person.

In using the above relation, the ratio of dimensions is the scale factor. What speed ratio to use is less obvious. PLWs, like other serviceability considerations, are judged on the basis of relatively common wind speeds rather than those used in the design of the structure and the building envelope. One possible choice is the ratio of the wind tunnel gradient wind speed to the full-scale gradient wind speed, with a recurrence interval ranging from 1 week to 1 year.

C3.3 MEASUREMENT TECHNIQUES

C3.3.1 Introduction

Many methods have been successfully used to investigate and measure pedestrian level winds in the wind tunnel. They range from simple flow visualization, with smoke in air or ink in water, to sophisticated laser Doppler methods. The most commonly used quantitative methods are the erosion of particles scattered in all areas of interest; the pressure probe invented by Irwin (1981); and hot-wires and/or hot-films. Each of these is discussed in detail below.

The laser-Doppler method can provide accurate measures of the wind speed, but the equipment is expensive and obtaining data is time consuming. It is used mostly in research projects. Many other methods have been tried, and new ones are under development. Infrared thermography has also been used for pedestrian wind evaluations (Wu and Stathopoulous 1997). See Wu and Stathopoulous (1993) for a review of current methods. Any method that results in accurate estimates of the average, rms, and peak PLW speeds is acceptable.

The final result of any wind tunnel study of PLWs is a prediction of how often a given wind speed is expected to occur at each location of interest. Two sets of data are needed for this prediction. The ratios of the pedestrian level wind speed at the location of interest to the gradient wind speed for all gradient wind directions [sometimes for the 16 major compass directions, but more typically at 10 or 15° intervals]; and a statistical description of the local wind climate at gradient height. The former is obtained in the wind tunnel and the latter comes from a statistical analysis of data from the nearest weather station, as described in Chapter 10. Thus, each of the measurement techniques mentioned above must provide a means of obtaining the ratio of PLWs (average, rms, and peak) to a gradient reference wind speed at each station for each direction.

C3.3.2 The Erosion Technique

For the erosion technique (Gandemer 1978, Grip 1982, Beranek 1984, Livesey et al. 1990, Gerhardt and Kramer 1992, Durgin 1992), it is assumed that the wind speed at pedestrian levels that causes the particles to move can be reliably determined. Knowing this wind speed and the reference gradient wind speed in the wind tunnel at which a station first becomes free of particles, one can obtain the required wind speed ratio. The accuracy of the erosion technique is limited by several factors. First, while the particles are known to respond to a combination of average and gust wind speeds, the exact combination seems to be dependent on test circumstances (Grip 1982, Durgin 1992), and, as noted in Section C3.4, it may not be the most meaningful measure of the wind speed. Second, the small particles that are used in most such studies result in the top of the particles being much lower than pedestrian height. Thus, the indicated wind speed will be too near the ground. The problem here is that in the vicinity of the building and/or in city streets, the variation of wind speed with height will be different at different stations and for different directions. Finally, results are dependent on how closely the particles are placed (Grip 1982), their size, shape, and drag as a function of wind direction (Durgin 1992) and so on. Durgin (1992) has found standard deviations of about 20% for predicted wind speeds of about 20 mph. Livesey et al. (1990) report using the technique with considerable success, but report errors as high as 30%.

This technique is especially valuable in looking at large areas and assessing the effects of adding several new buildings. The resulting images provide valuable insight into actual flow patterns and locating very windy areas. Architects find this technique very useful.

C3.3.3 Hot-Wires and Hot-Films

The hot-wire and hot-film probes typically consist of a very thin vertical element spanning, at model scale, the equivalent of 4 to 6 feet above the ground full scale. The element is heated to a constant temperature (such as 300 °C). The current required to maintain the constant temperature is a non-linear function of wind speed. Because the element is very thin and the gain of the controlling amplifier high, very good frequency response, typically up to several kHz, is obtained. With frequent calibration and checks, accuracies of 1% are attainable. Hot-wires or films are fragile and require frequent calibration, but are the most convenient accurate instruments for measuring PLWs at the present.

C3.3.4 The Irwin Probe

In 1981 Irwin reported an omni-directional pressure probe for measuring PLWs. It is very rugged and is made up of a round hole in the floor with a tube coming out of the center to some distance above the hole. Pedestrian level winds are determined by measuring the difference in pressure between the hole and the tube end. Irwin showed that the probe produced accurate results in a typical boundary layer and then did some experiments to show it also could measure PLWs in the flow around buildings. This probe is very convenient, because it can be used with the same pressure instrumentation needed for building pressure measurements (see Chapters 4 and C4) and will have a similar frequency response so that peak gusts and rms variations can be measured. In 1992 Durgin reported a careful study of the Irwin probe. He found that as long as the top of the tube was at the height at which the wind speed was wanted, the probe was accurate to approximately 5% for all kinds of flows. In view of the many other uncertainties in PLW studies, such accuracy is probably sufficient in most situations.

Irwin probes and hot-wires or hot-films have two common characteristics. They only measure the horizontal component of the flow. Because they are omni-directional, when used in highly turbulent flows (rms > 20%) in which the flow will reverse, they rectify the reverse flow. This results in the indicated average wind speed being too high and the rms being too low. The peak measurement is unaffected. Of course, it is the wind speed that people sense and that is still measured. The pulsed hot-wire (Bradbury 1976) eliminates the rectification for high rms, but has limited frequency response and is too time consuming to use in typical PLW wind tunnel studies.

Because most full-scale measurements are made with three cup anemometers, and they also rectify the reverse flow, such full-scale results are comparable with the Irwin Probe and hot-film or hot-wire results from wind tunnel studies. Also, when measuring PLWs, it is usually the windier places that are of most interest, and the turbulence intensities there are generally less than 20%.

C3.4 CRITERIA

Establishing criteria for pedestrian level winds has proven difficult and elusive because it must be expressed in probabilistic form and of necessity is subjective. In a hurricane or other major storm, because the wind usually changes direction during the storm, many locations can experience unacceptable and possibly dangerous winds. The issue becomes one of determining how winds affect any given pedestrian activity (see below) and how often a particular wind speed can be exceeded before a location is perceived as unacceptable for that activity. Establishing criteria is further complicated, because what seems windy to a fragile older person, may be acceptable for a physically robust individual. Also, what seems acceptable in a city like Boston, Massachusetts, which has an annual average yearly wind speed at the airport of 12.9 mph, may not be in a city like Orlando, Florida, where the wind speed is approximately 8.5 mph.

Many authors have attempted to define criteria for PLWs (Wise 1965, Melbourne and Joubert 1971, Davenport 1972, Penwarden 1973, Isyumov and Davenport 1975, Lawson and Penwarden 1975, Penwarden and Wise 1975, Hunt et al. 1976, Jackson 1978, Lawson 1978, Melbourne 1978, Murakami et al. 1979a and b, Visser 1980, Durgin 1985, Hosker 1985, Murakami et al. 1986, Durgin 1989, Ratcliff and Peterka 1990, Bottema 1992, Williams and Wardlaw 1992, Williams and Soligo 1992, and Durgin 1995). The above list is not exhaustive. Note the number of papers from the late 1970s and the apparent renewed interest in the 1990s.

References Penwarden (1973), Melbourne and Joubert (1971), Hunt et al. (1976), Melbourne (1978), and Murakami et al. (1979a) specifically deal with the physical effects of wind on people. The starting point for many criteria is the Beaufort wind scale version for pedestrian winds, as modified by Penwarden (1973). PLWs are unsteady and in order to define them, the average, the root mean square variation about the average, and the peak value over some period of time is needed. If the relationship between these three quantities were the same at all locations for all wind directions, then the average or any combination of the three could be used for establishing criteria, as was done in most of the early studies. Unfortunately, that relationship varies greatly and the most appropriate measure of wind speed has not been generally agreed on. What makes the problem difficult is that if enough loca-

tions and wind directions are considered, there are fixed average relationships between the three quantities (Durgin 1992). Using those average relationships will work for some directions for some locations, but not in all situations.

The studies of Hunt et al. (1976) and Murakami et al. (1979a) are particularly important with regard to defining what wind speed to use in any criteria. Both show that the gusting wind component is important in determining what people perceive as windy. Further, both found that gusts lasting less than 2 or 3 seconds do not affect people's balance. As a result, both these authors and the studies that followed began to use an effective gust speed V_{eff}, which is defined as

$$V_{eff} = \overline{V} + gV_{RMS} \tag{C3.2}$$

where $\overline{V}$ and V_{RMS} are the average and RMS wind speeds, and g is a constant. If the distribution of gusts were Gaussian, then for $g = 3.5$, V_{eff} would approximate the 2 or 3 second peak gust and lower values of g represent gusts lasting longer times. Hunt et al. (1976) chose 3.0 and Murakami et al. (1979b), chose 3.5. Other authors have chosen values from 1.0 to 3.5. There does not seem to be general agreement on the most appropriate value.

Durgin (1992) has proposed using a combination of average, effective gust, and peak gust, called an equivalent average speed. The equivalent average is defined as the largest of the average wind speed divided by 1.1; the effective gust wind speed divided by 1.43; and the peak gust wind speed divided by 1.88. Each wind speed is determined over a time equivalent of one hour full scale. The effective gust uses g =1.5, which turns out to approximately define the expected fastest one-minute gust during the hour; and the measured peak gust is measured to correspond to the expected fastest 2 to 3 second gust full scale. Using these constants, Durgin (1992) shows that the average wind speed will determine the equivalent average for turbulence intensities less than 20% and that the effective or peak gust will determine it for greater turbulence intensities.

As noted above, many authors have attempted to define criteria for PLWs. Categories in many criteria for PLW's include:

1. dangerous and unacceptable;
2. uncomfortable for walking;
3. comfortable for walking;
4. comfortable for short periods of sitting or standing; and
5. comfortable for long periods of sitting or standing.

In examining approximately 1000 data points from a large number of studies, Durgin (1992) found that the average wind speed determines the

equivalent average for 90 to 95% of stations, with predicted wind speeds greater than or equal to those associated with categories 1 and 2. Winds in categories 4 and 5 are more often determined by the peak and effective gusts. This is not surprising, because areas where categories 4 and 5 govern, tend to be in sheltered areas where the turbulence is expected to be higher.

Many authors defined their criteria in terms of a single velocity. For instance, winds are unacceptable and dangerous if the average wind exceeds 23 m/s more than once per year. This means they are using one point on the plot of average wind speed versus probability to define the criteria. Criteria for PLW were summarized by Isyumov and Davenport (1975b). In 1978 Melbourne plotted all the existing criteria on a single plot using average hourly winds. Recently three papers have come out (Ratcliff 1990, Williams and Wardlaw 1992, Bottema 1992 and Durgin 1995) that compare many of the existing criteria.

In the above criteria only the mechanical effects of the wind have been considered. In fact, the effects of wind on people are also influenced by precipitation, temperature, and humidity. These variables can become particularly important if individuals are not seasonably dressed. Recently a number of researchers (Fanger 1988, Williams and Wardlaw 1992, Soligo et al. 1995) have begun to include these effects in their studies of PLWs.

C3.5 COMPARISONS WITH FULL-SCALE MEASUREMENTS

Without comparisons to full scale, results from wind tunnel studies are unproven. Comparisons made by Isyumov and Davenport (1975) showed that wind tunnel model studies can provide reliable estimates of pedestrian level winds in full scale. In their book Simiu and Scanlan (1986) review many of the full-scale and wind tunnel studies performed before 1986. More recently studies have been reported by Carpenter (1990), Williams and Wardlaw (1992), and Isyumov (1995). In general it is found that while on any given day the agreement may be poor, when long term averages are used, the agreement is much better. This is not surprising, because wind tunnel data are taken using a neutrally stable approach flow, whereas neutral approach flows are infrequent in real life. Given enough time for averaging these non-neutral flows, the average, of day and night conditions, approaches values associated with neutral conditions. It is also found that local details such as landscaping, trees, wind breaks, and so on have a beneficial effect, and their exclusion from wind tunnel models can result in conservative estimates of full-scale conditions.

This page intentionally left blank

Chapter C4
LOCAL AND PANEL WIND LOADS

C4.1 GENERAL

This chapter describes procedures used to obtain information on local wind-induced pressures and suctions, as required in the design of components of exterior surfaces or the "envelope" of buildings and structures. Also discussed are methods for developing wind loading information on panels and the tributary areas of secondary structural members.

C4.2 SCALING WIND TUNNEL RESULTS TO FULL SCALE

Scaling measurements from wind-tunnel to full scale is illustrated for local pressure measurements, but the concepts apply to area average pressure measurements as well. Scaling is accomplished through a dimensionless pressure coefficient

$$C_p = (p_x - p_r)/q \tag{C4.1}$$

$$q = \tfrac{1}{2}\rho V_r^2 \tag{C4.2}$$

in which p_x is the pressure at a measurement pressure tap on the building model, p_r is the static, or the barometric, pressure at a reference location away from the influence of disturbed wind flow about buildings, q is the dynamic pressure of the wind at the reference location, ρ is the density of air, and V_r is the 10 minute to 1 hour mean wind speed at the reference location.

The numerator $p_x - p_r$ is measured directly by the laboratory pressure transducer as a differential pressure and represents the wind pressure acting at the pressure tap location (no internal effect included). The denomina-

tor q can be measured directly by the same pressure transducer (at a different time), by a separate pressure transducer, or by calculation after measurement of V_r and ρ. The air density ρ is usually calculated from measured temperature and barometric pressure. The location for the reference position is selected so that it has no interference from wind flow over any structure which might disturb the wind velocity or pressure field. This location is often at a height above ground of 100 to 500 m rather than at the height of the building under investigation as is common for reference velocities for building codes.

The velocity at the reference location may be influenced by the distribution of ground roughness and terrain upwind of the building site. If the surface roughness upwind of the site is not uniform for a sufficient distance over flat terrain (say 5 to 10 km or more), then there may be a benefit to performing a terrain model study at a small scale before the building model test to define the characteristics of the approach wind for the building site.

Pressure coefficients have been found to be in good agreement between model and full scale for most areas of sharp-edged bodies, providing the modeling techniques of Chapter 2 are satisfied. Extreme negative pressure coefficients measured in regions influenced by corner vortices are a possible exception. These tend to be highly localized with short duration peak values. Their practical consequence tends to be of limited importance in most situations. The pressure on the full-scale building can be obtained by multiplying the pressure coefficient by the full scale value of q, corresponding to the selected full-scale reference wind speed (see Chapter C10).

The value of V_r used in q must be transferred from a location where historical speeds have been recorded to the reference velocity location. If the winds at both historical location and reference velocity position are in equilibrium with the upwind roughness (the upwind roughness is relatively constant for a distance of 10 to 20 km), then relatively simple equations such as those found in the appendix of the national wind load standard ASCE 7 (ASCE, 1988) can be used to transfer data from the historical to reference site. If either site is not in equilibrium with the upstream roughness, then more complicated computations or wind tunnel tests may be needed to quantify the transfer.

C4.2.1 Local Pressures

A typical model pressure tap size of 1 to 2 mm corresponds to a diameter of 0.2 to 0.5 m on the full-scale building. Because reduction of local pressures as a result of area averaging in many cases does not begin until areas are more than 1.0 sq m (10 sq ft), a single pressure tap is normally sufficient to specify pressures for individual cladding elements or connections. Exceptions may be in areas with rapid variation of pressure with distance, such as within a vortex forming over a roof very near the roof corner or near the ori-

gin of a vortex which forms over wall cladding elements near a break in the vertical lines of a corner.

Full-scale data suggest that the largest peak local pressures acting on most buildings and structures have an effective duration of about 1 to 10 seconds. This duration is long enough to cause an element of cladding, such as a window or mullion with a natural frequency in excess of several Hz to respond fully to the load. Most cladding elements, for which single tap measurements are an appropriate measure of load, have natural frequencies of several Hz or more. For these cases, the application of a pressure for a few seconds is sufficient for the element to be in full equilibrium with the applied load. While the load is fully applied to the element, there are separate issues concerning the capacity of the material to withstand short-duration loading which may need to be considered. This is typically true of glass and wood, but not for most metals and connectors. In some instances, a rapid rise time of loading may contain higher frequencies, which might influence the quasi-steady loading.

The largest peak pressures on a structure can vary by 30% or more from one measurement to another, because of a natural variation in the largest peak during a measurement period. Several methods are available to obtain a stable estimate of the peak value corresponding to the mean or mode of the probability distribution of the largest values. The methods include averaging peaks from several measurement records, extrapolating the peak values obtained at a number of subrecords to the full record using analysis, obtaining the distribution of the largest peak by measuring all independent peaks in a record followed by analysis, and direct measurement of the distribution using a large number of sample periods with one measured peak in each (Peterka 1983, Irwin 1988). All these techniques work well.

Wind loads on cladding elements are mostly non-Gaussian in nature and usually occur in the presence of a mean load. The non-Gaussian nature of the loading often occurs as pressure pulses or spikes in the negative pressure direction and results in a highly skewed probability distribution. Changes in wind speed and direction over the structure life cause the amplitude and sign of these loads to change. Material fatigue, which might result from this complicated loading, may not follow typical fatigue charts based on sinusoidal loads with zero or nonzero mean. This is an active research area. Hurricane winds can be of sufficient magnitude and duration to cause fatigue damage. Attention to fatigue loading is especially important in hurricane regions and is often a failure point for connections in the structure.

C4.2.2 Panel Wind Loads

Area average pressures are useful in many applications. For cladding assemblies larger than about 1.0 sq m, the area average peak pressure may be reduced and is often, but not always, significantly lower than the peak pres-

sure measured at a single tap when the area exceeds 10 sq m. The area reduction in pressure can be a function of location of the area on the structure. Design of longer span roof trusses can frequently benefit from measurements of area averaged pressures. Examples of other situations in which area averaged pressures can be important include purlin or mullion loads, cladding subassembles, and glass walls supported mainly by structural silicone.

Two primary methods for measuring area averaged wind loads are available. The first is to measure pressures simultaneously at tap locations distributed throughout the area and to perform an average of pressures digitally in a computer at each instant in time. The second method is a pneumatic average in which all taps in the area are connected to a manifold that has one output to a pressure transducer (Stathopoulos 1975). Further discussion is provided in Section C5.2. Each method has its advantages and disadvantages. In either method, taps can be arranged so that the average provides an area average, moment, modal load, or other desired quantity. In the digital average, weighing functions can be used with each tap to calculate quantities such as moments or modal loads. It is important that the digital average be performed with all taps in the area measured sufficiently close in time that only an insignificant time shift is incorporated in the results. This requirement is not trivial and should be addressed in the data acquisition process. In the pneumatic average, it is important that the tubing system be designed to have the required frequency response and that the manifold system have very small internal volume and a geometry to provide equal weight to each tap (Surry and Stathopoulos 1978). In both methods, it is important to have sufficient taps to adequately define the load over the area in question.

C4.3 INTERNAL PRESSURES

The internal pressure is important because the net pressure applied to the building cladding system is the algebraic sum of pressures acting on the outer and inner sides. Internal pressures can be influenced by many factors. The size and distribution of openings in the building skin; permeability of the skin; location of air intakes and exhausts and their ability to modify external pressures before imposing them on the interior space; distribution of floors, partitions, doors, elevator shafts, climate control ducts, and other restrictions on pressure and air flow within the structure; volumes of internal spaces; and flexibility of the building envelope are all potentially important factors.

An opening in the building skin causes internal pressures to be influenced by the external pressure at the opening. There is no general agreement in building codes as to whether glass (which might be broken by flying debris) or tenant-operable windows or doors (which could be left open by

the tenant) should be considered to be an opening for internal pressure calculations. In many cases, determination of what constitutes an opening may be established by the design engineer in consultation with the owner. A building is often considered to be sealed if there are no tenant-operable windows or doors onto balconies. The ground floor entry doors might be considered sealed if they do not lead directly to a portion of the exterior wall, if they have double sets of doors, or if they are revolving doors. A building is often considered to have openings if the closure is under control of the tenant and not restricted to maintenance access.

Some studies have shown a potential overshoot in internal pressure when an opening is created suddenly, while other studies have not recorded such an overshoot. The presence of this effect may be influenced by turbulence in the approach wind and by factors not completely understood at this time. However, it has been found experimentally that in normally turbulent winds, the overshoot does not exceed the maximum peak external pressure at the opening under steady-state conditions.

For a sealed building, internal pressures are often accounted for in a wind-tunnel test by use of an internal pressure from a code or standard or from other analysis. For buildings with openings, calculations are sometimes performed to impose the external pressure at an opening on connected spaces within the building, accounting for volume of internal space and the instantaneous difference between pressures at various tap locations on the model building (Irwin 1988).

Internal pressures should not be neglected in calculation of frame forces. For example, on buildings with lightweight roofs, the failure of a truck door or large window can transfer a large positive pressure to the interior increasing uplift on the roof. Large panels or walls can be similarly loaded.

C4.4 ROOF PRESSURES

Roofs, pavers, and vented walls experience some wind-induced pressures on their back or undersides. This pressure equalization can reduce the total or differential pressure on these components. The extent of this equalization and the load transfer depend on the size and spacing of pavers or the size and distribution of vent ducts in a wall. The measurement or calculation of load distribution is not straightforward and is an area of active research. Direct modeling in the wind tunnel has been performed on a research basis for smaller buildings, but has not been tried for larger buildings, because of the small scale of the vented spaces.

This page intentionally left blank

Chapter C5

OVERALL WIND LOADS AND WIND-INDUCED RESPONSE

C5.1 GENERAL

There are several techniques for assessing overall wind loads on structures. The most appropriate technique for a particular case is determined by such factors as the novelty or uniqueness of the structure's design, the accuracy expected in the results, the relevance of the results to issues of public safety, and the time and funds available to complete the study.

At the one extreme are situations in which one or more of the following factors apply. The project

- is of essentially conventional structural design (typical low-rise buildings for example);
- has a relatively limited or fixed overall budget and design schedule; and
- has a limited design life with minor human risk factor (light standards).

For such cases, results may be required quickly and cheaply. To achieve this, some approximation in the results may be tolerated. Therefore a purely analytical or code-based estimation of wind loads may suffice, and one may forgo wind tunnel testing completely.

At the other extreme are structures for which there is

- a unique or novel design (super-tall buildings or sports facilities);
- less predictable aeroelastic behavior (bridges, towers);
- a significant human risk factor (sports facilities);
- a long design life and significant investment;
- a significant economic penalty for designing undue conservatism into the structure (any large project);

or some combination of these factors. For these structures, full wind tunnel model studies may be both necessary and cost effective for providing reliable wind loading evaluations. Such studies may use procedures described in this Chapter or may involve the aeroelastic wind tunnel models described in Chapter C6.

It should be noted that electronic measurement and computing technology directly related to these wind tunnel techniques have advanced considerably in the last decade, and continue to do so. Consequently, approaches that were simply not viable previously are now being successfully developed. Simultaneous measurements of instantaneous pressures at many locations and their on-line integration, the recording and maintaining of large numbers of digital time series, and the combination of wind tunnel data with numerical computation and computational fluid dynamics are now possible. The relative merits of such techniques, both economically and technically, are evolving rapidly. Because of this changing state of the technology, the following discussions focus more on the general physical and theoretical bases of different approaches and less on the particular mechanics of implementations.

C5.2 MEASUREMENT TECHNIQUES

C5.2.1 Pressure Averaging

Pressure Averaging for Area Loads. Averaging of pressures may be used to assess loads acting over specific areas or net loads acting across structural elements, parapets, roof pavers, and so on. Several techniques for this have been devised. These efforts have been largely driven by the cost and physical size of early pressure transducer instrumentation. The issues and logistics of sampling pressures are covered in Chapter C8, and the material presented here deals with the experimental approaches to the problem.

Pneumatic Averaging. Area loads may be assessed by measuring local pressures acting on tributary areas and averaging these pressures "mechanically" using small diameter tubing or pressure cavity systems. The simplest approach here is to place pressure taps at various points on the surfaces subjected to the wind-induced pressures and then to connect them to a common manifold through flexible plastic tubing (e.g. Stathopolous, 1975). The input pressures are physically averaged within the manifold, and the averaged pressure is in turn measured by a single pressure transducer. There are several important design considerations in this technique. The internal volume of the tubing and manifold system must be kept minimal, and geometries which induce acoustic pressure wave amplification must be avoided. These issues are discussed in detail by Surry and Stathopoulos (1978).

Weighted combinations of pressures, required in order to assess wind-induced moments for example, may be obtained by clustering together small numbers of pressure taps within common tributary areas on the exposed model surfaces. These in turn provide a discrete weighting to that tributary area by way of the averaging process within the manifold.

Ordinarily, pressures are measured relative to some reference pressure by connecting the reference pressure to a small cavity on one side of a pressure transducer membrane and the subject pressure to a cavity on the other side. One may, however, assess net wind-induced loads across structural elements by connecting single tap or manifolded pressures from different model surfaces to each side of the transducer membrane, thereby measuring the pressure differential. This approach then requires special consideration of the appropriate reference pressure that is no longer directly accounted for. It also requires small volumes on either side of the transducer membrane; not all commercially available transducers are suitable.

In all of these approaches, pressures at the surface of the model are transmitted to a pressure transducer located at some distance—either within the model or outside of the tunnel. Flexible plastic tubing with inner diameters of 1/16 in. or less is typically used. Except in the case where only mean loads are of interest, it is important that the frequency content of the fluctuating loads be correctly represented and that the average represents that of simultaneously occurring pressures. Therefore, it is crucial in these set-ups that the frequency response of the pneumatic transmission be properly considered. The fluctuating pressures at all frequencies of interest must be adequately transmitted to and measured by the transducer. Otherwise, some specific means of accounting for signal distortions must be implemented. Both the magnitude and phase of the frequency response should be considered. The magnitude consideration addresses the potential distortion in the signal level for various frequency components, while the phase consideration addresses potential distortion in the simultaneity of the pressures from different locations.

In all cases where the effective pressure acting over a tributary area is evaluated from a single pressure tap, it is necessary to consider carefully the extent of the tributary area and whether the measured localized pressure will adequately represent it. For example, appropriate tributary areas near sharp building corners should be smaller than those necessary in central areas of a building façade, because pressure gradients are typically greater near corners.

Porous-Polyethylene Cavities. More direct measurement of area pressures has been achieved using porous polyethylene materials in the model construction (e.g. Vickery et al. 1985). Porous polyethylene sheets approximately .005 to .020 in. in thickness are porous enough to effectively transmit fluctuating pressures in the dynamic range relevant for area loads, while still being solid enough to provide the aerodynamic geometry required for the

model surface. In this approach, a small cavity is built into the model and covered by a thin sheet of polyethylene mounted flush with the exterior surface of the model and leaving a small pressure equalization volume behind it. The wind-induced pressures acting over the exterior surface are transmitted to the cavity and the averaged cavity pressure is measured using a single internal pressure tap. The technique is effective and offers a greater spatial resolution than using the multiple pressure tap approach. However, the model construction is considerably more involved.

On-Line Averaging. Averaging of measured pressures can also be done by combining the electronic transducer signals from individually measured local pressures. Analog averaging of the electronic signals from the transducers is possible. However, this is now rarely undertaken because digital sampling and averaging are more powerful, flexible, and cheaper.

Simple weighting to account for tributary areas, as well as negative weighting for net or differential loads, or the evaluation of moment loads are all handled similarly by software programming of the appropriate weighting values. The approach is discussed in Surry and Stathopolous (1978).

As with the pneumatic averaging approaches, careful consideration must be given to the appropriate distribution of local pressure taps and the frequency response of the systems carrying the pressures to the transducers. Unlike those approaches, the digitized signals may be manipulated to account for frequency response distortions or asynchronous sampling procedures.

Pressure Averaging for Modal Loads. The approach described previously of averaging pressures pneumatically has often been used because it reduces the number of pressure transducers required. This is advantageous because of both the size and cost of pressure transducers; however, the advent of compact solid-state pressure transducers is changing this picture. The ability to simultaneously measure large numbers of local pressures has prompted the development of techniques that use pressures measured over much larger areas of the structure or even the entire structure. The drop in the cost of computing and data storage has made it feasible to collect and process much larger data sets than previously. The following approach is one result of these advances.

Modal Loads from Integrated Pressures. The approach of integrating individually measured local pressures to assess modal loads is an expansion of the on-line averaging approach described in the previous section. It offers an alternative to the force balance approach of measuring modal loads in appropriate situations. The potential exists to apply this technique to a wide variety of structures, including long-span roofs, stadia, and even bridges. It

can handle higher frequency modes, requires no mode shape corrections, and can be readily used to evaluate the generalized forces of modes with coupled degrees of freedom (3-dimensional mode shapes).

Proper measurements of overall loads require a large number of simultaneously measured local pressures in order to fully capture the pressure field acting on the exterior surface of the entire structure. The advent of solid-state pressure scanning instrumentation has made this a viable task, but the required pressure tap coverage remains an issue of debate. Opinions on the number of pressure channels for a typical high-rise building model, for example, range from 200 to as high as 1000. The following considerations should be kept in mind when determining the required number of local pressure measurements:

- In evaluating overall mean loads, the spatial resolution required is greater, because the static pressure field over the exterior surface of the structure must be adequately resolved and may have areas of high-pressure gradients, particularly near corners and other flow separation points. On the other hand, mean loads do not require that the pressures be measured simultaneously, so that pressures from sequential tests may be combined.
- The dominant contribution of any modal load is the result of pressures fluctuating at the modal frequency. Fluctuating pressures are generally correlated over distances inversely related to the frequency. In other words, the higher the fluctuating frequency, the more localized the fluctuating pressures. There are notable exceptions to this, such as vortex shedding, where the fluctuations can become highly correlated over a narrow range of frequency. For most large building structures the correlation distances of the pressures fluctuating at the important modal frequencies (i.e., the first two or three modes) are of the same order of magnitude as the structure itself. This fact helps to reduce the spatial resolution of measurements required for assessing modal forces.
- Pressure fluctuations at frequencies lower than that of the fundamental mode of the structure contribute to the quasi-static or background loads. These loads can be important for some structures and simultaneous pressure measurement can provide a good indication of their distribution and magnitude. A pressure tap distribution, appropriate for mean loads, is required in this case.
- For many structures, vortices form at the windward edge and travel along the side of the structure in more or less discrete packets. Pressure taps must be placed sufficiently close if they are to capture the resulting dynamic loads. Spatial aliasing is another concern. This requirement may exceed that for mean pressures loads.
- Many buildings and structures have complicated architectural treatments that are difficult to adequately cover with pressure taps.

- Where higher modes are important, simultaneous pressure measurements have a distinct advantage.

Until further experience is accumulated, the requisite number of simultaneously measured pressures ought to be judged with particular care and on a case by case basis.

The modal loads acquired from this technique may be accumulated and analyzed in either the time or frequency domain. The methodology is discussed in Steckley et al. (1992) and Irwin and Kochanski (1995).

C5.2.2 Direct Load Measurements

High-Frequency Force Balance. The high-frequency base balance technique, first reported by Tschanz (1982), is based on an earlier approach used by Whitbread (1975). It is now a widely accepted technique for wind tunnel model studies. It offers a relatively economical and expeditious alternative to the more involved aeroelastic procedure. The technique involves the use of a very stiff high-frequency balance-model system that models only the exterior geometry of the structure. The wind tunnel study may be carried out at a stage in the design when only the exterior geometry of the structure has been fixed. When they become available, the remaining structural properties are combined analytically with the wind tunnel data to determine full-scale responses. The measured quantity in the aeroelastic procedure is the final response. In the base balance technique, on the other hand, it is the spectra of modal forces that are measured experimentally. The responses of the structure to these modal forces are then determined analytically. Changes in the structural properties can be readily accommodated by iteration of the analytical procedures. Parametric studies, in which the responses are predicted as functions of the structural parameters, are often feasible. Importantly, it is unnecessary to retest a new wind tunnel model unless significant changes in the exterior geometry are made.

The idea of measuring the modal force spectrum and then calculating the responses as they would occur for varying structural parameters had been considered prior to the development of the current base balance technique. Saunders and Melbourne (1975) attempted to record the modal spectrum by measuring it as seen through the mechanical admittance of an aeroelastic model. By knowing the model properties, reverse calculation yielded the modal spectrum which could then be combined with the desired structural properties. Major difficulties with this procedure are the errors introduced through the aeroelastic model properties, in particular the estimate of the damping. Measurements of modal force have also been made using pressure models, and this is discussed in the previous section.

Principles and Assumptions. The fundamental premise of the base balance technique is that the generalized or modal forces resulting from the wind can be estimated from the measured base moments experienced by a stationary model. The modal force is defined as the integral of the applied force weighted by the mode shape at the point of application.

A fortuitously similar quantity to the modal force occurs in the more easily measured base overturning moment. In this case, the applied forces incur a weighting naturally through the moment arm influence line, which varies linearly with height. When the mode shape is proportional to the influence function, then the modal force and the base overturning moment are also proportional.

A similar approach can be taken for the twist modal force and modal torque. In this case, the loading is the torque per unit height, but the base torque influence line which is constant over the height of the structure, is less representative of twist mode shapes.

The base moments, including two overturning moments and the base torque, represent direct and exact measurements of the modal forces on a structure when the following conditions are met:

- The first three natural modes of the structure are decoupled and geometrically orthogonal in two sway directions and one twist direction.
- The fundamental sway mode shapes are linear functions of height and pivot at a point where the moments are measured.
- The fundamental twist mode shape is a height independent constant over the height of the structure.
- There are no significant motion-induced forces involved and so the nature of the forcing remains the same on a responding structure as it is on a stationary structure.
- The balance-model system is essentially rigid, with a high natural frequency, so that the measured moments are not significantly amplified by the mechanical admittance of the system in the frequency range of interest.

In practice these conditions are never fully met. However, in most situations adjustments can be made for all of these difficulties, with the exception of the possible effects of motion-induced forces.

The technique is also limited in that only the fundamental modes in each direction can be reasonably estimated. It must be assumed that contributions to the response from higher modes are negligible. Also, only limited information is obtained on how the mean and non-resonant time-varying loads are distributed over the structure. Such information, however, can be estimated or measured in a companion study of local pressures. A "second-generation" base balance approach, aimed at overcoming some of these limitations, is discussed in a later section.

Adjustments for Base Balance Mechanical Admittance. It is necessary that the base moments used to represent the modal forces be the moments as measured on a nearly rigid model. If the balance-model system responds dynamically to the wind loading, then the measured base moments will include the inertial loading effects of the system itself. If the motions are large, then the aerodynamic interaction of the model with the wind could also contaminate the measurements. Therefore an attempt is made to make the balance-model system as rigid as possible, while still being sensitive enough to provide reasonable signal strength. In this way the frequency range of interest falls at the low end of the mechanical admittance function of the model-balance system, where the dynamic amplifications are small. In some cases the natural frequency of the system cannot be raised sufficiently high and the base moment measurements are amplified. There is in principle no difficulty in adjusting the spectral density measurements to account for this, providing the mechanical admittance of the system is well identified and may be treated as linear and uncoupled. It is always assumed, however, that the frequency is still high enough that the model motion is insignificant.

Adjustments for Mode Shape. The assumption of a constant twist mode shape with height or that the modal amplitude of the fundamental torsional mode is independent of height is never true for real structures. A typical fundamental twist mode shape of most tall buildings lies somewhere near a linear function of height. In practical cases, the majority of the contribution to the torsional modal force comes from the upper half of the structure. The measurement of the base torque from the base balance may be made more representative of the generalized torque by artificially sheltering the lower portion of the model in such a way that the aerodynamic interference of the sheltering device is minimal. This is not easy to achieve and a more practical approach is to make adjustments to the measured base torque, as was suggested by Tschanz (1982). He argued that a realistic measure of the base torque relative to the generalized torque is given by the ratio of the measured base shear and base moment. Some experimental data for such comparisons are available. It is generally agreed that a value of about 0.70 represents an adequate empirical adjustment factor to apply to the measured base torque.

Although approximating the sway mode shapes by a linear function is sufficient in many cases, tall buildings and structures having mode shapes that significantly deviate from this approximation are not uncommon. The variation in mode shape can have a significant effect on the similarity of the modal force and the measured base moment spectral densities. Measurements aimed at quantifying these effects have been carried out by various researchers. The effect, which deviations from a linear mode shape function have on the final predicted response, differs depending on the type of

response considered. The most notably affected response is the predicted acceleration. In the case of acceleration, the mode shape appears in the analytical portion of the response estimate, as well as the measured quantity. This accentuates the errors arising from the assumption of a linear mode shape. Typical corrections to predicted accelerations near the top of a structure because of non-linearly varying mode shapes may reach 20%. Further discussions of the effect of mode shape on building response estimates derived using the force balance technique are given in Vickery et al. (1985), Holmes (1987), and Boggs and Peterka (1989).

Treatment of Coupled Degrees of Freedom. Many structures, particularly buildings of more complex design, can exhibit coupling between the sway and twist motions and between the two sway directions. Modified base balance techniques may be used to estimate the modal forces in situations of coupled modal coordinates. Multi-degree-of-freedom aeroelastic models are another alternative.

Ideally, a relatively complete approach to the problem would be to measure, in any convenient coordinate system, the complete spectral density matrix of the actual modal forces, including the cross-spectra. The spectral density matrix can then be combined with the mechanical admittance matrix, as defined in a consistent coordinate system, to get the spectral density of the response. Because the mechanical admittance is most easily defined in the modal coordinates, it would be prudent to first transform the spectral density matrix of modal forces to the modal coordinate system.

The practical difficulty is the measurement of the modal forces. It must be remembered that the base moments only represent an approximation to the modal forces and only do so when measured in the modal coordinates. Coupled degrees of freedom represent a further complexity when making these representative measurements. Some progress can be made in cases in which it can be assumed that the base moments and torque represent proportional measurements of separate modal forces. This means that the twist response is largely contained in one mode and that the sway modes, although coupled, still lie in basically vertical planes. It then becomes valid to measure the base moments in a predefined coordinate system and then transform them to modal coordinates. Consideration should still be given to the poorer representation for the twist mode provided by the base torque.

Some linear combination of the measured base moments at each time instant may be used as an approximation to the generalized modal load. The weight factors for each moment must be carefully synthesized by a process that accounts for the component coupling as well as for the nonideal mode shapes. Once the generalized load is transformed to a generalized response by the mechanical admittance, it is frequently required that the response be decomposed into the various component directions. The total dynamic resonant response in each component direction can then be obtained by mean-

square addition of the corresponding component from each contributing mode. See Tschanz (1982) and Irwin and Xie (1993) for details.

In frequency domain analyses for lightly damped systems with well separated frequencies, it is an accepted practice to neglect the off-diagonal terms of both the spectral density matrix of the modal force and the mechanical admittance matrix because they contribute little to the final response. Neglecting the cross-terms, however, only applies to the matrices AFTER transformation to the modal coordinates. In general, cross-spectra measured in standard or predefined coordinates can make significant contributions to the autospectra in the modal coordinate system. Note also that by the very nature of coupled systems, the frequencies may not be well separated. Only separation of a few percent in frequency is necessary to diminish the cross-modal response, but in situations in which this cannot be ensured, it is advisable to consider these effects. Where needed, a method to avoid this complication is to perform all calculations in the time domain. Time domain analysis has complications of its own and must be implemented carefully.

Force Transducers on Substructures. It is possible to mount components of a structure on force transducers and to get direct measurements of the wind-induced forces that are experienced. Examples are sections of bridge decks, segments of roofs, masts, and antennae, and so on. Such transducers must be sufficiently stiff to avoid local resonances of the transducer/substructure system.

C5.2.3 Miscellaneous

There are other techniques, which are less commonly used, but which have advantages for some applications. Two of these are briefly discussed in the following sections.

Multi-Level Force Balance. An extension of the high-frequency force balance technique that is usually implemented as a base balance is the multi-level force balance (Reinhold and Vickery, 1990). This has also been referred to as a second generation force balance. By measuring moments and shears at multiple levels, an improved estimate of the modal loads may be obtained, particularly in cases where the real mode shapes are not well represented by the idealized mode shapes inherent in the base balance approach. This is particularly true of torsion about the vertical axis of the structure and non-linearly varying sway modes.

The multiple force balance technique has the advantage that it does not require extensive pressure transducer equipment. However, it does require a specialized balance and more complicated models than its alternatives.

Forced Oscillation. The forced oscillation technique is used to determine information about the motion-induced or aeroelastic forces acting on a structure. These are the wind forces on a structure which are induced by the motion of the structure through the air (Scruton 1963). In absolute terms, these forces are often relatively small compared to the random wind forces and the inertial and elastic forces of the structure itself. However, because they are correlated with the structural motion, they can be thought of as wind-induced damping and stiffness forces, which effectively modify the structural damping and stiffness.

The technique of forced oscillation has become more common with the advent of solid-state pressure transducer equipment.

This page intentionally left blank

Chapter C6
AEROELASTIC SIMULATIONS

C6.1 GENERAL

Aeroelasticity describes phenomena involving the interaction between aerodynamic forces and structural deformations or motions. Such body motions can introduce additional forces not experienced by a stationary object. An aeroelastic instability occurs when body motion-induced or "aeroelastic" forces act to increase the amplitude of the motion. The instability can be oscillatory or statically divergent in character. Aeroelastic simulations are studies of this phenomenon, using models which replicate the deformation or motion of prototype buildings and structures in a simulated flow field. Body motion-excited or "aeroelastic" forces can become important for some lightweight, flexible, and lightly damped structures. This includes vertical structures, such as tall buildings, towers, masts, and chimneys; long-span suspension and cable-stayed bridges; cables and transmission lines; flexible air and cable-supported roofs, and others. These potentially important additional forces cannot be measured with stationary models, such as are used in pressure and force balance model studies.

In the early stages of the development of wind engineering, aeroelastic model studies were primarily prompted by concerns for aeroelastic instability. It is still common practice to use such tests to ascertain the stability of unusual bridge sections and flexible structures of novel aerodynamic shape. In addition to concerns for the unexpected, aeroelastic simulations are valuable in improving the design of many structures that are sensitive to wind-induced dynamic excitation. Two approaches are common in such studies. Aeroelastically scaled models are used to provide empirical data for analytical formulations of wind-induced effects. This approach is effective for line-like structures in which the wind-induced excitation, including possible aeroelastic effects, can be analytically described. In other situations, aeroelastic studies can be used to simulate the response of a structure in par-

ticular surroundings. This latter approach is effective in providing "direct" estimates of the wind-induced response, when it is difficult to develop analytical descriptions of the wind loading process.

In addition to the similarity of the flow field, the exterior geometry, and the aerodynamic forces, such studies require a representative similarity of the inertia, stiffness, and damping characteristics of the prototype structure.

For structures with sharp-edged exterior geometries, aeroelastic studies can provide reliable direct indications of prototype behavior. As in the case of other types of wind tunnel tests, adjustments are necessary when predicting the behavior of prototype structures with Reynolds number sensitive shapes (circular or rounded). This may involve corrections to the aerodynamic drag and lift forces. Finally, aeroelastic simulations are primarily limited to the study of the elastic behavior of buildings and structures. Correspondingly, extrapolations are needed when predicting structural performance beyond the linear elastic range.

C6.2 ADDITIONAL REQUIREMENTS

Once the geometric scale of the simulation has been established, similarity of the flow-structure interaction requires similarity of the static and dynamic response of the structure under the action of the simulated aerodynamic forces. The similarity requirements, outlined in Section 6.2, can be determined by dimensional analysis or from the non-dimensional equations of motion. These have been extensively treated in the literature. As in all other wind tunnel model techniques, strict similarity of all aeroelastic scaling parameters is impossible to achieve at a reduced scale. Fortunately, good progress can be made with partial simulations as long as these capture the most significant aspects of the wind loading process. For many structures, the practical importance of wind action is limited to its lower modes of vibration, and their dynamic response can be studied with relatively simple aeroelastic models.

Difficulties with Reynolds number scaling have already been discussed in other parts of the Manual. These are compounded in aeroelastic simulations, because these tend to be carried out at wind speeds lower than those commonly used for pressure measurements. For example, for structures in which gravitational forces are important, including suspension bridges, transmission line systems, guyed towers, and so on, the velocity scaling is determined by the Froude number and becomes the square root of the length scale. Length scales are typically in the range of $1{:}100 > \lambda_L > 1{:}500$ and corresponding velocity scales are in the range of $1{:}10 > \lambda_V > 1{:}22$. The need to test at low wind speeds also arises with aeroelastic models of structures, which are dominated by elastic forces. In such situations, it is important to cover a velocity range from common wind conditions, which influ-

ence serviceability questions, to extreme speeds at and beyond the design value. The influence of wind-induced motions on occupant comfort and satisfaction at common wind speeds is an important consideration for the design of tall buildings (Hansen et al. 1973, Davenport 1975, Isyumov 1993). The upper end of the wind speed range is normally extended to explore possible aeroelastic instabilities. Test speeds should exceed the design wind speed by at least the square root of the load factor.

When planning an aeroelastic model study it is important to carefully consider the following:

1. *Influence of the Siting and the Surroundings of the Structure To Be Studied.* The geometric scale and the choice of the type of model to be used is often influenced by the siting and immediate surroundings of the prototype structure. For example, the presence of unusual topographic features and/or other structures may result in substantially higher wind loads and unusual variations of the response with wind direction. In this situation, a full aeroelastic model is preferable to a partial or a section model, which would only provide information on wind effects for some wind directions. This is a particularly important choice for horizontal structures, such as bridges, roofs, and so on.
2. *Predictions of Full-Scale Behavior.* Wind tunnel model studies provide information on the effects of wind for particular chosen wind speeds and wind directions. In other words, such models can be used to "map" the response expected for different possible wind conditions. Full advantage of this information is taken only when these aerodynamic data are properly combined with the statistical characteristics of the local wind climate. Procedures for providing such predictions are discussed in Chapter 10.

C6.3 TYPES OF AEROELASTIC MODELS

Practicable aeroelastic simulations range from replica models, used in studies of slender chimneys, and tubular structures to various types of continuous or discrete (lumped parameter) equivalent models, designed to selectively simulate the dynamic properties of the prototype structure in those modes of vibration that can be excited by wind action. A thorough understanding of the dynamic characteristics of the prototype structure is an essential prerequisite for the selection and design of an aeroelastic model.

C6.3.1 Replica Models

Scaled replica models are practicable only for structures whose elastic properties are concentrated along the exterior geometry and which can be

reproduced at the required geometric scale. For free-standing structures, Froude number scaling can usually be relaxed and the scaling of stiffness is based on maintaining the equality of the Cauchy number.

For strict similitude, all dimensions are consistently scaled and the velocity scale is determined from the equality of Ca in the model and the prototype. Since equality of the density ratio must also be maintained (see Chapter 6), the velocity scale becomes:

$$\lambda_V = \frac{V_m}{V_p} = \sqrt{\frac{E_m}{E_p}} \tag{C6.1}$$

The success of replica models thus depends on finding a model material with acceptable mass and damping properties and a Young's modulus low enough to allow a significant range of full-scale velocities to be examined in the wind tunnel. Furthermore, for a strict replica model, it may be necessary to maintain equality of the Poisson ratio. A metalized epoxy, sold under the trade name Devcon, has been used in the construction of aeroelastic models of concrete cooling towers (Isyumov 1972) and other shell structures. The Young's modulus of this material, is about 0.7×10^6 psi (4800 MPa), its unit weight is about 150 lb/ft^3 (2400 kg/m^3), its Poisson ratio is 0.23, and its material damping is just under 1% of critical damping. These properties can be somewhat adjusted by changing the amount of hardener used in the mixture. For typical strength concrete, the use of this material leads to velocity scales of $\lambda_V \approx 1/2.5$ to 1/3. A replica aeroelastic model of a 375 ft (114 m) high hyperbolic paraboloidal cooling tower is shown in Figure C6.1.

For situations, in which membrane stresses predominate and for slender thin-wall tubular structures, it is sometimes possible to maintain similarity of overall dimensions while distorting the wall thickness. Scaling an equivalent or effective modulus, taken as $E_{eff} = E\tau/L$, allows greater flexibility in the choice of the model material. In the absence of Froude number effects, the velocity scale is determined from

$$\lambda_V = \sqrt{\frac{E_{eff_m}}{E_{eff_p}}} = \sqrt{\frac{(E\tau)_m}{(E\tau)_p} \times \frac{1}{\lambda_L}} \tag{C6.2}$$

where τ is the wall thickness.

An example of a major concrete structure modeled as an approximate replica aeroelastic model using Devcon, is the 1815-ft (553-m) CN Communications Tower in Toronto. An elevation of this tower and typical sections are shown in Figure C6.2. The concrete shaft of this tower, extending up to about 1500 ft (457 m) above ground, was modeled aeroelastically at a geometric scale of 1:450. The exterior geometry of the shaft was modeled cor-

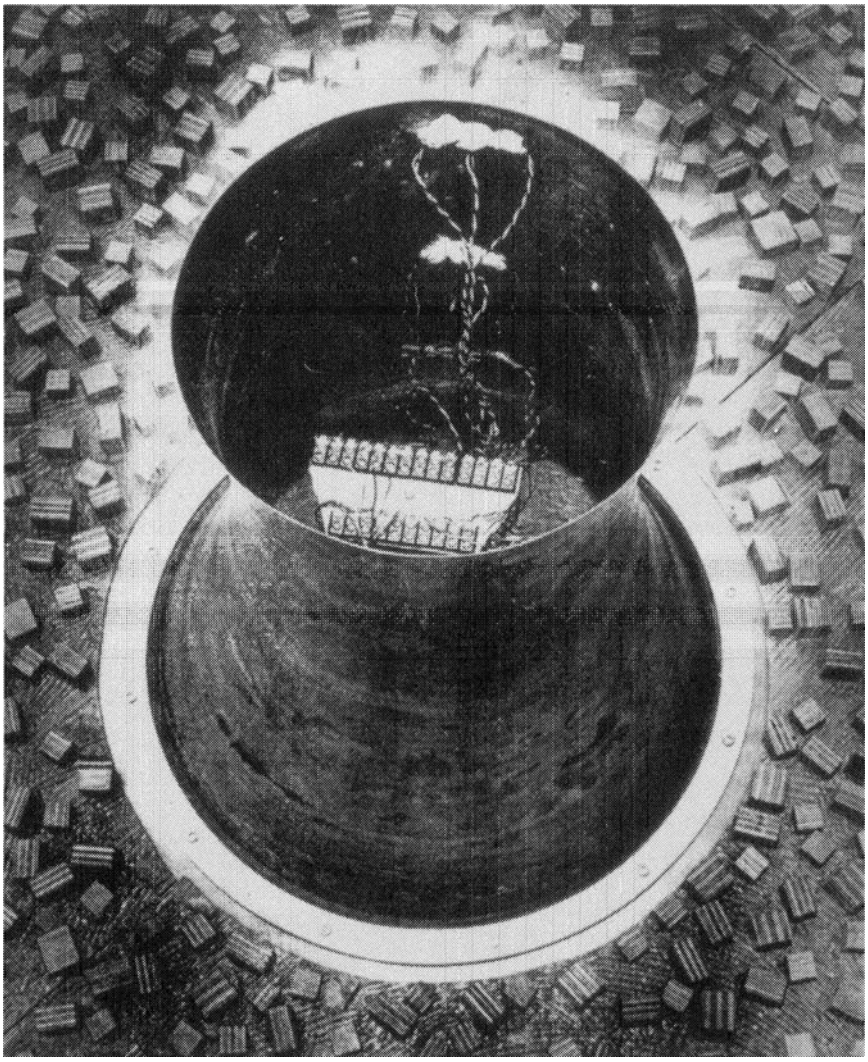

FIGURE C6.1. Photo of Replica Aeroelastic Model of a 375-Foot High Cooling Tower Model Scale $\lambda_L = 1{:}300$).

rectly, but the wall thickness was distorted to achieve the desired model stiffness. The structural system of the steel antenna above elevation 1715 feet was simulated by an equivalent spine. Full-scale measurements have confirmed the wind tunnel findings for this project (Isyumov et al. 1984).

The distortion of wall thickness results in a departure from strict replica modeling and leads to incorrect modeling of shell structures, where both axial and bending stresses are important. The equality of the mass scaling

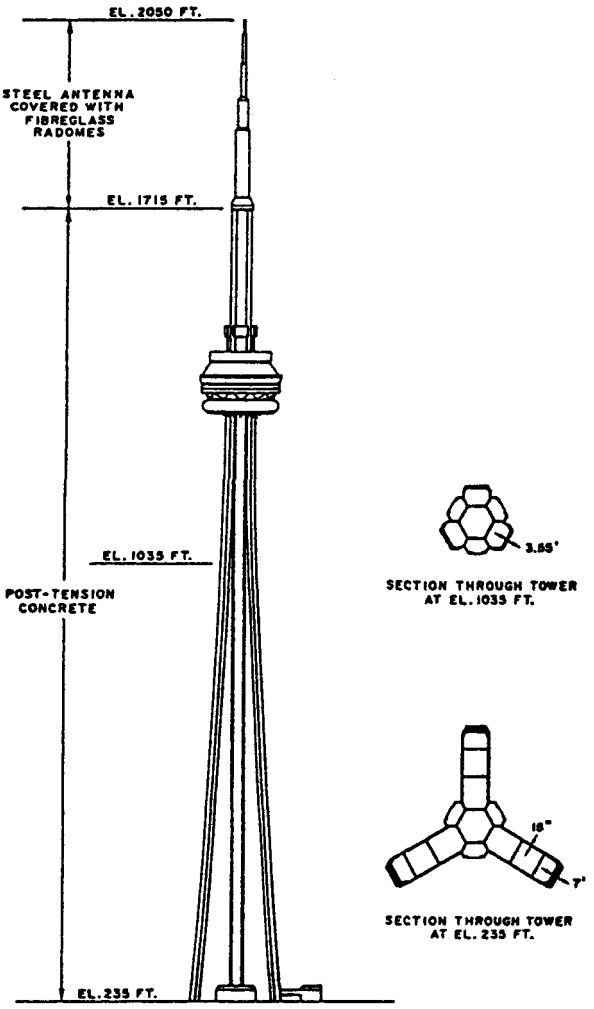

FIGURE C6.2. CN Tower, Toronto, Ontario.

parameter is a lesser problem, concentrated or distributed ballast weights can be added to adjust the mass of the model.

Replica aeroelastic models are valuable for unusual structures where analytic estimates may be difficult. For sharp-edged structures, such aeroelastic models provide direct estimates of full scale wind-induced effects. Corrections are necessary for rounded shapes when there are difficulties in achieving a similarity of aerodynamic forces at a reduced geometric scale. Despite their advantages, there are also some drawbacks. Such models tend to be expensive and are not suited for parametric studies in which structural parameters, such stiffness, mass, and/or damping are varied.

C6.3.2 Equivalent Models

Equivalent aeroelastic models are mechanical analogs designed to simulate only some aspects of the dynamic characteristics of the prototype structure. Usually, such models use a nonstructural exterior "skin" to maintain similarity of the exterior geometry and hence the aerodynamic forces, and some internal equivalent structural system, often referred to as a "skeleton" or "spine." The equivalent aeroelastic model allows greater flexibility of design and choice of model materials. However, unlike replica models, which directly lead to full dynamic similitude, equivalent aeroelastic models are designed to simulate only selected structural behavior. Consequently, the stiffness characteristics and the important modes of vibration of the full-scale structure must be determined beforehand. Both continuous and discrete structural model analogs are used. Such models are suited for both Froude number dependent and independent structures.

6.3.2.1 Continuous Equivalent Models. Continuous equivalent or "spine" models are effective for structures in which flexural, torsional, or axial force effects predominate. If the spine is to simulate only flexural and/or torsional behavior, the effective moduli become $E_{eff} = EI/L^4$ and $G_{eff} = GC/L^4$, where C is the torsional constant.

Froude Number Dependent Structures. For situations in which Froude number scaling must be observed, for example in the modeling of a suspension bridge, the velocity scale is constrained by the requirement to achieve similarity of gravity forces. The scaling of the elastic properties of the deck and cables are determined from

$$\frac{(EI)_m}{(EI)_p} = \frac{(GC)_m}{(GC)_p} = \lambda_V^2 \lambda_L^4 = \lambda_L^5 \tag{C6.3}$$

$$\frac{(EA)_m}{(EA)_p} = \lambda_V^2 \lambda_L^2 = \lambda_L^3 \tag{C6.4}$$

The attainment of an acceptable similarity of aerodynamic forces becomes an important constraint for small scale models of Froude number sensitive structures. With a geometric scale of 1:400, λ_V becomes 1:20. On the other hand, the velocity scale of a Froude number insensitive structure, with the same geometric scale, can be typically around 1:4 to 1:5. The resulting differences in the body Re can be an important limitation.

Froude Number Insensitive Structures. If the stiffness properties are predominantly the result of elastic action, the velocity scale is based on Ca similarity

and is determined by such practical constraints as available model materials and the operating velocity range of the wind tunnel. Consequently, the velocity scale for structures governed by flexural and axial force action becomes respectively,

$$\lambda_V = \sqrt{\frac{(EI)_m}{(EI)_p} \times \frac{1}{\lambda_L^4}} = \sqrt{\frac{(GC)_m}{(GC)_p} \times \frac{1}{\lambda_L^4}} \tag{C6.5}$$

and

$$\lambda_V = \sqrt{\frac{(EA)_m}{(EA)_p} \times \frac{1}{\lambda_L^2}} \tag{C6.6}$$

The quantities $(EI)_p$, $(GC)_p$, and $(EA)_p$ are chosen to reflect the total effective flexural, torsional, and axial properties of the full scale structure. For example, an allowance for shear and/or $P-\Delta$ effects can be included in $(EI)_p$, and $(GC)_p$ can reflect warping effects, as well as Saint-Venant torsion. In summary, continuous equivalent aeroelastic models can be highly effective for slender, vertical, and horizontal structures, where the dominant wind-induced structural action can be clearly delineated.

An example of a continuous equivalent aeroelastic model is the antenna of the CN Tower model, shown in Figure C6.2. The flexural properties of this antenna were simulated by an equivalent spine, built from thin-wall hypodermic needles. Nonstructural styrofoam radomes were added to achieve the required exterior geometry. Another example is the 1:400 model of a giant portal shipyard crane (Isyumov 1981), shown in Figure C6.3. In this case the flexural properties of the main girder and the two portal supports were simulated by spines with equivalent flexural, torsional properties, and fixity conditions. The model "structure" was then enclosed by nonstructural balsa-wood sections to reproduce the outside geometry.

6.3.2.2 Discrete Equivalent Models. For complicated structural systems, it is often convenient to represent the full-scale structure by an equivalent lumped parameter system comprised of a number of elastically interconnected discrete or "lumped masses." Aeroelastic modeling in such cases reduces to the simulation of the full-scale discrete parameter system by an equivalent mechanical analog, which correctly scales the prototype mass *(M)* and stiffness *(K)* matrices. These are related as follows

$$(M)_m = \lambda_M (M)_p \tag{C6.7}$$

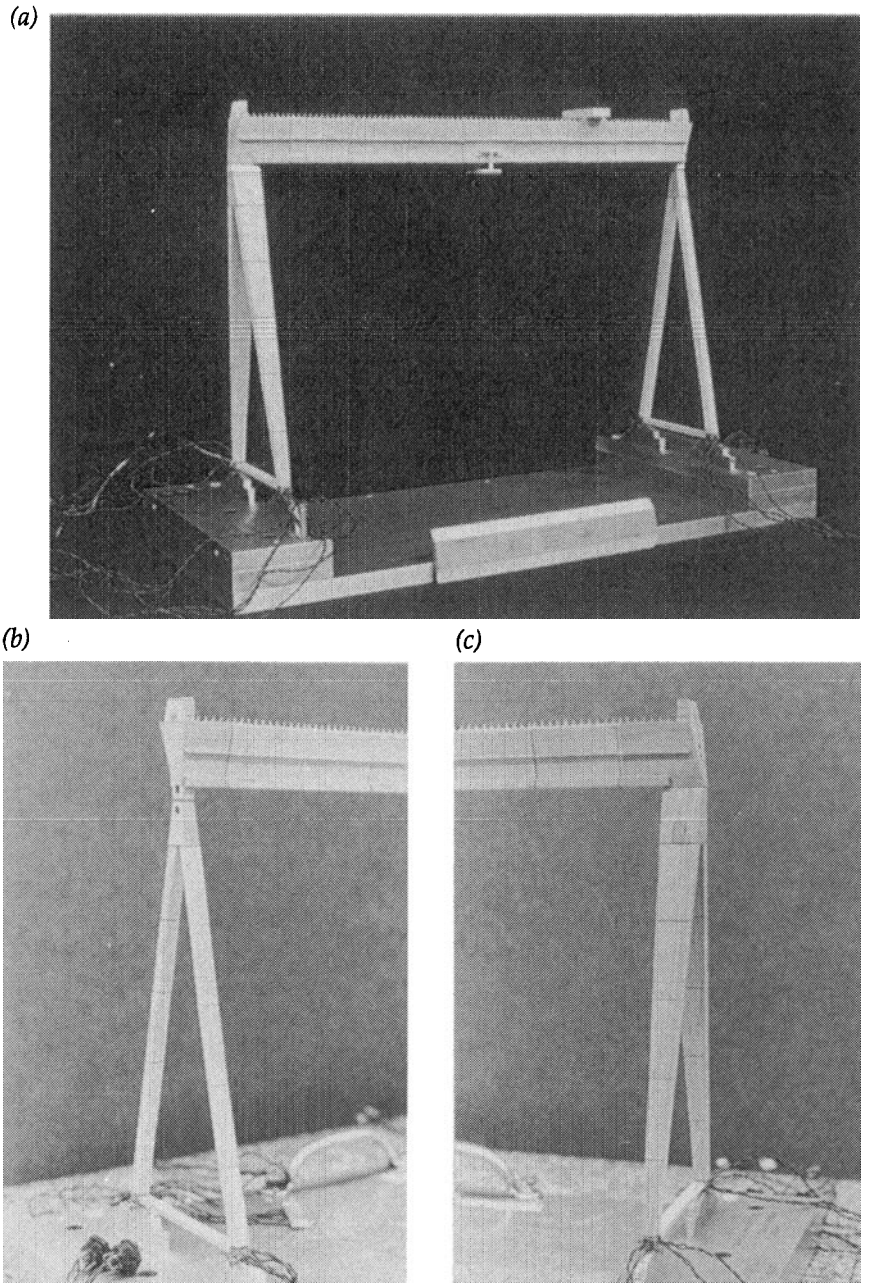

FIGURE C6.3. Photograph of Aeroelastic Model of a Shipyard Crane (Model scale $\lambda_L = 1{:}400$). (a) View of Completed Model. (b) Close-up of Pinned A-Frame Support. (c) Close-up of Fixed A-Frame Support.

and

$$(K)_m = \lambda_K (K)_p \tag{C6.8}$$

where λ_M and λ_K are the mass and stiffness scaling parameters.

The mass scaling parameter λ_M becomes as follows:

For Translation:
$$\lambda_M = \frac{L_m^3 \rho_{s_m}}{L_p^3 \rho_{s_p}} = \lambda_L^3 \lambda_{\rho_s} \tag{C6.9}$$

For Rotation:
$$\lambda_{I_M} = \frac{L_m^5 \rho_{s_m}}{L_p^5 \rho_{s_p}} = \lambda_L^5 \lambda_{\rho_s} \tag{C6.10}$$

In most situations $\rho_{s_m} \approx \rho_{s_p}$ and λ_M and λ_{I_M} become $\lambda_L{}^3$ and $\lambda_L{}^5$ respectively.

The stiffness scaling parameter λ_K is determined by the Cauchy number, using the actual or the effective elastic modulus, as in the case of approximate structural systems. In the absence of Froude number scaling requirements, the velocity scale is constrained by practical considerations and by the need to achieve a minimum body Reynolds number.

For a consistent scaling of all relevant modes of vibration, the velocity scale becomes,

$$\lambda_V = \frac{V_m}{V_p} = \lambda_L \lambda_f = \frac{\lambda_L}{\lambda_t} \tag{C6.11}$$

where $\lambda_t = 1/\lambda_f$ is the overall time scale of the simulation.

Having chosen the velocity scale for the simulation, the stiffness scaling becomes,

For Translation:
$$\lambda_K = \frac{\lambda_M \lambda_V}{\lambda_L \lambda_t} = \lambda_L \lambda_V^2 \lambda_{\rho_s} \tag{C6.12}$$

For Rotation:
$$\lambda_K = \frac{\lambda_M \lambda_V}{\lambda_t} \lambda_L = \lambda_L^3 \lambda_V^2 \lambda_{\rho_s} \tag{C6.13}$$

In most wind tunnel simulations, $\rho_m \approx \rho_p$ and, consequently $\lambda_{\rho_s} \approx 1$. Nevertheless there may be situations where the densities of the model and prototype are different. For example, measurements carried out in a wind tunnel, situated near sea level are not directly applicable for a structure to be located

in a mountainous region. The air density ratio in such a case may typically be $\rho_m/\rho_p = 1.15$, and adjustments become necessary to all previously presented equations in which the air density ratio was assumed to be unity.

The use of discrete models offers distinct advantages for aeroelastic simulations of tall buildings. With a suitable mechanical analog, it is usually possible to adequately simulate both inertial and elastic properties, including both inertial and elastic coupling. The choice of the degree of detail necessary for a representative aeroelastic model depends largely on the anticipated complexity of the full-scale response to wind loading. For example, the dynamic wind-induced response of many tall buildings is predominantly in the two fundamental sway modes of vibration. Consequently, if torsional loads are not expected to be significant, a rigid aeroelastic model, spring mounted at the base to simulate two translational degrees of freedom, may be sufficient. Because of its inherent simplicity, this type of model with linear mode shapes offers maximum freedom for varying the building mass, the frequency ratio, and the structural damping. Multi-degree-of-freedom models, with typically 4 to 7 lumped masses, each with two translational and one rotational (about the vertical axis) degrees of freedom, are sufficient for most buildings, where a more detailed modelling is justified.

C6.3.3 Section Models

Dynamically scaled partial or "section" models are valuable tools to study the action of wind on certain slender, high aspect-ratio structures. These include such line-like structures as long-span bridges, cables, and slender chimneys and towers, where body motion induced effects can be significant. The study of the aerodynamic stability of bridge sections is a particularly important application (see Section C6.8).

Section model tests are used to evaluate various aerodynamic derivatives, used in conjunction with theoretical models of the process (Scanlan 1982, Vickery 1982). Such models provide a rigid representation of a portion of the structure mounted dynamically. Sometimes, these models are "driven" externally. This approach is an important technique for studying non-linear aspects of the process including the aerodynamic damping (Steckley 1989). Such tests can be carried out in smooth flows or in turbulent flows generated with coarse grids or active turbulence generators (Bienkiewicz et al. 1983, Davenport and King 1984, Scanlan 1982, Vickery 1982).

Important advantages of section models are their simplicity and the use of relatively large models. The larger geometric scale permits the inclusion of details and results in a larger body Reynolds number. Principal disadvantages are difficulties with achieving a representative flow simulation and the inability to examine the effects of wind direction and the influence of the immediate surroundings.

C6.4 AEROELASTIC MODELING OF TALL BUILDINGS

C6.4.1 Introduction

As discussed elsewhere (Isyumov 1982), aeroelastic models of tall buildings tend to be of the discrete type, with the complexity of the model chosen to capture the anticipated wind-induced structural action of the prototype structure. An important consideration in studies of tall buildings is their complex environment, which must be included in the simulation. Such "proximity" models reproduce all major buildings and structures in the "near field," typically taken as 300 to 800 m from the site. Of particular importance is the inclusion of major nearby buildings, which could lead to aerodynamic interference effects. Two commonly used aeroelastic building models are briefly discussed below.

C6.4.2 Traditional "Stick" Aeroelastic Models

This earliest type of aeroelastic model used in wind tunnel studies of tall buildings is schematically shown in Figure C6.4. The building is represented by a rigid body model, pivoted at the base or some other location and restrained with springs to simulate 1 or 2 orthogonal fundamental sway modes of vibration. The mounting hardware consists of a set of gimbals located at the selected pivot point and a rigid rod extending below the model and restrained with appropriately selected springs. The other components are force transducers, which measure the wind-induced overturning moment, a ballast weight, adjustable to achieve correct inertial scaling, and an electro-magnet that provides eddy-current damping to the model.

This type of model, with variations in the supporting hardware, has traditionally been used in studies of slender tall buildings for which the wind-induced response is principally in the two fundamental sway modes and in which the fundamental torsional and higher modes of vibration are judged to be secondary considerations. This tends to apply to buildings of compact shape with a tube-like structural system, or in situations where the across-wind vortex-shedding induced response is expected to dominate.

The mass and stiffness matrices for a stick model are (2 × 2) diagonal matrices, and it is convenient to use rotational degrees of freedom to describe the model motion. Normally, the full-scale mode shapes are only approximately linear, and the generalized mass of the prototype building in each of the two fundamental sway modes of vibration is used to determine the model mass moment inertia about the pivot point, $z = a$. Based on the mode shape in the x-direction,

$$I_{M_m} = \lambda_{I_m} \left[(h-a)^2 \int_0^h m(z)\, \mu_x^2(z) dz \right]_p \qquad \text{(C6.14)}$$

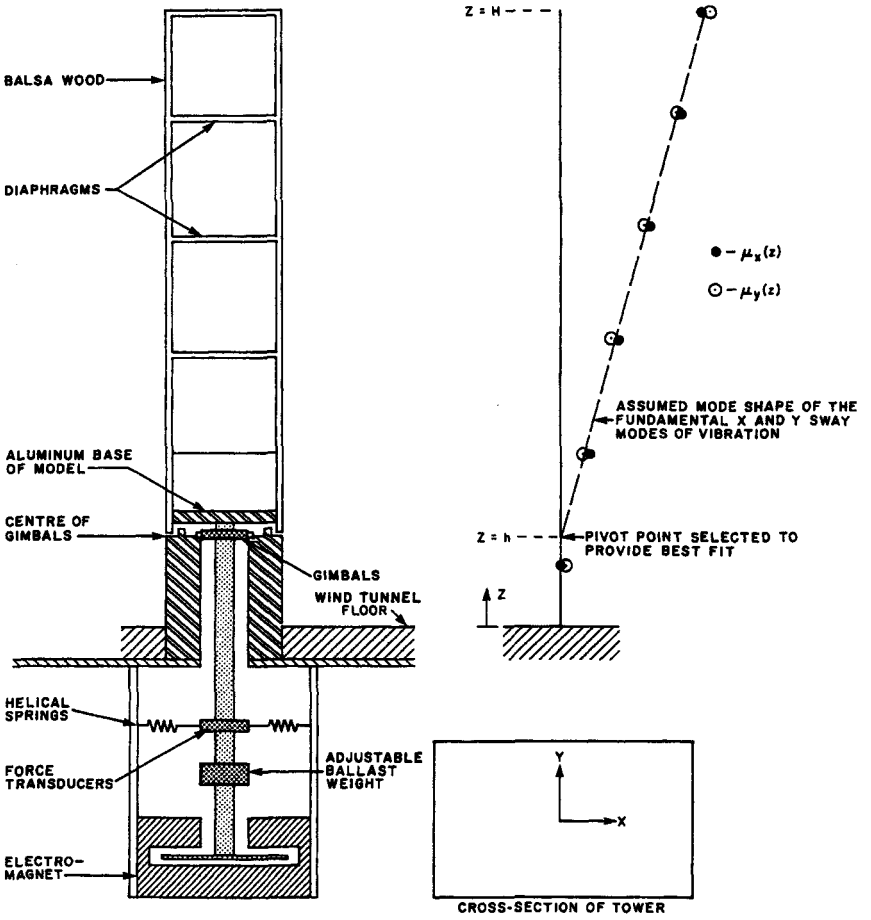

FIGURE C6.4. Schematic Representation of a "Stick" Aeroelastic Building Model. Source: Isyumov 1982; reprinted with permission of Cambridge University Press.

where $m(z)$ is the mass per unit length of the building and $\mu_x(z)$ is the normalized x-direction fundamental mode shape [$\mu_x(z = h) = 1$].

A similar expression for I_{M_m} is obtained using the mode shape in the orthogonal y direction. The pivot point $z = a$ is selected to provide the best fit for these two estimates. With prototype mode shapes significantly different from a linear variation with height, corrections should be considered. Such corrections should examine the sensitivity of the joint acceptance functions in the fundamental modes to differences in mode shape and require information on the cross-spectra of the time varying wind load at various heights along the building (Vickery et al. 1985).

The simplicity of the "stick" model is both its principal advantage and disadvantage. The model is cost and time effective and offers flexibility in examining variations in the building mass, stiffness, and damping. On the other hand, its use is limited to studies of buildings governed by drag or lift induced sway loads.

C6.4.3 Multi-Degree-of-Freedom Models

This type of model is suited for aeroelastic studies of more complex buildings, where torsional effects are judged to be important and/or in situations where the modes of vibration are highly three-dimensional because of inertial and/or elastic coupling. A schematic representation of a typical multi-degree-of-freedom aeroelastic model is presented in Figure C6.5. In this case, the building has been divided into four zones, each represented by a lumped mass. The masses are primarily concentrated at the rigid or flexible floor diaphragms. The diaphragms are connected by flexible columns and the entire mechanical system is enclosed by a nonstructural skin, which reproduces the exterior geometry. This skin is discontinuous with slits separating the various zones of the model. The mass of the flexible columns, the exterior skin, and any added instrumentation are included in the total mass budget of the model. The structural damping is usually obtained by adding interfloor dampers. These range in complexity from visco-elastic columns to damping tapes attached between adjacent floors. Other possibilities are miniature dash-pots and eddy-current devices. Generally, the required damping is attained by trial and error.

The four lumped mass, 12-degree-of-freedom representation, as shown in Figure C6.5, is sufficient for the study of most tall buildings. Up to 7 lumped masses have been used in unusually complex buildings, whereas 3 lumped masses have been found to be sufficient for buildings of intermediate height (Isyumov 1982). The sway wind-induced response of tall buildings is predominantly in the fundamental sway and torsional modes of vibration, and the inclusion of higher modes results in marginal improvements (Isyumov and Halvorson 1984).

The mechanical systems of multi-degree-of-freedom models vary in complexity. Relatively simple structures can often be modeled with "lumped" masses, represented by rigid plates interconnected with elastic columns. More complicated structural systems may require the modeling of column shortening and/or the bending of the floors. Schematic representations of stiffness elements used in such models are shown in Figure C6.6. The flexible columns are "built-in" at the floor diaphragms in all cases. The floors remain essentially horizontal in the Type 1 element. Floor rotation is achieved in the Type 2 and 3 elements by the addition of extension elements at the inflexion points of the columns (see Type 2), or the addition of bending elements in the floors (see Type 3). In the latter case, the floor is represented by two rigid diaphragms

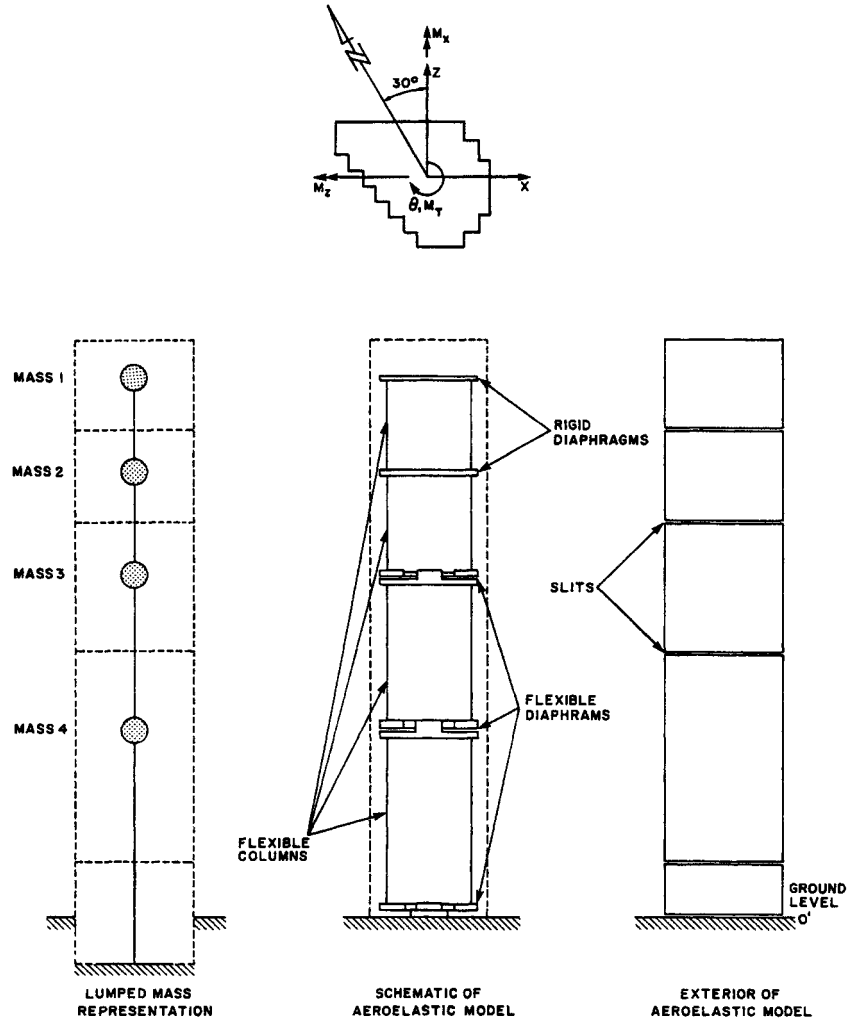

FIGURE C6.5. Schematic Representation of a Multi-Degree-of-Freedom Aeroelastic Building Model.

Source: Isyumov 1982; reprinted with permission of Cambridge University Press.

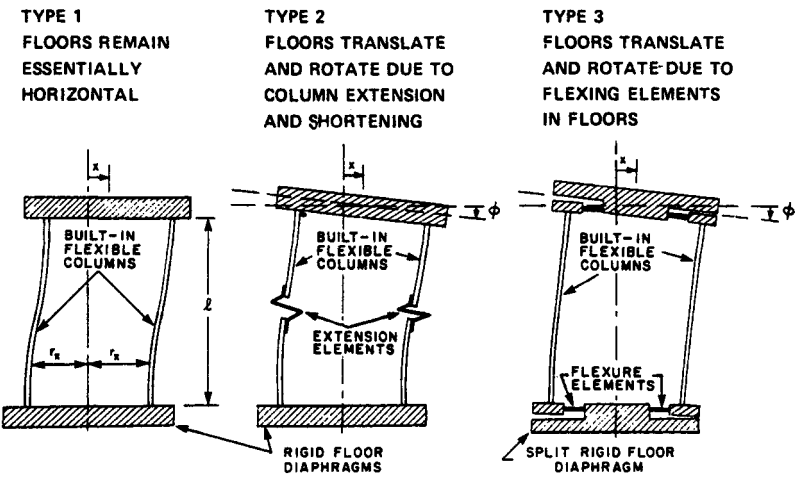

FIGURE C6.6. Stiffness Elements Used in Multi-Degree-of-Freedom Aeroelastic Building Models.

Source: Isyumov 1982; reprinted with permission of Cambridge University Press.

connected by leaf-springs. A photograph of a model using bending floor elements is given in Figure C6.7. The simple Type 1 mechanical element, is usually satisfactory for situations in which the ratio of the fundamental torsional to the fundamental sway frequencies is less than about 1.5. A more complex system is usually needed for higher frequency ratios (Isyumov 1982).

The main advantage of the multi-degree-of-freedom model is its ability to simulate complex structural behavior, including both sway and torsional degrees of freedom. Its main disadvantages are its greater complexity of design and fabrication—and consequently greater cost. Also it is more difficult to vary such structural properties as stiffness, mass, and damping.

C6.5 TOWERS, MASTS, AND CHIMNEYS

The aeroelastic modeling of towers, masts, and chimneys frequently use equivalent models. Freestanding structures are often simulated by models which reproduce the flexural characteristics, using appropriately designed "spines" (see Section C6.3.2.1). For guyed masts, as in the case of suspension bridges, it becomes necessary to observe Froude number similarity. Chimneys and some masts and towers often have circular cross-sections, and Reynolds number scaling becomes an important complication. In such situations, it is necessary to make Reynolds number corrections when translating the results of wind tunnel tests to full scale. Results in the wind tunnel are typically carried out at subcritical Reynolds numbers and adjustments to

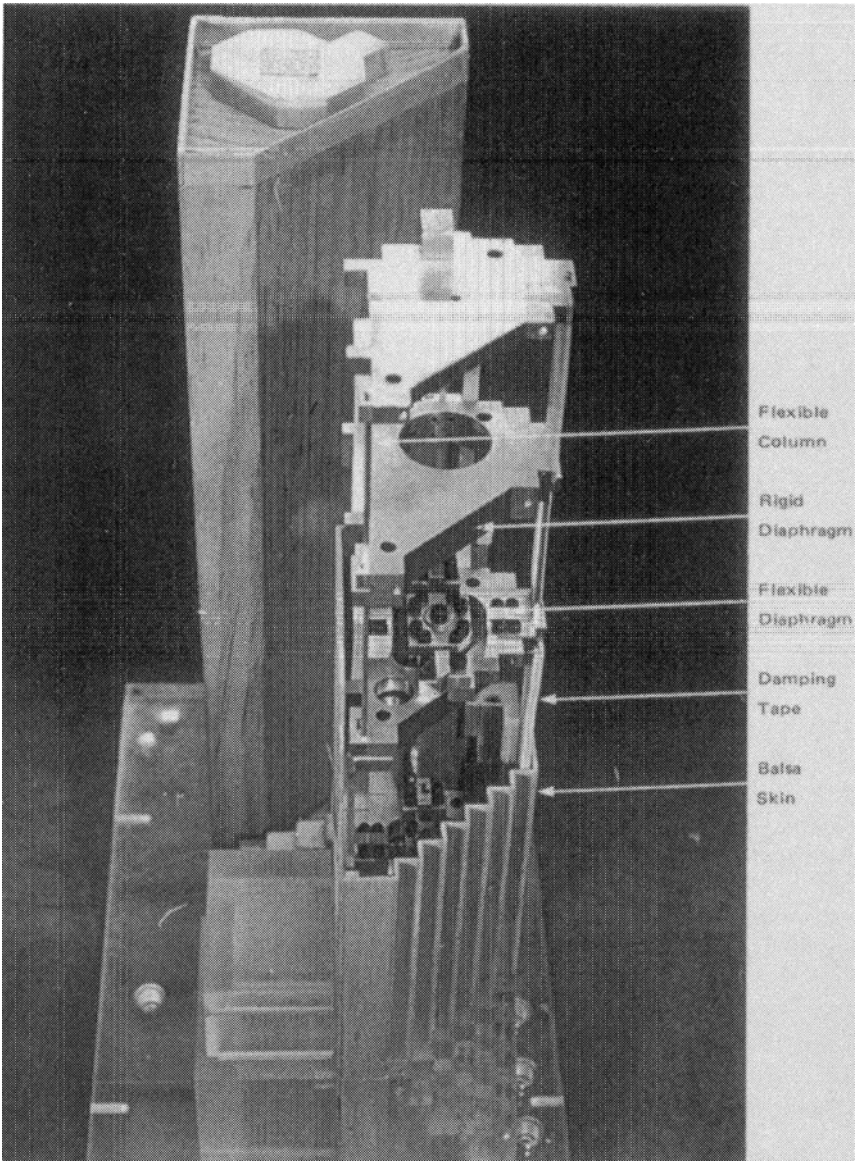

FIGURE C6.7. Photo of Components of a Multi-Degree-of-Freedom Model of a 670-Foot Building (Model Scale λ_L = 1:500).

the static and dynamic drag coefficients, the dynamic lift coefficient and the Strouhal number are appropriate. Without such adjustments, wind tunnel tests at subcritical Reynolds numbers can be prohibitively conservative.

A common approach for modeling latticed towers and masts is to scale the product of $d \times C_D$, where d is a typical member dimension and C_D is the drag coefficient. Namely,

$$\frac{(dC_D)_m}{(dC_D)_p} = \lambda_L \tag{C6.15}$$

Although this technique is effective for single members, it can lead to errors for groups of members in which interference effects can be important. In view of the difficulties of directly transferring model information to full-scale, wind tunnel model studies of towers, masts, and chimneys are often carried out to support analytical models rather than to provide information that directly predicts full-scale behavior.

C6.6 COOLING TOWERS

Aeroelastic studies of cooling towers have used replica aeroelastic models. Unfortunately, the availability of model materials with sufficiently low Young's moduli is limited. As a result, it becomes difficult to simulate significant full-scale wind speeds in most boundary layer wind tunnels. A distortion of the wall thickness poses difficulties, as both bending and membrane stresses are important for these structures.

Dissimilarities of model and prototype Reynolds numbers are a complication. Fortunately, the aspect ratio of cooling towers is relatively small and the tip effect becomes important. As a result, overall horizontal forces, and hence vertical strains and stresses, are not particularly Reynolds number sensitive. On the other hand, circumferential pressure patterns do vary substantially with Reynolds number, and corrections are appropriate.

Much of the dynamic response of cooling towers is the result of the excitation by background turbulence. Aeroelastic effects are not particularly important and the principal advantage of an aeroelastic model is that it can provide direct information on wind-induced stress distributions within the cooling tower shell. This requires a replica aeroelastic simulation.

C6.7 FLEXIBLE ROOFS

Flexible roofs which resonate under wind action are unusual, and aeroelastic models of these structures are carried out either in situations in which there

is a considerable uncertainty about the overall or local dynamic behavior of the roof or for unusually complicated geometries that cannot be effectively studied through measurements of local pressures and suctions. Current experience indicates that wind-induced resonant vibrations are unlikely if the fundamental frequency of vibration exceeds about 1 Hz. Figure C6.8 illustrates the additional resonant contribution to the peak bending moment in a roof girder of a large hangar. The full scale fundamental frequency of the roof in this case is 0.5 Hz. For this girder, 90% of the variance, or about 95% of the RMS bending moment, is the result of vibrations associated with excitation by background turbulence. As a result, the scaling of mass and structural damping which influence resonant vibrations can be more approximate.

Examples of situations where the modeling of the pneumatic stiffness of air-supported, fabric, and other flexible roof structures can be found in Tryggvason and Isyumov (1977) and Tryggvason (1979).

The pneumatic stiffness of internal volumes plays an important role for air-supported structures and roof systems with fully or partially enclosed internal volumes. To obtain similarity of pneumatic stiffness, enclosed internal volumes must be scaled to achieve

$$\lambda_{vol.} = \frac{\lambda_L^3}{\lambda_V^2} \tag{C6.16}$$

The development of solid-state pressure scanning systems that allow simultaneous measurements of fluctuating pressures at many locations (see Chapter C5), has largely replaced the use of aeroelastic models for these structures. Simultaneously measured time-varying pressures can be used to determine the generalized forces for particular modes of vibration. Estimates of the response are then made analytically. The aerodynamic damping must be assumed in such estimates. In many situations this results in conservative estimates of the resonant induced vibrations, as the aerodynamic damping tends to be positive. However there can be exceptions.

C6.8 LONG-SPAN BRIDGES

C6.8.1 Introduction

It is advantageous to carry out a study of the wind characteristics at the proposed site to assist in the planning of the wind tunnel model study. This should examine the effects of location and fetch on both extreme winds and the expected turbulence at the bridge. These considerations, dealt with elsewhere (Cermak 1982), will not be treated in detail in the present commentary.

The steady horizontal forces resulting from the wind on the bridge are usually adequately accounted for (i.e., conservatively estimated) in struc-

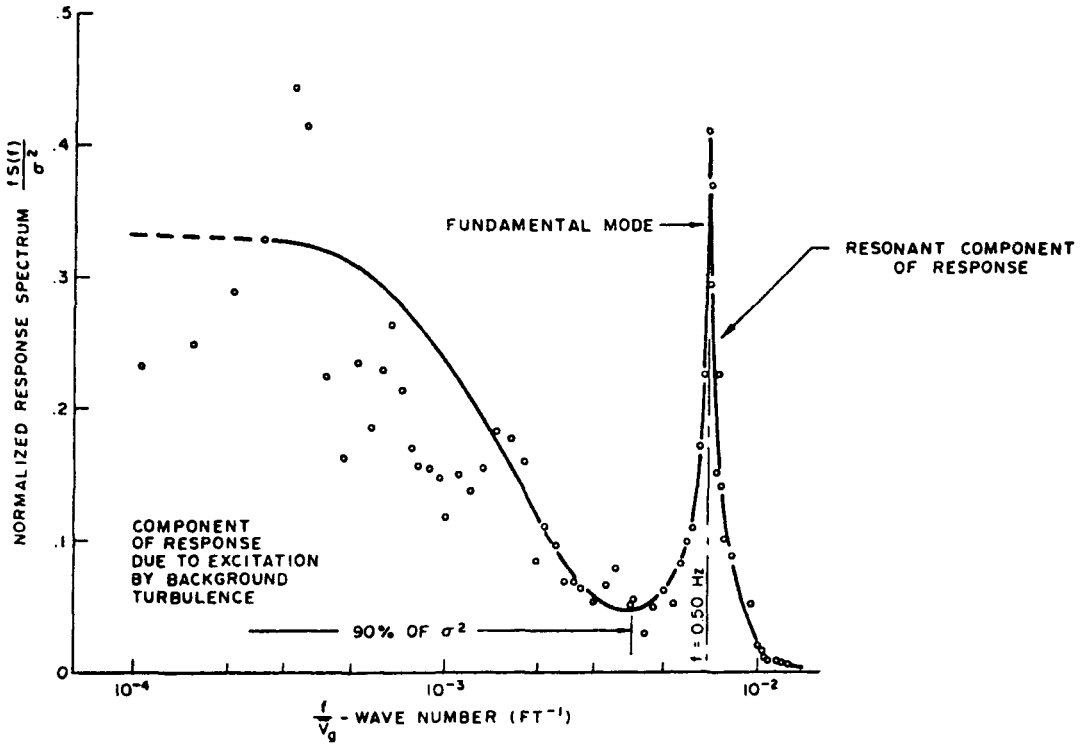

FIGURE C6.8. Illustration of the Relative Importance of the Effects of Resonant Vibrations for a Large Hangar Roof.

tural analyses. This is because long-standing experimental results for drag forces on bluff bodies are by now quite well known and adequately specified in codes and elsewhere. However, there also are unsteady forces that require special attention. The most important of these are the result of either the turbulence of the wind or the motion of the structure.

Wind turbulence may occur in either the approach flow (generated by the upstream fetch) or, more locally, as a "signature" effect caused by the bridge itself, as the flow passes by its windward edges and continues downstream across and under the deck.

Long-span bridges can deflect appreciably under the action of wind forces; this motion can cause new wind forces to be generated. In the historical case of the Tacoma Narrows Bridge, oscillations of the bridge deck increased in amplitude and led to an instability of the structure.

To preclude such occurrences, all important new bridge designs—particularly long, flexible spans—are routinely subjected to stability and buffeting studies. Of these, the stability study must be considered the primary one, because large amplitude oscillations and—at worst a recurrence of a Tacoma-like disaster—are unacceptable. A buffeting analysis based on experimental studies provides information on the wind loads at design wind speeds.

Although, as mentioned above, it is usually possible to make a theoretical, conservative estimate of the drag (along-wind) forces on a bridge deck and towers, it is more difficult to make a theoretical estimate of the lift (vertical, across-wind) and torsional forces. It is virtually impossible to make theoretical estimates of the time-varying forces acting on an oscillating bridge. For these reasons, it is necessary to have recourse to the wind tunnel, using bridge test models as "analog computers."

C6.8.2 Models and Scaling

Full bridge and partial bridge models have been used. The latter have taken a number of different forms. The most basic of the partial bridge models has been the section model, which represents a section of the deck mounted on springs. Other partial models have included deck simulations variously supported across the wind tunnel with taut wires, tubes, or other support systems.

For a model to serve as an analog source of force or response data, certain scale ratios must be established and respected. Typical model-to-prototype scale ratios include λ_L (geometric length); λ_ρ (density); λ_V (velocity). The density ratio λ_ρ is usually near unity, while λ_L and λ_V are fixed mainly by the size of the model and available wind tunnel speeds. If turbulence is introduced into the wind tunnel flow, it is important that its intensities correspond to those in full-scale and that typical turbulence (eddy) lengths are scaled in accordance with λ_L. Full scaling of the atmospheric turbulence is

impractical at geometric scales used in section model tests. In such cases, partial simulation of turbulence up to scales of turbulent eddies comparable to that of the deck width have been found effective. Quasi-steady theoretical adjustment to the response can be done with confidence to allow for the effects of larger eddies (Davenport and King 1984).

Occasionally, especially for full models of suspension bridges, Froude number similarity is required in situations in which gravity forces substantially contribute to the stiffness. In such cases, the Froude numbers for model and prototype must be equal, that is,

$$\left(\frac{V^2}{Bg}\right)_m = \left(\frac{V^2}{Bg}\right)_p \tag{C6.17}$$

where

V = velocity of wind
B = typical dimension, usually deck width
g = acceleration of gravity

Since the acceleration of gravity is unchanged between model and prototype, $\lambda_g = 1$ and Froude scaling implies that

$$\frac{\lambda_V^2}{\lambda_L \lambda_g} = \frac{\lambda_L}{\lambda_t^2} = \lambda_L \lambda_f^2 = 1 \tag{C6.18}$$

where λ_t and λ_f are time and frequency scales, respectively. Hence the scale of the oscillation frequencies becomes,

$$\lambda_f = \frac{1}{\sqrt{\lambda_L}} \tag{C6.19}$$

while the wind velocity is scaled as

$$\lambda_V = \sqrt{\lambda_L} \tag{C6.20}$$

In studies involving full bridge models of cable-stayed bridges, it is usually possible to avoid Froude number scaling if a pretensioning of the stay cables to the design dead-load tension is performed to avoid the slackening of the model stays during a test.

The scaling of the reduced velocity is required in all dynamic modeling situations. Correspondingly,

$$\left(\frac{V}{fB}\right)_m = \left(\frac{V}{fB}\right)_p \tag{C6.21}$$

where f is the frequency of interest, either of the fluid or the structure.

For dynamic models in free oscillation, the damping ratio ζ (proportional to the logarithmic decrement) must be the same in the model as in the prototype.

Under all scaling available in atmospheric wind tunnels, the Reynolds number is generally too low by several orders of magnitude. This practical obstacle requires that structural features deemed to be Reynolds number sensitive be given particular aerodynamic attention. In general, this implies that fine geometric details may develop excessive drag, while curved surfaces may exhibit model flow characteristics not fully representative of the prototype. For surfaces with sharp edges, however, Reynolds number effects are minimal providing that the model *Re* exceeds some minimum value (see Chapters 2 and C2). A general review of wind tunnel scaling is presented in Simiu and Scanlan (1986).

C6.8.3 The Full Bridge Model

Full bridge models require engineering attention both to geometric/aerodynamic form and to bridge structural dynamics. To minimize Reynolds number effects, the geometric scale λ_L should be made as large as feasible. Scales as large as 1:100 have recently been realized for full bridge models. However, large scale models require comparably large wind tunnel facilities (Davenport and King 1984, Miyata et al. 1992, Reinhold et al. 1992, Irwin 1992). In a few cases, special wind tunnels have been constructed to this end.

It is difficult to construct models to required scales that are simply of the "structural replica" type (i.e., exact structural duplicates with all dimensions at geometric scale). In most cases, it is necessary to create a substitute internal structural system, which simulates the main deflectional characteristics of the structure. For example, the deck structure may be represented by an equivalent spine or flexible strip to which light non-structural geometric duplicates of the deck are attached. Mass and damping must be correctly scaled in such equivalent systems. Cable elements typically have stiffness duplicated by fine wires with mass duplicated by spaced, concentrated weights. Analogously, tower structures typically have a flexible structural skeleton, enclosed with appropriately shaped light, external forms.

An important consideration is to construct the model accurately enough so that the successive, scaled modes and frequencies of the entire structure align with those of the prototype. The damping of each mode should correspond to that assumed for the prototype. For the reasons enumerated, the

creation and use of a properly scaled full bridge model become a major engineering challenge.

The structural response can be monitored with appropriate instrumentation such as strain gauges, accelerometers, deflection transducers, and so on.

Full bridge models, once correctly established, offer the possibility of extensive explorations of prototype conditions, such as the effects of winds at various approach angles, velocity profiles, turbulence levels (which also must be appropriately modeled), special effects that may be caused by unusual topography and upwind obstacles, and so on. Such models are highly effective in studies of bridge performance during different stages of construction. A full aeroelastic model of a long-span cable stayed bridge is shown in Figure C6.9. Erection stages as well as the completed bridge were tested.

C6.8.4 The Section Model

In view of the extent of technical care required to create and exploit full bridge models, various limited or abridged models are often sought. The most elementary and, in a number of ways, the most productive and economical of these is the section model.

This consists of a typical rigid section of the deck of the long-span bridge, geometrically/aerodynamically similar to the prototype, mounted in the wind tunnel in such a way as to permit measurement of the wind-produced static and dynamic lift, drag, and moment and dynamic motion-related forces.

This section model is usually equipped with end plates channeling the flow over it, or is located between parallel walls of the wind tunnel.

In a fixed position, the section model can be instrumented to measure lift, drag, and moment per unit length of the bridge deck. Typically these are specified as follows

Lift: $$L = \tfrac{1}{2}\rho V^2 B C_L \tag{C6.22}$$

Drag: $$D = \tfrac{1}{2}\rho V^2 B C_D \tag{C6.23}$$

Moment: $$M = \tfrac{1}{2}\rho V^2 B^2 C_M \tag{C6.24}$$

where ρ is air density, B is deck model width, and C_L, C_D, and C_M are dimensionless lift, drag, and moment coefficients, respectively.

As first used in early applications, the section model was conceived of as a kind of "stand-in" for the prototype bridge. Because its dynamics and aero-

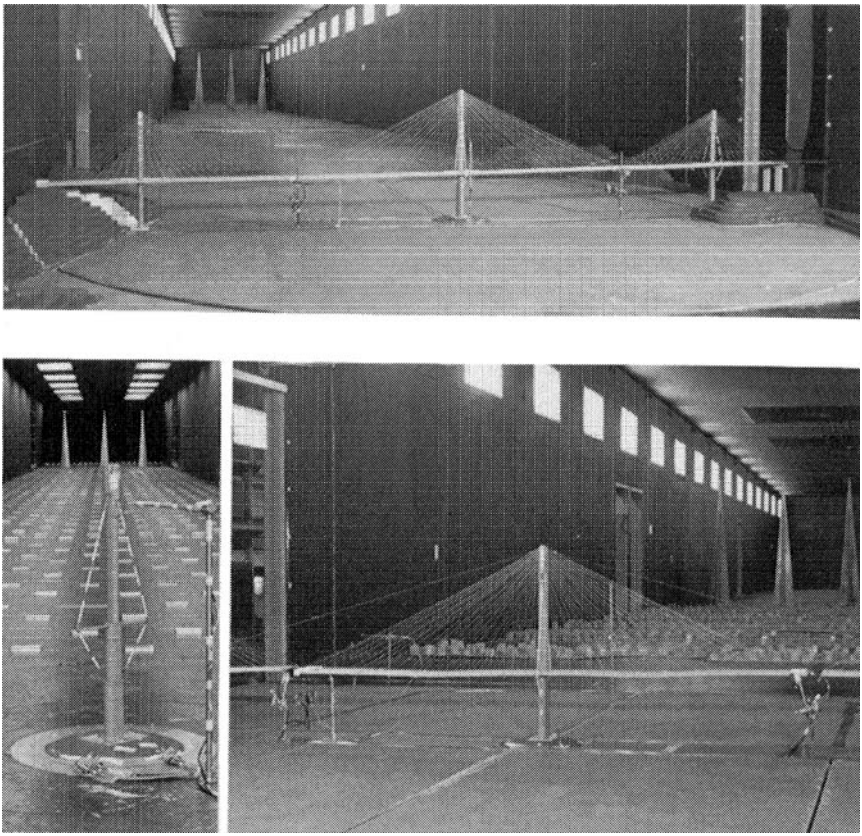

FIGURE C6.9. Photos of Aeroelastic Models of a Long-Span Cable-Stayed Bridge Tested at Various Stages of Completion (Model Scale $\lambda_L = 1{:}250$)

dynamics cannot fully duplicate those of the full bridge, interpretation of its role is required. Research in recent years has emphasized this fact and has better defined the limited but very important role of the section model.

Mounted on springs, with scaled mass, mass moment of inertia, structural damping, and natural frequency, the section model is commonly used to investigate the dynamic response as a result of vortex shedding; to ensure that the section is aerodynamically stable up to an acceptably high prototype wind speed; and to determine the response to turbulent buffeting (Hjorth-Hansen 1992). Usually, the effect of turbulence is to reduce or mask the vortex shedding-induced amplitude peaks. For this reason, tests are conducted in flow conditions with a low turbulence intensity in order to conservatively estimate the amplitudes of motion. Various edge treatments can be

investigated to improve the response to vortex shedding. The model is also tested with the same low turbulence flows to provide conservative estimates of the flutter behavior of the section. The response is often investigated at various structural damping ratios.

A uniform grid, spires, or active turbulence generators are used to provide simulations of scaled atmospheric turbulence. Measured buffeting response can be interpreted using an appropriate theory to provide estimates of prototype wind loading that can be used in the design specifications for the bridge, during construction and when fully completed (Davenport and King 1984).

Just as the section model is an analog source for the measurement of static-force coefficients, so also it can be employed to measure motion-related effects. Mounted on springs, or driven through sinusoidal motions, the section model in the wind attracts aerodynamic forces proportional to the bridge motion and to the time derivatives thereof. These so-called "flutter" forces are usually measured and codified with the aid of a background theoretical framework. The latter has been provided in the literature (Scanlan 1982, Davenport and King 1984, Scanlan 1992). Section model tests can, therefore, provide information on static-force coefficients and on "flutter derivatives" which, used later in the dynamic theory of the entire bridge, serve to predict its performance and ultimate stability. In this role the section model serves a very fundamental purpose.

An important parallel role, in this regard, is that flutter derivative tends also to serve as a kind of information index as to stability tendencies for any given section shape. Thus, in the design stage, certain evolutions of the flutter derivatives with wind velocity (notably the torsional damping derivative) act as indicators of the effect of deck geometry on bridge stability. As such they can be—and are—used to aid in bringing a bridge deck contour to a satisfactorily stable form.

In the process of exploiting flutter derivatives, a number of schemes for obtaining them in an efficient manner have been developed (Sarkar et al. 1992, Davenport et al. 1992, and Raggett and Scanlan 1993). Two basic approaches to extract the flutter derivatives have been (1) to permit free oscillation of the section model and to infer the derivatives from the observed model motion (typically, decaying sinusoidal oscillation) and (2) to drive the model through prescribed sinusoidal motions and collect—via numerous pressure taps—the alternating pressures acting over it, and integrate these pressures to obtain the oscillatory forces. The freely oscillating schemes have the advantage of simplicity, while the forced oscillation, pressure-integration techniques allow working at wind speeds offering somewhat greater Reynolds number independence, as well as studies in turbulent wind. References such as Simiu and Scanlan (1986) and Scanlan (1992) discuss some of the major uses of section models.

C6.8.5 Other Bridge Models

A model possessing certain spanwise dynamic properties may consist of an elastically simulated deck extended across the wind tunnel, as for example by tensioned wires. Such a model (often called a "taut strip") provides a full-span simulation of the bridge, which can be tested in representatively scaled turbulent boundary layer flows (Davenport et al. 1992). It has the important advantage of being exposed to and integrating three-dimensional effects of wind turbulence, which can be quite accurately simulated. The model can sometimes also be endowed with elastic properties causing it to possess modal forms approximating the lower modes of the prototype bridge.

With all models, it is necessary to *interpret* the action of the model when predicting prototype behavior. To transfer taut-strip model results to the prototype invariably requires an analytical interpretation.

C6.9 CABLES AND TRANSMISSION LINES

Aeroelastic models are essential to the study of aerodynamic forces on cables which can undergo large wind-induced motions. Often this is achieved through section model tests or aeroelastic models of particular spans. The methodology here is similar to that described in connection with bridges (see Section C6.8). A particularly important question is the "galloping" of iced conductors. Reynolds number similarity is important for both uniced and iced cables.

As in other "line-like" structures, it is possible to develop reliable analytical models, and wind tunnel tests are often used to provide information on aerodynamic coefficients and derivatives.

This page intentionally left blank

Chapter C7
DISPERSION AROUND BUILDINGS

C7.1 GENERAL

Much progress has been made with numerical models of various atmospheric dispersion scenarios. Nevertheless, physical modeling in wind tunnels remains an indispensable tool for evaluating atmospheric dispersion in complex settings. These include:

1. The effects of unusual topography which can lead to unexpected impingement of plumes or situations of aerodynamic downwash and entrapment of plumes.
2. Situations of unusual thermal stratification which may lead to exceptionally slow or rapid dispersion. Frequently this is compounded by the additional effects of unusual topography.
3. The dispersion from elevated or ground sources in very rough terrain, as experienced in built-up urban areas. This includes the street canyon problem, as well as the dispersion from low and intermediate point sources.
4. Reingestion of exhaust gases into fresh air intakes or through operable curtainwalls.

Guidelines for physical model studies of atmospheric diffusion have been developed by the EPA (Snyder 1981). Although the dispersion around buildings is addressed, these guidelines emphasize the dispersion of plumes from elevated sources in both neutral and stratified flows. Other valuable contributions to the topic of dispersion around buildings are by Blumen (1990), Hosker (1984 and 1985), Meroney (1982), and Meroney et al. (1995a and b). The material presented here is intended to supplement that information, with emphasis on the dispersion of vehicular and building exhausts, which are important sources of pollutants in urban areas.

Guidelines for modeling dense gas cloud dispersion can be found in Meroney (1987).

C7.2 MODEL STUDIES OF VEHICULAR EXHAUST EMISSIONS

Significant simplifications in the similarity requirements can be made for approximately non-buoyant pollutants from point and area sources during neutral atmospheric conditions. Most vehicular exhaust problems fall into this category.

The representative simulation of the atmospheric boundary layer determines the geometric scale λ_L of the study. The additional requirements for simulating the dispersion of vehicular exhaust gases are

A consistent scaling of all velocities

$$\left(\frac{W_s}{V}\right)_m = \left(\frac{W_s}{V}\right)_p \tag{C7.1}$$

where W_s is the exhaust speed of the pollutant and V is a characteristic wind speed. W_s is obtained from the emission rate of the pollutant per unit area of the strip source along a particular street.

An equality of the density ratio

$$\left(\frac{\rho_s}{\rho_a}\right)_m = \left(\frac{\rho_s}{\rho_a}\right)_p \tag{C7.2}$$

where ρ_s is the density of the emitted exhaust at the source, and ρ_a is the ambient air density.

The geometric similarity of the source

$$\frac{A_{s_m}}{A_{s_p}} = \lambda_L^2 \tag{C7.3}$$

where A_s is the cross-sectional area of the source.

The requirement to scale W_s/V can be relaxed in most situations and the choice of the velocity scaling can be largely based on convenience. W_s is small both in model and in full scale and thus does not significantly affect

the flow field. Buoyancy effects of the exhaust are relatively minor and there is essentially no momentum rise of the emanating gas. The density or temperature ratio requirement is approximately satisfied because both carbon monoxide and typical tracer gas used in model study are of approximately the same density as air and the temperature of the exhaust is near ambient. Because of the near neutral buoyancy of the pollutant, gravity forces are minor and it is not necessary to observe Froude number scaling, which would require that

$$\lambda_V = \lambda_{W_s} = \sqrt{\lambda_L} \tag{C7.4}$$

The source geometry requirement is approximately satisfied by emanating the pollutant from continuous strip sources. Because of practical limitations, it is usually necessary to exaggerate the source strength. This does not affect the diffusion process as long as the exit velocity remains small in comparison to the mean wind speed near ground level.

For small concentrations, the exaggeration of the source strength does not alter the flow environment nor the mixing process. The scaling of concentrations from model to full scale, however, must allow for the exaggeration of the source strength. In the absence of any distortion of the source strength

$$\left(\frac{c}{c_s}\right)_m = \left(\frac{c}{c_s}\right)_p \tag{C7.5}$$

where c is the concentration of a particular pollutant at some location and c_s the corresponding concentration at the source.

When the source strength is distorted in order to achieve sufficient model flow rates, the scaling of concentrations becomes

$$\left(\frac{c}{c_s}\right)_m = \left(\frac{c}{c_s}\right)_p \frac{1}{\lambda_L^2}\frac{1}{\lambda_V}\frac{(W_s A_s)_m}{(W_s A_s)_p} \tag{C7.6}$$

or

$$\left(\frac{c}{c_s}\right)_m = \left(\frac{c}{c_s}\right)_p \phi \tag{C7.7}$$

where ϕ is a source strength distortion factor defined as

$$\phi = \frac{(W_s A_s)_m}{(W_s A_s)_p} \times \frac{1}{\lambda_L^2} \frac{1}{\lambda_V} \tag{C7.8}$$

An important practical difficulty in model studies of vehicular emissions is the development of a strip source which is uniform spatially and invariant with time. Studies, reported in the literature, show concentration fields downwind of strip sources, calibrated in homogeneously rough terrain. Although uniformity of the concentration field along the length of such a source does prove that there are no biases in the construction of the source nor differences in internal pressure, it does not guarantee uniformity of emissions in non-homogeneous built-up terrain. In such situations, wind-induced pressure gradients along the street may feed-back into the source and disturb the uniformity of emissions.

Studies have shown that proper operations of strip sources along a city canyon can be achieved by:

1. Maintaining large difference between the pressure within the source and the ambient static pressure, and
2. Using a source that is compartmentalized to avoid the feedback of aerodynamic pressures into the source, which can occur with a continuous source plenum.

The dispersion of vehicular exhausts in city streets is largely an aerodynamic problem and can be satisfactorily carried out in model flows simulating the atmospheric boundary layer during neutral conditions. An extensive data set for such a study is reported by Wedding et al. (1977). The importance of stable stratifications cannot be completely ruled out and its evaluation awaits studies in stratified flow or water tunnels.

C7.3 MODEL STUDIES OF BUILDING EXHAUSTS

Studies to evaluate the performance of building exhausts and possible reingestion problems are becoming increasing important as regulatory bodies tighten clean air requirements. Of particular concern are low-level roof exhausts, which often vent chemical fume hoods or other sources of potentially toxic gases.

In many situations, these exhausts are at temperatures near ambient and the modeling can avoid Froude number or densimetric Froude number scaling. The scaling in such situations becomes that of simulating the atmospheric flow field and maintaining the equality of (W_s/V) in model and in full scale. It is important to maintain minimum Reynolds numbers based on

characteristic building dimensions and internal diameters of exhausts, as outlined in Chapter 7.

The minimum value of Re_b of about 10,000 is based on data reported by Golden (1961) (actually Golden quoted $(Re_b) \geq 11{,}000$). Work by Castro and Robins (1977) and Snyder (1994) suggests that the critical Re_b for a building immersed in a simulated ABL can be considerably smaller and in the neighborhood of 4000. Recent measurements by Neff and Meroney (1995) on the other hand suggest that $(Re_b)_{\min}$ is influenced by source location and geometry. Neff and Meroney recommend that $Re_b \geq 15{,}000$.

C7.4 EXPERIMENTAL METHODS

Quantitative studies of concentrations usually rely on measurements of tracer gas concentrations. Smoke flow visualization has traditionally been a qualitative technique to identify overall plume behaviour. Digital image processing techniques are used to determine plume trajectories and relative concentrations using model plume exhausts with an admixture of visible tracer smoke. This technique provides information on concentrations in a selected plane and is a powerful tool for locating plume trajectories and identifying situations of potential aerodynamic entrainment. This is then followed with detailed relative concentration measurements where appropriate. Several instrumentation systems are available for measuring tracer gas concentrations at particular locations. When planning a study it is important to select instrumentation with a time constant which is sufficiently short to also evaluate the time-varying, instantaneous peak concentrations. These can be substantial in complex settings. Instantaneous peaks, with durations of several seconds, can be several times the hourly mean values of the concentration.

This page intentionally left blank

Chapter C8
INSTRUMENTATION

C8.1 GENERAL

Wind is, by its very nature, a random process. This means that it is not possible to predict future values of wind speeds or wind effects from present or past values except in terms of statistical representations such as mean values, extreme values such as peaks, variance or root-mean-square values, power spectral density functions, probability density functions, correlation functions, and various derived characteristics describing these representations. Consequently, all wind tunnel model studies involving simulated natural wind conditions require measurement of random fluctuating quantities such as wind speeds, pressures, forces, motion, or concentrations of tracer gases. In some instances it will be sufficient to determine the mean value of the quantity being monitored. However, frequently it is necessary to measure and characterize the fluctuations associated with the random variable.

There are many types of instruments available for measuring various quantities of interest in wind tunnel model studies. It is not the intent of this section to try and catalog all the various instruments along with their strengths and weaknesses. However, it is important to recognize that a particular instrument or system may only be suitable for certain types of measurements. For example, flame ionization detectors (FID) are frequently used to measure concentrations of tracer gases in pollution dispersion tests. If the gas samples are being routed to the FID through long tubes, the gas will mix in the tubes and the system should only be used for estimating mean values of gas concentrations. If data on fluctuations were required, a different set-up and probably a different instrument with a remote burner would be required in order to minimize the sample tube length.

Rather than focus on specific instruments, this section deals with general issues of precision and accuracy which are important to the measurement of random variables. Accurate measurement of random variables requires both

precise quantification of the variable and its monitoring for a sufficient amount of time to establish stable estimates. Bendat and Piersol (1986) provide an excellent guide to the measurement and analysis of random data. The following discussion draws from this reference as well as practical experience in the measurement of wind loads and wind effects. The discussion centers on both questions of precision and stability or repeatability (accuracy) of the measurements. While a single detailed example is given, similar calculations can be developed for other applications based on the equations given and basic knowledge about the instrumentation used in the experiments.

C8.2 PRECISION

Wind tunnel tests usually involve scale models which are much smaller than the prototype and which are tested at wind speeds that are lower than design values. In fact, if an aeroelastic model is constructed with Froude number scaling, the properly scaled wind velocity is lower than the prototype speed by the square root of the geometric scale. For a 1:100 scale model, the model wind speed would be 1/10th of the prototype velocity of interest. For nonaeroelastic models and models, in which Froude number scaling is not employed, the test velocity is generally selected large enough to ensure that Reynolds number effects are either not important or can be accounted for in model design or analysis of results. Once this issue is dealt with, the actual speed selected represents a trade-off between increased signal level (higher speed leading to larger pressures or forces) and reduced frequency requirements (at lower speeds, fluctuations occur at a slower rate and frequency response requirements of the instrumentation are reduced).

A basic relationship used throughout wind engineering studies to relate wind speeds, model scales and time or frequencies is

$$\left(\frac{fL_b}{V}\right)_m = \left(\frac{fL_b}{V}\right)_p \tag{C8.1}$$

where:

f = frequency or 1/time
L_b = a characteristic dimension
V = wind velocity, and
subscripts m and p refer to model and prototype respectively.

Rearranging terms produces the relationship between model frequencies or time, t, as

$$\frac{f_m}{f_p} = \frac{\frac{1}{t_m}}{\frac{1}{t_p}} = \frac{L_{b_p}}{L_{b_m}} \frac{V_m}{V_p} \tag{C8.2}$$

These relationships allow the wind tunnel operator to judiciously select the appropriate wind tunnel test velocity or instrumentation frequency response characteristics for a given model scale and prototype wind conditions. In most cases, the frequency response characteristics of the instrumentation are restrained by the physical or electrical characteristics of the instrumentation system used. For example, it is well known that the frequency response characteristics of common tubing systems used for pressure measurements are dependent on the length of the tubing, any changes in diameter of the tubing, restrictions in the tubing lines, and the control volume of the pressure transducer. For lengths of tubing approaching 0.5 m, the nominal range of frequencies where the response is flat is less than 40 Hz unless restrictions are added or equalizers are used to compensate for the effect of the tubing system on the dynamic pressures (the tubing system transfer function) (Irwin et al. 1979, Stathopoulos 1975, Gerstoft and Hansen 1987).

The frequency response, sensitivity, stability, and noise characteristics of the instrumentation must all be considered when the laboratory is establishing its test protocol for each type of testing conducted. The following example is given to help illustrate the considerations involved in establishing a proper wind tunnel test protocol from the standpoint of instrumentation requirements.

Example: The minimum peak loading corresponding to a one-second duration at full scale is needed for design of roof or wall panels on a tall building. The wind tunnel is about 3 m wide and a 1:400 scale is selected to allow modeling of buildings within approximately 600 m (2,000 ft) of the site. The approximate design wind speed at the site has been determined and the corresponding mean hourly wind speed at gradient height, z_g, has been estimated to be 40 m/s. The pressure transducer system has a flat frequency response up to about 200 Hz, an output voltage range of ±2.5 volts at ±0.69 kPa (±0.1 psi) and the analog to digital (A/D) converter on the wind tunnel's data acquisition system is a 12-bit system with ±10.0 volt range.

These characteristics are not intended as a specification of minimum acceptable values for acceptable measurements, because different combinations of properties can yield sound measurement systems. Instead, emphasis should be placed on answering the following questions.

Typical questions to be answered include:

1. What wind speed should be used in the tests?
2. What sampling rate should be used?

3. How long should data be taken at a given tap?
4. What gain should be used if any?
5. What will be the smallest possible resolution of pressure coefficients?
6. What will be the typical precision of the measurements?
7. How repeatable are the results? (see Section C8.3 as well)

Approaches to answering these questions are suggested below.

The question concerning the wind speed to be used in the tests can be answered to some extent by using the relationship presented earlier. By setting the model frequency at 200 Hz and the prototype frequency at 1 Hz, the resulting expression is

$$V_m = V_p \frac{f_m L_{b_m}}{f_p L_{b_p}} = (40 \text{ m/s})\left(\frac{200 \text{ Hz}}{1 \text{ Hz}}\right)\left(\frac{1 \text{ m}}{400 \text{ m}}\right) \tag{C8.3}$$

Thus, the maximum wind speed that can be used in the wind tunnel before the instrumentation response can no longer follow the fluctuations of interest is 20 m/s. A lower speed may be used provided the transducer, instrumentation system, and computer has sufficient sensitivity and resolution. As will be noted in the subsequent discussion, there are other issues related to instrumentation sensitivity that can influence the selection of the velocity to be used in the tests.

The sampling rate to be used must be at least twice the highest frequency of interest, and the signal should be filtered to remove contributions or noise at higher frequencies than the highest frequency of interest. This requirement is based on eliminating aliasing where fluctuations at higher frequencies appear as if they occur at lower frequencies in digital data (Bendat and Piersol, 1986). However, it should be emphasized that this is a minimum requirement based largely on digital signal processing requirements. If the experiment is to capture peak values at frequencies close to the highest frequency of interest, significantly higher sampling rates are required. A sampling rate 10 times the highest frequency of interest will ensure much better resolution of the peak values. Thus, in our example, if the test is conducted with a wind tunnel mean gradient speed of 20 m/s and there is concern that peak fluctuations will contain contributions close to 200 Hz, the suggested sampling rate would be 2,000 samples per second on each channel. If the maximum sampling rate possible with the wind tunnel computer data acquisition system were 1,000 samples per second on each channel, it would be necessary to reduce the mean gradient height velocity used in the model tests to 10 m/s and filter the pressure signal at 100 Hz.

Where peak pressures are not influenced by frequency contributions close to the maximum frequency of interest, acceptable measurements are obtained at significantly lower sampling rates. At least one laboratory

reports excellent results at sampling rates as low as 250 samples per second with wind tunnel speeds of 17 m/s. Additional discussion of frequency response requirements for pressure and force measurements is given by Durgin (1982). The kinds of computations outlined above provide some initial estimates for design of experiments. However, emphasis should be placed on laboratory demonstration of accuracy and repeatability of results, including comparison with results from field data or other laboratories.

The question dealing with how long to take data will be deferred to the next section, where questions concerning measurement accuracy and repeatability for random signals are discussed.

Questions four through six are all related and will be discussed together. To improve the precision of the measurements, it is important to create large signals which utilize as much of the dynamic range of the analog to digital converter as possible. When this is done, the laboratory operator must be conscious of the possibility of exceeding the range of the analog to digital converter. The best data acquisition software will test for values equal to the limits of the analog to digital converter and report how many values reach the limits. For spectral analysis and other types of digital signal processing, which involve transformation from the time domain, it is frequently acceptable to allow the limits to be exceeded for a small portion of the sampling time. However, for pressure measurements where peak values are important, the wind speed or signal gain should be reduced and tests repeated if the analog to digital converter's limits are exceeded. It should be noted that a relatively common 12-bit analog to digital converter was used in the example. The use of a 16-bit analog to digital converter significantly improves the dynamic range and precision of measurements and can solve some of the problems illustrated, provided the signals from the sensors are sufficiently free of distorsion and noise to allow an effective use of this increased precision in the conversion of analog signals to digital values.

For the above test conditions and instrumentation, the minimum voltage which can be resolved by the analog to digital converter is 20 volts divided by the number of counts in the converter (i.e. 2^{12}, or 4,096). Thus the minimum voltage step that can be resolved is 0.0049 volts, or 4.9 millivolts. With a gain of unity, the minimum voltage step would correspond to a pressure of 0.0014 kPa. Assuming that the tests are carried out with a mean velocity at gradient height of 20 m/s, the mean dynamic pressure at gradient height will be 0.2452 kPa (0.0356 psi) and a pressure coefficient equal to 2.81 (based on the mean gradient velocity pressure) will correspond to a pressure of 0.69 kPa (0.1 psi). Thus, peak pressure coefficients greater than or equal to ±2.81 would indicate that the pressure has reached or exceeded the nominal range of the transducer, and the wind tunnel test speed should be reduced unless the transducer calibration has been verified beyond the nominal range. If the pressure coefficients never exceed ±2.81, then the tests should be acceptable. Running the tests with a mean gradient wind speed of 10 m/s would

reduce the dynamic pressure by a factor of 4, and pressure coefficients less than ±11.24 would fall within the nominal limits of the transducer pressure range.

With a gain of unity and the mean gradient speed set at 20 m/s, the minimum voltage step of the analog to digital converter (4.9 millivolts) corresponds to 0.0014 kPa or a pressure coefficient of about 0.006 based on the gradient velocity pressure. The precision could be increased by applying a gain of 4 to the pressure signals so that the nominal maximum or minimum pressure will produce a voltage of ±10 volts, the analog to digital converter limit. With a gain of 4, the analog to digital converter will be able to resolve signals for increments in pressure coefficients of 0.0014. Higher gains will be acceptable if the pressures are smaller than the nominal maximum for the transducer. If the tests were conducted with a mean gradient wind speed of 10 m/s, and a gain of unity were applied to the pressure signal, the 0.0014 kPa pressure would correspond to a pressure coefficient based on the gradient velocity pressure of 0.023. Applying a gain of 4 to the pressure signal would improve the resolution to a pressure coefficient increment of 0.006.

The electrical noise of the pressure measurement system must also be considered in estimating the precision of the measurements. If the peak to peak noise is 20 millivolts when a gain of 4 is used, the measured pressure could be in error by ±0.0028 kPa. This would correspond to an uncertainty of ±0.046 in the value of the peak pressure coefficient for tests with a mean gradient velocity of 10 m/s, and an uncertainty of ±0.0114 in the value of the peak pressure coefficient for tests with a mean gradient velocity of 20 m/s. If the peak pressure coefficients of greatest interest for design are around ±2.0 or larger, representing the higher typical loading on the cladding, the percent error in measurements because of precision would be of the order of 2.3% for the 10 m/s tests with gain set at 4 and of the order of 0.6% for the 20 m/s tests with gain set at 4.

For high-rise buildings, the peak pressures near corners will occasionally produce pressure coefficients, related to the gradient velocity pressure, exceeding 3 or even 5. Cases have been reported in which pressure coefficients exceeding 10 have been measured. Consequently, testing at a gradient mean velocity of 20 m/s using transducers with a range of ±0.69 kPa (±0.1 psi) would not be advisable unless extreme care were taken to ensure that the transducer range was not exceeded. If it was exceeded, it would be acceptable to retest the critical pressure taps at a lower speed. This approach would improve the precision of the measurements at taps exposed to lower pressures, but would require careful examination of the data and retesting of critical taps for certain wind directions. Testing at a mean gradient velocity of 10 m/s would work well for most high-rise building studies carried out in the facility described above since the transducer's range would not be exceeded for pressure coefficients up to 11.24 and the nominal precision error for pressure coefficients with magnitudes of 2.0 or larger would be less than 2.5%.

End of Example: It is not the intent of this section to establish particular performance criteria. Instead, the example is given to illustrate that wind tunnel operators have the ability to estimate the performance of their systems and that the client can request information on the typical accuracy and repeatability of the experiments. In particular, the precision estimate of 2.5% listed at the end of the last paragraph should not be taken as a performance criterion. As discussed in the following section, precision is only one factor affecting the overall accuracy and repeatability. The need for precise measurements should be balanced against the inherent variability in measuring random processes.

C8.3 ACCURACY

From the discussion in the introduction to this section, it should be clear that the overall accuracy of the wind tunnel measurements depends on the precision of the measurements (as discussed in the previous section) the characteristics (random nature) of the quantity being measured, and the type of statistical quantity being determined. The time interval over which data are gathered and the method of analysis are frequently more important to the overall accuracy of the measurement in a turbulent wind environment than the precision of the instrumentation. Snyder (1981) provides a discussion of some of the considerations involved in selecting an appropriate averaging time and associated targets for accuracy. Mean values generally require the shortest amount of time to establish stable estimates, the root-mean-square values and variances require somewhat longer times to obtain stable estimates than the mean. Extreme values or peaks, higher order correlations including spectral analysis, correlation functions and coherence functions may require lengthy sampling times and special analysis procedures to establish stable estimates. The relative sensitivity of the accuracy or stability of the measurements to sample time is illustrated in Figure C8.1. This figure presents a measure of the variability in the measurement of typical velocity characteristics based on repeated tests for various sampling times with the wind tunnel running continuously at a single velocity setting of about 4 m/s (Reinhold and Brinch, 1992). (This speed is typical for small scale aeroelastic models or pollution dispersion studies in which Froude number scaling is employed. For pressure studies in which higher velocities are utilized, the required sampling times would be significantly reduced.) Note the relatively small variation in the values of the mean velocity even at sample durations of only 30 seconds. The variability in the root-mean-square values as illustrated by the turbulence intensities I_u and I_w, are reduced by a factor of about 2 as the sample time is increased from 45 seconds to 120 seconds. The variability in the Reynolds stress, which represents a higher order correlation, also is reduced as the sample time is

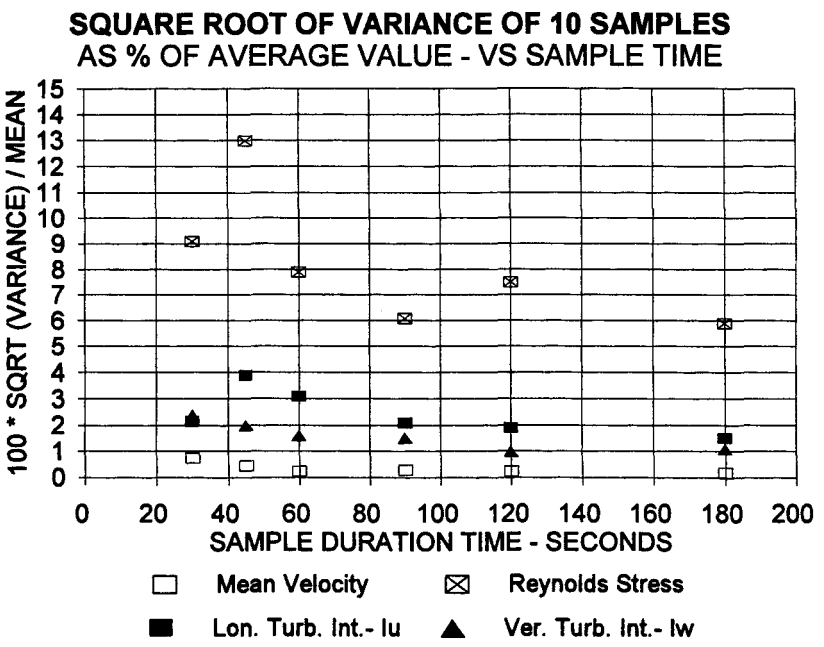

FIGURE C8.1. Plot of Variation in Measured Wind Velocity Characteristics as a Function of Sample Time.

increased but at a much slower rate. These trends are typical of the way in which increased sample times reduce the variability in the measurement of characteristics of stationary random processes. If the full-scale sample time remains constant, equation (C8.2) indicates that the wind tunnel sample time increases linearly with the inverse of the wind tunnel speed. Consequently, for tests requiring low speeds, the sampling time required to produce small variations in results can become quite large.

This Manual suggests measurements for periods of time corresponding to about 1 hour in full scale. This is appropriate for determining stable estimates of mean, root-mean-square and to some extent extreme values such as peaks. However, in areas of flow separation where large fluctuations are observed, the extreme values obtained from a simple measurement of the maximum or minimum peak pressure may exhibit considerable variability for times corresponding to one hour full scale. Many laboratories have instituted probabilistic methods for obtaining more stable estimates of extreme values by measuring a number of peaks and using analysis techniques such as the Lieblein-BLUE approach to estimate the expected peak for a period of time of one hour full-scale (Lieblein 1974).

If spectral analysis, correlation functions, or higher order correlations are to be determined, a time period corresponding to about 5 or more hours at

full scale should be used to obtain enough data to produce stable estimates. This does not correspond to an analysis of a single 5-hour record, because most analyses will involve ensemble averages of results for shorter data blocks. The 5 hours is a rough estimate of the quantity of data required to achieve stable ensemble averages.

The laboratory operator and end user should both be aware that increased accuracy requires increased testing time and that the increases can be significant for some types of measurements and depend on the speeds used in the model tests. The target levels of precision and accuracy should be established with a realistic appreciation for the budget implications and consideration of all the other sources of uncertainty including the wind climate. Since uncertainties are generally independent and the combined uncertainty is estimated from the square root of the sum of the squares of the individual values, it may be a waste of resources to quadruple the sampling time in order to reduce the uncertainty in the peak pressure coefficient from 10 to 5%, particularly if the uncertainty in the wind climate is 15%. Assuming that these are the only two uncertainties involved, reducing the uncertainty in the peak pressure coefficient from 10 to 5% would only reduce the total uncertainty from 18 to 16%.

This discussion is not intended to suggest that accuracy should not be a major focus in the laboratory study. Rather it is intended to reinforce the understanding that the study of wind effects on structures involves the management of many potential sources of uncertainty, some of which would be common to both physical models and analytical or numerical studies. Thus, the operator and client should not develop unrealistic expectations for overall accuracy based on close attention to one or two parameters when a balanced overall treatment of all the sources of uncertainties would produce more reliable predictions.

This page intentionally left blank

Chapter C9

QUALITY ASSURANCE OF WIND TUNNEL DATA

C9.1 GENERAL

The purpose of quality control of wind tunnel testing and wind engineering analysis is to ensure that they are carried out to satisfactory standards (American Society of Mechanical Engineers (ASME) 1996, Canadian Standards Association (CSA) 1991) and that the results are reliable and consistent with the expectations of the sponsor.

In particular the objectives of quality control are to ensure

- that the scaling and representation of the properties of the natural wind conform as far as possible to the full scale; where they do not conform, it should be noted and understood;
- that the scaling and representation of the models and physical processes affected by the wind also conform to the full scale and perform as intended;
- that instruments used in experiments function correctly and consistently and are calibrated accurately;
- that computer programs for data acquisition, processing, editing, and analysis perform reliably and accurately;
- that theoretical interpretations suitably reflect the realities of the problem and the limitations and assumptions are stated and understood;
- that as a long-term industry objective, full-scale verification of all key assumptions should be sought (examples include testing of standard buildings such as CAARC, CIBC Toronto, Texas Tech University, Aylesbury);
- that steps are taken to minimize the likelihood of human error in all aspects of the study; and
- that reporting is complete and understood by the sponsor.

The following outlines some practical procedures for achieving these objectives. In doing so it should be recognized that the procedures used in wind engineering are not absolute in character and are steadily evolving and expanding.

C9.2 GENERAL CONDUCT OF TESTS AND ANALYSIS

It is recommended that in all phases of wind tunnel testing and wind engineering analysis, careful project and facility records should be kept. These should include:

- dates and times;
- the persons responsible for defining the tasks to be performed, setting up the experiments, running programs, checking installations, scheduling, and controlling documentation;
- wind tunnel condition and servicing, cleaning of screens, and so on;
- photographs of experimental set-ups;
- the identification and condition of equipment, calibration of instruments, gain settings, and so on;
- operating schedule, interruptions;
- computer software used (including identification of the particular version), file names of data; and
- archiving of all results and data.

All errors encountered should be discussed openly, avoiding recriminations, and investigated fully. Steps should be taken to avoid their recurrence. This process should be fully recorded. Good communications should be emphasized.

C9.3 ASSURANCE OF CORRECT MODELING AND SCALING

For the wind, the correct scaling generally can be achieved through consistent scaling of all dimensions of length, time, mass, and, in some instances, temperature. Alternatively, characteristic dimensions of length, velocity, and density may be compared in model and in prototype.

Correct scaling of the wind and the physical process being investigated is a key issue in assuring accurate results. This involves the scaling of

- the roughness length in the far field of the flow approaching the building or structure under study, and the geometry of the boundary in the near field;
- the mean velocity profile;

- the turbulence intensity profile;
- the spectra of the velocity components;
- the cross-spectra of the velocity components at various spatial separations; and
- the probability distributions.

Site visits and evaluation of roughness and topography from maps and aerial photographs is recommended. Other properties of the flow may be more difficult to reproduce. These include the effects of buoyancy or density gradients in the flow, the Reynolds number, and the Rossby number. In these instances, the discrepancies should be noted and the likely effects noted.

The following properties should be carefully scaled in constructing models of buildings and structures:

- the geometry of the structure;
- the texture of the building surface; this may require exaggerated roughness to ensure transition to turbulence in the boundary layers;
- in aeroelastic models, stiffness and mass distribution (this can be alternatively described through the natural mode shapes and natural frequencies);
- the structural damping in the case of aeroelastic models; and
- porosity (leakage paths).

Modeling of drifting of snow and other particulate material (not covered by this Manual) requires scaling of

- the terminal "fall" velocity of snow particles; and
- stability of particles on the ground or other surface.

Modeling of plumes requires scaling of

- efflux velocities;
- mass flow;
- densities;
- concentrations; and
- atmospheric stability (in some cases).

C9.4 SOURCES OF ERROR

Human errors are the most difficult to avoid. They are influenced by attitudes toward work, the sense of professional responsibility, organization, and experience. The following approaches can be helpful in reducing and eliminating human and other errors.

- Assign responsibility for checking the quality. In some instances it is desirable to assign a Quality Officer who is not otherwise involved in the test.
- Establish clear responsibilities for the tasks, with definition of checks to be performed and signed off.
- Ensure that instrumentation and software used has been properly checked and commissioned. If software is modified, ensure it is checked and modifications clearly recorded.
- Clear and frank discussion of errors when they occur should be encouraged.
- Have all work checked by a second person.
- Perform periodic quality audits, in which the Quality Officer checks that all quality assurance procedures are being followed.

The following techniques can be useful in identifying human and other errors.

- *Repeat measurements.* Repeated measurements of key quantities, such as the reference tunnel wind speed, made at intervals during a test sequence will detect changes in wind tunnel or instrument performance.
- *Dual instrumentation.* Use of two instruments in parallel will identify malfunctions of key instrumentation.
- *Standardization.* Standardization of experimentation and computations reduces risks from unfamiliar procedures.
- *Graphical display.* Graphical display of measurements can lead to rapid recognition of anomalous results and data points. For example, this can be useful in recognizing trends in the variation of pressure coefficients with azimuth.
- *Interdependency and redundancy.* Interdependent and redundant experimental results can be exploited to demonstrate internal consistency in measurements and hence to verify their accuracy. Integration of mean pressures on a tall building, for example, should be consistent with direct measurements of base shear or moment.
- *Comparisons with theory.* Approximate theoretical estimates made in anticipation of experimental results should provide preliminary indication of the accuracy of results.
- *Pressure sensors.* In setting up pressure models, the tubing from the model to the pressure sensor should be checked for correct connection and for leaks.
- *Logs.* All people involved should keep daily logs of their activities. A detailed log of all testing activities should also be kept.

C9.5 STRATEGY

Errors of various kinds can easily defeat the purpose of the testing—to improve the overall accuracy of the estimation of the effects of wind. Application of the principles of quality control should be applied to eliminate these sources of error.

This can be accomplished by building up an environment for wind tunnel testing in which

- the importance of quality is clearly articulated;
- responsibilities are clearly assigned and understood;
- the assumptions and limitations of the scaling and modeling are identified;
- instrumentation is carefully checked;
- computer programs are checked and documented;
- procedures for experimental measurement contain a suitable number of checks for internal consistency and reliability;
- as a long-term goal, full-scale verification of key modeling assumptions should be undertaken.
- human errors are openly discussed and procedures to avoid them laid out; and
- comprehensive records are kept of all details of the test.

This page intentionally left blank

Chapter C10

WIND CLIMATE AND PREDICTION OF FULL-SCALE BEHAVIOR

C10.1 GENERAL

The final product derived from a boundary layer wind tunnel test is usually a prediction of a load, response, or local wind speed as a function of return period or recurrence interval. To obtain the predicted load or response, the results from the wind tunnel tests are combined with information on the wind climate at the location of interest. This chapter discusses a number of different types of winds (thunderstorms, extratropical storms, hurricanes, and so on) and provides information on some of the techniques used to combine wind tunnel test results with the wind climate model to obtain the predicted load or response.

C10.2 WIND TYPES AND THEIR EFFECTS ON THE WIND DATABASE

Throughout the various regions of the United States, extreme winds are governed by different meteorological phenomena. Along the Gulf and Atlantic coasts of the United States, extreme winds are driven by the influence of tropical cyclones or hurricanes. In the Great Plains and the southeastern portion of the country, thunderstorms dominate the extreme wind climate. In some areas of the western mountain states the mountain ranges can induce large amplitude atmospheric waves that may dominate the extreme winds. Over much of the remainder of the country, the extreme wind climate is dominated by the passing of large-scale extratropical storm systems. At any one location, the record of wind speeds measured by an airport anemometer is likely to contain winds produced by more than one of the above storm types. The present state-of-the-art prediction of structural loads and responses separates hurricane winds from other wind types, but

thunderstorms and downslope winds are not, in general, treated any differently than the winds produced by large-scale extra-tropical storms. A review of the aforementioned wind types is given in Golden and Snow (1991). They are briefly discussed in the following sections.

C10.2.1 Extra-Tropical Storm Systems

Extensive pressure system (EPS) or extra-tropical storm winds are produced by the large scale high- and low-pressure systems that move across North America from the West. The winds associated with these storms are produced by severe low pressure systems that occur throughout the year. However, the most intense storms generally occur during the winter months. The winds in these extra-tropical storms are produced through a balance in the pressure gradient forces and the Coriolis force. The mean wind speed at gradient height V_g, for a stationary EPS storm is described through the relationship,

$$\frac{1}{\rho}\frac{\partial p}{\partial n} = \pm\frac{V_g^2}{r} + f_c V_g \qquad \text{(C10.1)}$$

where ρ is the density of air, $\partial p/\partial n$ is the pressure gradient normal to the isobars, f_c is the Coriolis parameter, and r is the radius of curvature of the isobars. The gradient wind speed has a direction nearly parallel to the isobars. The wind speed at the surface is reduced because of frictional effects, and the wind direction is changed, also a result of surface friction. The characteristics of the boundary layer associated with the extratropical storm winds are reasonably well understood, and it is these winds that are well modeled in the boundary layer wind tunnel.

C10.2.2 Thunderstorms

Thunderstorms constitute a violent form of atmospheric convection and are generally composed of short-lived cells, consisting of regions of strong vertical air motion. With favorable conditions, a supercell may develop (Browning 1964) in which updrafts and downdrafts coexist for periods of an hour or more. The cold downdraft air often produces a sharp gust front, the so-called first gust.

The strongest downdraft velocities in the thunderstorm vary widely and tend to occur at altitudes lower than the peak updrafts. The cold downdraft air diverges in all directions at the ground. Much of this downdraft air is left behind the storm, but some initially flows out ahead or at one side of the storm giving rise to a gust front. Wind speeds associated with outflows moving ahead of the storm are increased by the forward motion of the storm system itself. The gust front associated with an intense, quasi-steady thunder-

storm is usually found 5 to 6 km ahead of the leading edge of the main precipitation core (Auer et al. 1969). The variation of the horizontal wind speed with height within a thunderstorm gust front is somewhat uncertain, and the characteristics of the change in velocity with height vary significantly from event to event and are not well understood. In addition to the thunderstorm winds associated with the gust front, smaller scale more violent phenomena associated with thunderstorms are downbursts and tornadoes discussed below.

C10.2.2.1 Downbursts. Downbursts, introduced by Fujita (1976) as distinct meteorological phenomena, are strong downdrafts that produce an outburst of winds near the grounds. By the mid-1980s, the meteorological community had accepted the downburst as distinct from the well-known large-scale downdrafts associated with gust fronts and cold air mass fronts. A macroburst is a large downburst with winds greater than 4 km in horizontal dimension, whereas a microburst is a small downburst with damaging winds extending less than 4 km. Downbursts propagate outward very slowly and the wind directionality is more uniform in azimuth than thunderstorm or extratropical cyclone winds.

Notable differences in microburst winds versus thunderstorm gust front winds are discussed by Bedard and LeFebvre (1986) for events studied at Denver Airport. The vertical profiles of downbursts are thought to be significantly distinct from other storms. In a full penetration microburst, the horizontally divergent winds will result in a very thin layer of high wind speeds near the ground, generally maximum winds are within 100 to 150 m (300 to 500 ft) above the ground.

The scale of downbursts is thought to be at least one order of magnitude less than thunderstorm gust fronts. Due to the relatively small size and frequency of occurrence, downbursts are not well represented in National Weather Service (NWS) station wind records. Databases of downbursts are limited to several airport sites investigated by the FAA. These include Oklahoma, Dulles Airport, Chicago, Denver, Boulder, Memphis, Huntsville, Kansas City, and Orlando. Fujita (1985) has developed microburst hazard curves for the Chicago and Denver areas based on these measurements. These results are very preliminary, but indicate that downbursts probably do not contribute significantly to the wind climate for return periods of less than approximately 1000 years.

C10.2.2.2 Tornadoes. A tornado is a violently rotating column of air whose circulation reaches the ground. It is often observable as a condensation funnel attached to the cloud base or as a rotating dust cloud rising from the ground. Horizontal wind speeds in the most intense 2% of all tornadoes may exceed 90 m/s (200 mph), although over 50% of tornadoes have peak winds less than about 40 to 50 m/s (90 to 110 mph) The peak winds occur

over an area generally less than 20% of the tornado damage path. The probability of a tornado strike for a point target located in any part of the United States is less than 10^{-3} per year (Twisdale 1978), however the strike probability varies significantly with geographic area. Hence, on average, tornado winds generally do not influence the wind hazard curve for point targets and small buildings for annual exceedance probabilities greater than 10^{-3} (a mean return period of less than 1000 years). There are large uncertainties associated with tornado hazard analysis, particularly for gust wind speeds greater than about 55 m/s (125 mph). Key aspects of tornado hazard analysis include databases, wind speed transformations from observed damage, and the integration of these elements into a hazard model.

C10.2.3 Hurricanes

The most devastating windstorms in the United States are those produced by hurricanes (tropical cyclones or typhoons as they are referred to elsewhere). Although they are small compared to extra-tropical pressure systems and are relatively infrequent, when they make landfall in urban areas the damage they produce is unequaled by any other single wind event. Tropical cyclones occur most frequently in the late summer and early fall, when ocean temperatures and air humidity are the highest. Tropical cyclones originate over tropical ocean water near latitudes of 15°. These low-pressure systems intensify in the presence of warm, moist air. Fully developed hurricanes have typical diameters in the range of a few hundred kilometers. However, the strongest damaging winds are concentrated near a few tens of kilometers from the center of rotation. In general, as a tropical cyclone becomes stronger, the size (or eye diameter) tends to decrease. Once the tropical cyclones pass over land their intensities diminish rapidly, because their source of energy from the warm waters is removed. As a result, tropical cyclones or hurricanes are only important for locations within about 100 km of the coast for return periods of less than about 100 years. In the United States the hurricane season is the period from June 1 to November 1, but the most severe storms occur from late August through to early October. The intensity of tropical cyclones as categorized on the commonly used Saffir Simpson scale is given in Table C10.1.

C10.3 COLLECTION AND ANALYSIS PROCEDURES FOR WIND DATA AVAILABLE IN THE UNITED STATES

C10.3.1 Background

Historical records of surface wind speed and direction in the United States are available in the form of one- to two-minute averages recorded

TABLE C10.1. Classification of Tropical Cyclones.

Category	Central Pressure (mbar)	One Minute Average Wind Speed 10 m above Water (m/s)	One Minute Average Wind Speed 10 m above Water (mph)
Tropical Depression	—	<17	<39
Tropical Storm	—	17–33	39–74
Hurricane Category 1	>980	33–42	74–94
Hurricane Category 2	965–979	43–49	94–110
Hurricane Category 3	964–945	50–58	110–130
Hurricane Category 4	944–920	59–69	130–155
Hurricane Category 5	<920	>70	> 155

once per hour (or once per three hours) and daily maximum peak gust or fastest-mile data. The peak gust wind speeds have durations on the order of two to three seconds. The averaging time, T, in seconds, associated with the fastest-mile wind speed is

$$T = \frac{3600}{V_{fm}} \tag{C10.2}$$

where V_{fm} is the fastest-mile wind speed in miles per hour. For fastest-mile wind speeds of engineering interest, the averaging time is in the range of 30 to 120 seconds. There are two basic methodologies used to combine the wind speed data with wind tunnel data to derive estimates of response as a function of return period. The first of these methodologies employs the hourly measurements of wind speeds and direction, combined with an upcrossing approach, and the second method makes use of the annual extreme values directly. The methodologies are discussed in the two following subsections. Because the experimental data derived from wind tunnel tests are usually referenced to a mean wind speed at gradient height, when using either the extreme value approach or the upcrossing approach, the surface wind speeds must be converted to equivalent hourly mean values at gradient height. This conversion is usually made assuming a power law relationship relating the mean wind speed at surface level to the mean wind speed at gradient height. Note that when the parent probability distribution of the hourly wind speed is derived from the one- to two-minute sample measurements taken at hourly intervals, the wind speed measurements are not converted to hourly values, but are treated as samples of a random process.

In the case where the wind climate is to be determined using annual extreme values of fastest-mile or peak gust data, these wind speed measure-

ments must first be converted to equivalent mean hourly values. This conversion is usually made with the assumption that the wind speeds were produced by an extra-tropical storm, and that the relationship developed by Durst (1960) (see Figure C10.1), relating the wind speed averaged over an arbitrary length of time to the wind speed averaged over one hour is valid. Because most wind speed measurements are obtained assuming a uniform open country type terrain, the relationship between the gradient wind speed and the surface wind speed is given as

$$V_g = V_a \left(\frac{z_g}{z_a} \right)^{1/\alpha} \tag{C10.3}$$

where V_a is the mean surface anemometer wind speed, and V_g is the mean gradient level wind speed, z_a is the height of the anemometer and z_g and $1/\alpha$ are the gradient height and power law exponent respectively (see Table C2.2). In instances where the airport stations are surrounded by extensive urban or suburban terrains, different values of z_g and $1/\alpha$ may be required.

C10.3.2 Hourly Wind Speed Data—The Parent Distribution Approach

The use of hourly measurements of wind speed to define the parent probability distribution of wind speed and direction, coupled with an

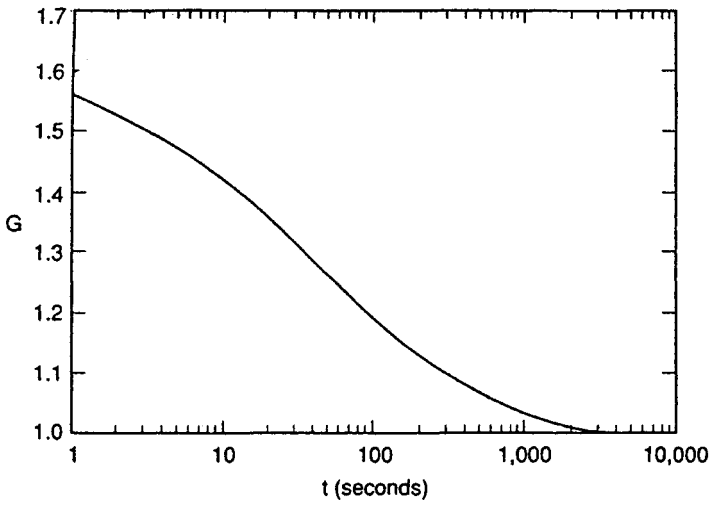

FIGURE C10.1. Relationship Between Wind Speeds Averaged over an Arbitrary Time to the Wind Speed Averaged over One Hour.

upcrossing approach to derive the extremes, was first discussed by Davenport (1968), and further examined by Gomes and Vickery (1978).

Using the hourly measurement of wind speed, the parent probability distribution of wind speed, independent of direction, can be modeled with a Weibull distribution given as

$$P(v > V) = \exp\left[-\left(\frac{V}{C}\right)^k\right] \tag{C10.4}$$

where $P\ (v > V)$ is the probability that the wind speed, v, is greater than V, and C and k are the Weibull distribution parameters. The Weibull parameters are obtained by fitting the wind speed data using standard methods, including method of maximum likelihood, method of least squares, methods of moments, and so on. Figure C10.2 shows an example of the observed and modeled distribution of the mean wind speed at gradient height for Oklahoma City.

The parent probability distribution of wind speed provides information on the fraction of time the wind can be expected to be greater than a specified value, but does not provide any information on how often a particular wind speed can be expected to be exceeded. The expected number of exceedances, $N_v(v)$, of a specified wind speed, v, is obtained using theory by Rice (1945). Namely,

$$N_v(v) = \int_0^\infty \dot{v} p(v, \dot{v}) d\dot{v} \tag{C10.5}$$

where $\dot{v}$ is the time derivative of the velocity, $p(v,\dot{v})$ is the joint probability density of v and $\dot{v}$, and $N_v(v)$ is the number of upcrossing (exceedances) of the wind speed v. For a stationary Gaussian process the joint probability distribution $p(v,\dot{v})$ is given as

$$p(v, \dot{v}) = p(v)p(\dot{v}) \tag{C10.6}$$

and thus the crossing rate $N_v(v)$ is given as

$$N_v(v) = C_1 \lambda \sigma_v p(v) \tag{C10.7}$$

where for a Gaussian process C_1 is equal to $\sqrt{2\pi}$, and λ is the average cycling rate of the process $v(t)$, which is in the range of 500 to 1000 cycles/year and σ_v is the long-term standard deviation of the wind speed. Gomes and Vickery (1977) found, from direct measurements, that the constant C_1 is equal to 2.26.

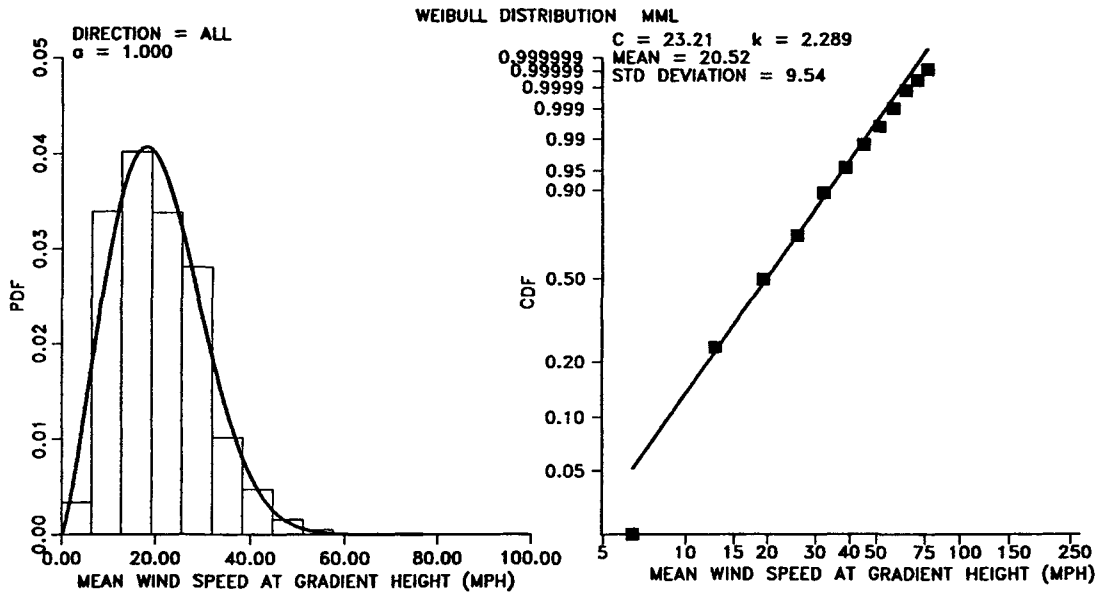

FIGURE C10.2. Weibull Distribution of Wind Speeds at Oklahoma City.

If the cycling rate is given in terms of cycles per annum, then the return period associated with the exceedance of the velocity V is

$$RP_v(V) = \frac{1}{N_v(V)} \tag{C10.8}$$

The combination of Eqs. (C10.4), (C10.7), and (C10.8) provides the necessary information to determine wind speed as a function of return period, independent of direction. The resulting predicted wind speeds correspond to an averaging time of approximately one hour, and can be used with wind tunnel test results to obtain upper-bound estimates of response versus return period.

The upcrossing approach was extended to determine the number of crossings of a directionally dependent, wind-induced response as discussed by Davenport (1977). The details of the methodology used to combine the probability distribution of wind speed and direction with wind tunnel test results to obtain prediction of wind-induced response as a function of return period are discussed in detail in Davenport (1977, 1982, 1983) and Surry and Davenport (1979). The joint wind speed and direction probability distribution derived from hourly wind speed measurements is usually well modeled with a Weibull distribution, where

$$P\left(v > V | \theta \pm \frac{\Delta\theta}{2}\right) = \exp\left\{-\left(\frac{V}{C(\theta)}\right)^{k(\theta)}\right\} \tag{C10.9}$$

where $P[v > V | \theta \pm (\Delta\theta/2)]$ is the probability that the wind speed v exceeds V, given that the wind is approaching from the direction $\theta \pm (\Delta\theta/2)$, and $C(\theta)$ and $k(\theta)$ are directionally dependent Weibull distribution parameters. The probability of exceeding the wind speed V within a sector $\theta \pm (\Delta\theta/2)$ is

$$P(v > V, \theta) = A(\theta)\exp\left\{-\left(\frac{V}{C(\theta)}\right)^{k(\theta)}\right\} \tag{C10.10}$$

where $A(\theta)$ represents the fraction of time the wind approaches within the direction sector $\theta \pm (\Delta\theta/2)$.

From the results of a wind tunnel test, the wind-induced response of a structure or component (cladding pressure, base bending moment, acceleration, and so on) can be expressed in the form

$$R(V, \theta) = a(\theta)V^{b(\theta)} \tag{C10.11}$$

where $a(\theta)$ and $b(\theta)$ are directionally dependent constants and $R(v,\theta)$ is the response as a function of wind speed and direction. In the case of a cladding pressure, $b(\theta)$ takes on a value of 2.0, and $a(\theta)$ is equal to $\frac{1}{2}\rho C_p(\theta)$, where ρ is the density of air and $C_p(\theta)$ is a pressure coefficient obtained from wind tunnel tests for a wind direction, θ. In the case of the dynamic response of a tall building, $b(\theta)$ typically varies between 2 and 3 and is a function of wind direction. The wind speed required to exceed a specified response level, R, is

$$V_R(\theta) = \left[\frac{R(v,\theta)}{a(\theta)}\right]^{\frac{1}{b(\theta)}} \tag{C10.12}$$

As described in Davenport (1977), the number of crossings of the response level, R, is approximated as

$$N_R(R) = C_1 \lambda \sigma_v \int_0^{2\pi} \left[1 + \left(\frac{1}{V_R}\frac{\partial V_R}{\partial \theta}\right)^2\right]^{1/2} p_v(V_R,\theta)\,d\theta \tag{C10.13}$$

where $p_v(V_R,\theta)$ is the probability density function of wind speed and direction derived from Eq (C10.10), and the terms C_1, λ, and σ_v are the same as in the non-directional case. The return period associated with exceeding the response level, R, is $1/N_R(R)$.

An alternate form of the two-dimensional upcrossing approach was developed by Lepage and Irwin (1985). Using the methodology described by Lepage and Irwin (1985), the average number of upcrossings of a response level, R, is

$$N_R(R) = \frac{1}{2}\int_0^{2\pi} \overline{|\dot{V}|} \left[1 + \left(\frac{\overline{|\dot{\theta}|}}{\overline{|\dot{V}|}}\frac{\partial V_R}{\partial \theta}\right)^2\right]^{1/2} p_v(V_R,\theta)\,d\theta \tag{C10.14}$$

where $\overline{|\dot{V}|}$ and $\overline{|\dot{\theta}|}$ are the mean magnitudes of the rates of change of the hourly wind speed and direction. Empirical relationships of $\overline{|\dot{V}|}$ and $\overline{|\dot{\theta}|}$ as a function of the mean hourly wind speed are given in Irwin (1987), where it is seen that $\overline{|\dot{V}|}$ increases with wind speed and $\overline{|\dot{\theta}|}$ decreases with wind speed.

The upcrossing method can also be used with the probability distribution of wind speed and direction derived from upper level (balloon) measurements of wind speed. Details of the methodology are described by Vickery (1973). Balloon or upper-level wind speed measurements are available for a

number of locations in the United States and depending on the station, balloons are released either twice daily or four times per day. Measurements of wind speed and direction (1-minute averages), temperature, and so on, are recorded at standard pressure levels (950 mbar, 900 mbar, etc.). Measurements taken at the 900-mbar level correspond to a height of approximately 500 m above sea level. The main advantage of using the upper-level wind speed measurements is that the data are free from the influence of terrain effects, nearby vegetation, structures, and so on. The main disadvantage of the approach is that the wind speed measurements taken only two or four times a day provide less data than those taken at surface level, and consequently there is more uncertainty built into the statistical models used to fit the data. The speed values obtained from the balloon measurements represent an average value over a height range, because the balloon is ascending during the measurement period.

C10.3.3 Wind Speed and Response Prediction Using Extreme Value Analysis

In instances where the annual extreme wind speed data are extracted from a continuous record of wind speed, the annual probability of exceeding a wind speed, V, can be determined by fitting the wind speed data to a Type I extreme value distribution given as

$$P(v > V) = 1 - \exp\left\{-\exp\left[-\frac{(V - U_a)}{a_a}\right]\right\} \tag{C10.15}$$

where U_a is the mode of the distribution and a_a is the dispersion. The use of a Type I extreme value analysis of wind speeds at 129 stations in the United States given in Simiu, Changery, and Filliben (1979) forms the basis for the non-hurricane design wind speeds given in ASCE-7-88. In the United States, the annual maximum wind speeds have been recorded in the form of either peak gust or fastest-mile values. For use with wind tunnel test data, the peak gust or fastest-mile wind speed data must be converted to equivalent mean hourly values using the methodology described in Durst (1960) or the modified Durst method given in Simiu and Scanlan (1986). As in the case of the hourly wind speed data, the distribution parameters are determined using standard methods, including the method of moments, method of least squares, or method of maximum likelihood. The form of the Type I distribution given in Eq. (C10.15) can be expressed in the form

$$V_{RP} = U_a - a_a \ln\left[-\ln\left(1 - \frac{1}{RP}\right)\right] \tag{C10.16}$$

where RP is the return period of interest, and for larger return periods, (RP > 10 years)

$$V_{RP} = U_a + a_a \ln(RP) \tag{C10.17}$$

Figure C10.3 shows an example of the observed and modeled distribution of extreme winds for Grand Rapids, Michigan, derived from 22 years of annual maximum peak gust data. Substituting the mode (U_a = 60.2 mph) and dispersion (a_a = 7.14 mph) given in Figure C10.3 into Eq. (C10.17) results in an estimated 100-year return period mean hourly wind speed at gradient height of 93 mph.

Peterka (1992) has shown that predictions of 50-year-return-period wind speeds from record lengths of 20 to 40 years at a single station can have a significant uncertainty associated with sampling error (the uncertainty in knowing the true statistics because of a short record length). Grouping nearby stations with statistically independent records was shown to be a technique for reducing the sampling error.

To take into account the effect of directionality, Eq. (C10.15) is modified so that

$$P(v(\theta) > V) = 1 - \exp\left\{-\exp\left[-\frac{V - U_a(\theta)}{a_a(\theta)}\right]\right\} \tag{C10.18}$$

where $P(v(\theta) > V)$ is the probability of exceeding the wind speed, V, within the directional sector defined by $\theta \pm (\Delta\theta/2)$, and $U_a(\theta)$ and $a_a(\theta)$ are the mode and dispersion of the distribution which are a function of wind direction. For most surface stations in the United States, the annual fastest-mile or peak-gust data are reported for the eight or 16 major compass directions ($\Delta\theta$ = 45° or 22.5°). The directionally dependent mode and dispersion are obtained by fitting the largest annual wind speed recorded within a directional segment to the Type I distribution using the same techniques employed in the non-directional case.

In instances where only relatively short records of extreme winds are available, monthly extremes can be used to estimate the 50- or 100-year-return-period wind speeds (Simiu et al. 1982). Assuming the monthly maximum wind speeds are independent of one another, then the mode and dispersion of the annual Type I distribution are obtained from the mode and dispersion of the monthly extremes using the expression

$$U_a = U_m + \ln(12) a_m \text{ and } a_a = a_m \tag{C10.19}$$

where U_m and a_m are the mode and dispersion derived from the monthly extremes, and U_a and a_a are the derived mode and dispersion for the annual maxima.

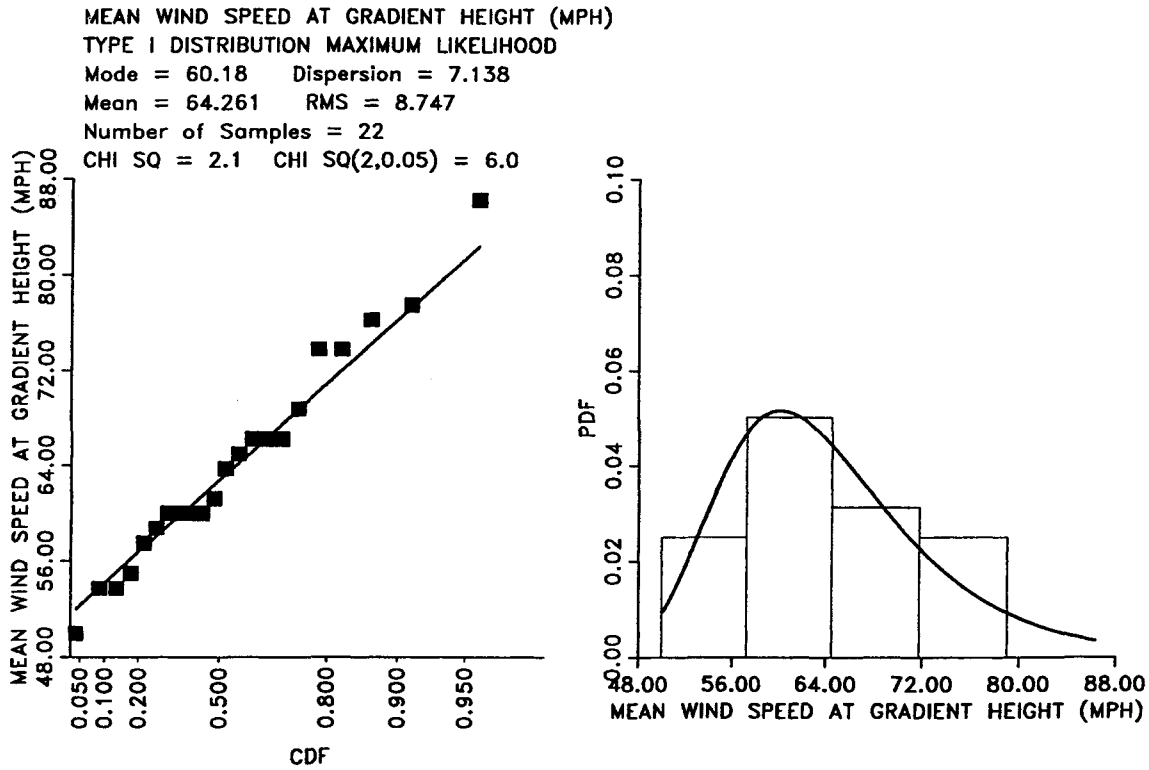

FIGURE C10.3. Type I Distribution of Wind Speeds at Grand Rapids.

One approach for using the annual extremes for the prediction of wind induced loads and responses is outlined in Simiu and Filliben (1981) and Simiu (1983). Using this approach a random variable, r_{1j} during year j, is defined as

$$r_{1j} = \max\left[C_p(\theta_i)^{1/2} V_j(\theta_i)\right] \tag{C10.20}$$

where $C_p(\theta_i)$ is the maximum pressure coefficient within the direction sector $\theta_i \pm (\Delta\theta/2)$, $V_j(\theta_i)$ is the actual value of the maximum mean hourly wind speed recorded in that year (converted to gradient height) in the same direction segment, and max[ ] implies the largest value over all azimuths. The response variable, r_{1j}, is the annual maximum value of the response and has units of wind speed. The maximum value of r_{1j} is determined for all years where annual maximum wind speed were obtained, and a prediction of the random variable, r_1, versus return period is obtained using a Type I distribution, using the methods outlined earlier. A second variable is defined as

$$r_2 = \max\left[C_p(\theta_i)^{1/2}\right] V_{RP} \tag{C10.21}$$

where V_{RP} is the predicted wind speed (independent of direction) associated with a return period of RP years and $\max[C_p(\theta_i)^{1/2}]$ is the maximum value of the square root of the pressure coefficient measured over all azimuths. The design pressure, P_{RP} associated with a return period RP, taking into account directional effects is then

$$P_{RP} = \left(\frac{r_1}{r_2}\right)^2 \tfrac{1}{2}\rho \max\left[C_p(\theta_i)\right] V_{RP}^2 \tag{C10.22}$$

The above method is strictly only valid for the predictions of responses which vary in accordance with a V^2 relationship. A simpler and more robust method involves calculating what the maximum response value of the structure would have been over the period of record for which wind speeds were obtained. Using this approach a set of N annual maximum response estimates, r_j, are obtained through

$$r_j = \max\left[a(\theta_i) V_j(\theta_i)^{b(\theta_i)}\right] \tag{C10.23}$$

where $a(\theta_i)$ and $b(\theta_i)$ are as defined earlier, and $V_j(\theta_i)$ is the maximum wind speed recorded in the jth year for a direction $\theta_i \pm (\Delta\theta/2)$. The vector of annual maximum responses, r_j, for the period of record is then fitted to a Type I dis-

tribution, and predictions of response versus return period are obtained using standard methods. The structural load or response vector derived from the wind tunnel data are proportional to velocity raised to a power in the range of two to three and will converge to a Type I distribution faster than the annual maximum wind speed measurements themselves (Cook 1982). Additional methods for taking into account the effect of wind direction on predicted wind induced responses include Holmes (1986).

C10.3.4 Comparison of Wind Climate Models and Example of Predicted Responses

The description of the wind climate at a given location often varies with the analysis technique and wind speed data used to derive the wind climate model. Each of the techniques described herein has advantages and disadvantages and in general, no one method is considered to be superior to any other method. However, in regions where the extreme wind climate is dominated by thunderstorms, the hourly wind speed measurements often do not include the effect of the short duration thunderstorm winds (Twisdale and Vickery 1992, 1993). An example of the differences in the wind climate models derived using annual extremes, hourly surface level, and upper-level wind speed measurements are given in Figure C10.4 for a major U.S. city. The annual extreme wind speeds were recorded as fastest-mile values at one of the city's two airports, the hourly surface-level data were recorded at the other airport, and the upper-level data were recorded near the second airport station. Figures C10.4a and b present the parent probability distribution of the mean hourly wind speed and direction at gradient height derived from upper-level and surface-level measurements respectively. The contours represent the wind speeds exceeded for specified probabilities of exceedance within directional segments of 22.5°. The strongest winds, as indicated by the lowest probability contour [$P(>v) = 10^{-6}$], are seen to approach from the south in the wind climate model derived from upper-level winds, and from both easterly and westerly directions in the model derived from surface-level wind speed measurements. Figure C10.4c shows the predicted 50- and 100-year-return-period wind speeds as a function of direction derived from annual extremes. The contours represent the wind speed expected to be exceeded an average of once every 50 or 100 years within an azimuth sector of 45°. Figure C10.4c indicates that the strongest winds approach from the west and northeast.

The effect of the different wind climate models on the final predictions is shown in the following example, where the 100-year return period predicted negative pressures (suctions) at four locations on a building are derived using the three wind climate models given in Figure C10.4 and two simplified representations of the wind climate. In this example, the wind climate models have been adjusted so that they all produce a predicted 100-

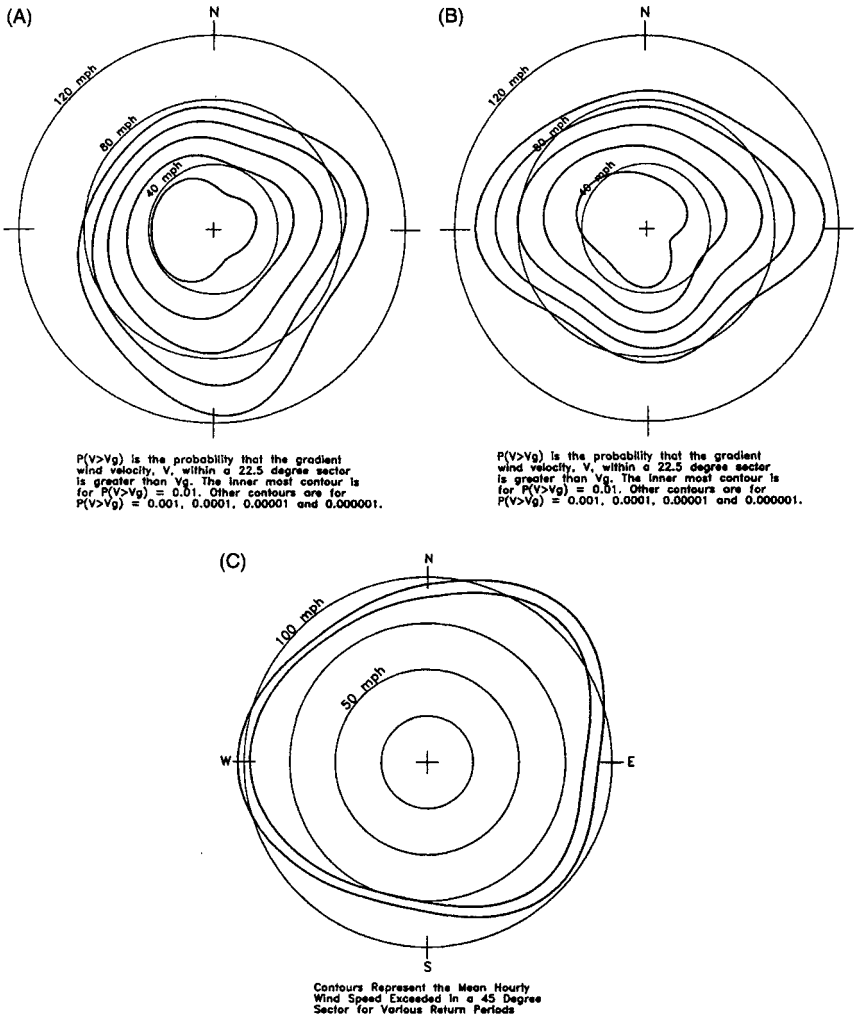

FIGURE C10.4. Wind Climate Models Derived from Various Sources for a Major U.S. City.

(A) Gradient-level wind climate derived from upper-level measurements wind speed; (B) gradient-level wind climate derived from surface-level wind speed measurement; and (C) gradient-level wind climate derived from surface-level annual extremes.

year-return-period mean wind speed at gradient height of 47 m/s, so that the example shows the effect of wind direction alone. Without this adjustment, the three wind climate models yield mean hourly 100-year return period wind speeds at gradient height ranging between 43 m/s and 47 m/s. The first of the two simplified models assumes that the 100-year-return-period wind speed approaches from the aerodynamically worst direction (i.e., code type approach) and the second simplified model assumes a circular wind climate. The aerodynamic characteristics of the pressures coefficients at the four pressure taps are shown in Figure C10.5, in which it is clear that the worst negative pressures (bottom curve) occur for winds approaching from different directions.

The predicted 100-year-return-period suctions obtained using the five different approaches are presented in Table C10.2. The results clearly indicate that ignoring the influence of wind direction produces conservative results, and that the selection of a wind climate model has a significant impact on the final predictions. In the case of TAP 1, where the highest suctions are produced by northeasterly winds, the prediction obtained using the wind climate model derived from the fastest-mile wind speeds, where the strongest winds are predicted to be northeasterly, yields the largest predicted suction. In the case of TAP 2 and TAP 3, where the highest suctions are produced by southerly winds, the predictions derived using the upper-level wind climate model exceed those derived using either of the wind climate models derived from surface level winds.

The differences in wind directionality shown in the wind climate models given in Figure C10.2 and the resulting differences in predicted pressures

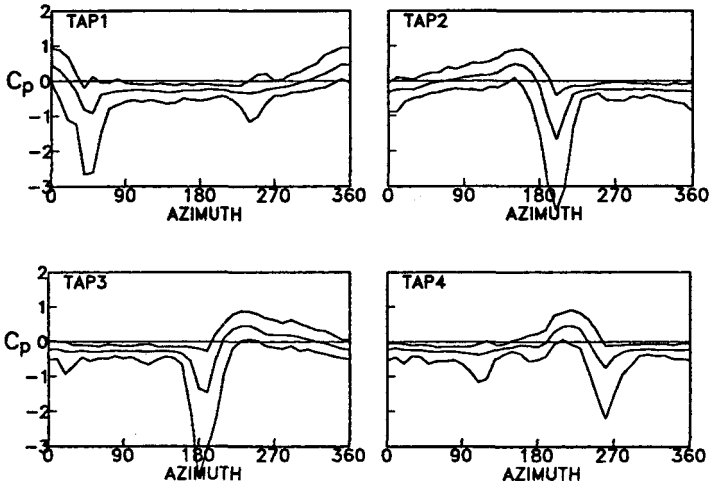

FIGURE C10.5. Pressure Coefficient versus Wind Direction.

TABLE C10.2. Effect of Wind Climate Model and 100-Year Return Period Predicted Wind-Inducedpressures

	Predicted 100-Year Return Period Suction (kPa)				
Pressure Tap	Wind Direction Not Taken into Account	Circular Wind Climate	Wind Climate from Upper Level Measurements (Figure C10.4a)	Wind Climate from Hourly Surface Measurements (Figure C10.4b)	Wind Climate from Surface Fastest-Mile Wind Speed Measurements (Figure C10.4c)
TAP1	3.6	2.8	2.0	2.3	3.6
TAP2	5.0	3.6	3.9	2.4	3.1
TAP3	5.2	3.8	4.5	2.9	2.9
TAP4	3.0	2.1	1.6	2.3	2.5

given in Table C10.2 indicate the importance of predicting the wind-induced response with multiple wind climate models to ensure that the final results are not nonconservative. The results also indicate that even though the directional characteristics of the three wind climate models differ significantly, using the highest predicted response from these climates still yields lower predictions than the simple and conservative code approach. Most locations do not show as much variability in the wind climate, as is shown in Figure C10.4 and Table C10.2. The uncertainty in the definition of the wind climate model is in most cases the largest contributor to the overall uncertainty in the wind tunnel testing process. The uncertainties in the wind climate modeling arise from a combination of sampling errors (associated with the number of years of data), and errors produced by terrain effects, climatological changes, applicability of relationships between surface and gradient level winds, sampling of wind speeds produced by different meteorological phenomena, and the suitability of models converting wind speeds from one averaging time to another.

Discussion of sampling errors associated with predicting wind speeds using a Type I distribution are given in Simiu and Scanlan (1986), and Cook (1985). Peterka (1992) presents information on site-to-site variability associated with a combination of sampling errors and terrain effects. The effect of deriving a wind climate model in regions influenced by a combination of thunderstorms and extratropical storms is described in Gomes and Vickery (1978) for Australia, and Twisdale and Vickery (1992, 1993) for the United States. It is noteworthy that the current state of knowledge with respect to the effect of thunderstorms on the wind-induced response of structures is extremely limited. Assuming the aerodynamic response of a structure in a thunderstorm wind is similar to that produced by a non-thunderstorm

wind, then the current approach of treating thunderstorm winds as having the same effects as non-thunderstorm winds is in most cases probably conservative for tall buildings. This conservatism is expected since the mean and gust velocity profiles in strong thunderstorms do not show the monotonic increase with height evident in the case of extra-tropical storm winds.

Because of uncertainties in the wind climate modeling it is suggested that multiple wind climate models should be developed using the various data sources available at a given site, and that the final predicted responses should be the largest of the resulting predictions. Alternatively rotating the wind climate model by ±22.5° can help to account for some of the uncertainty in the wind climate modeling.

C10.4 HURRICANE WINDS

Along most of the Gulf and Atlantic coasts of the United States, the design wind speeds are dominated by the influence of tropical cyclones or hurricanes. Reliable estimates of long-return-period wind speeds in these hurricane-prone regions cannot be derived using the more traditional techniques outlined in Section C10.3. The traditional approaches cannot be used because at any given location there are very few direct measurements of hurricane wind speeds. These direct wind speed measurements do not exist because hurricanes are relatively small storms, occurring infrequently (at any one location). Furthermore, the maximum wind speed produced by the storm are often not recorded because the anemometers fail or power is lost or the station is left unattended with no recording device.

To overcome the difficulties associated with the lack of direct hurricane wind speed measurements at a prescribed location, an indirect method first proposed by Russell (1971) is used to determine design wind speeds produced by hurricanes. This method owes its success to the fact that, although hurricane wind speed measurements at a given location are not available, information on key parameters describing a hurricane, including the central pressure, position and time data, and storm size are available. Using these data, statistical distributions for the central pressure (Δp), storm heading (θ), translation speed (VT), distance from the site (d_{min}), and radius to maximum winds (R_{max}) can be derived. This information is then used in combination with mathematical models of a hurricane windfield to simulate many thousands of hurricanes near the site. The final result of the procedure is a large number of simulated wind speed traces generated from site-specific statistics of key hurricane parameters, thus retaining the local hurricane climatology.

Once the simulated storms have been generated, the annual probability of exceeding a given wind speed, $P(v > V)$, is obtained through

$$P(v > V) = \sum_{x=0}^{\infty} P(v > V|x) P_t(x) \qquad \text{(C10.24)}$$

where $P(v > V|x)$ is the probability of exceeding the velocity V given the occurrence of a storm (derived from the simulated storms) and $P_t(x)$ is the probability of x storms occurring in any one year. At most locations, the arrival process of tropical storms is adequately modeled using a Poisson distribution, and for $P(v > V)$ of less than 0.05 (return periods longer than 20 years), Eq. (C10.24) can be accurately approximated as

$$P(v > V) = \lambda \cdot P(v > V|x) \qquad \text{(C10.25)}$$

where λ is the mean annual rate of occurrence of storms in the region. The simulation methodology is outlined in Figure C10.6.

Details of the use of mathematical simulation methodology as applicable to the United States are described, for example, in studies by Russell and Schueller (1974), Tryggvason et al. (1976), Batts et al. (1980), Georgiou et al. (1983), Georgiou (1985), and Vickery and Twisdale (1995a and b). Tropical cyclone wind speeds along the Northern Australian coast have been studied

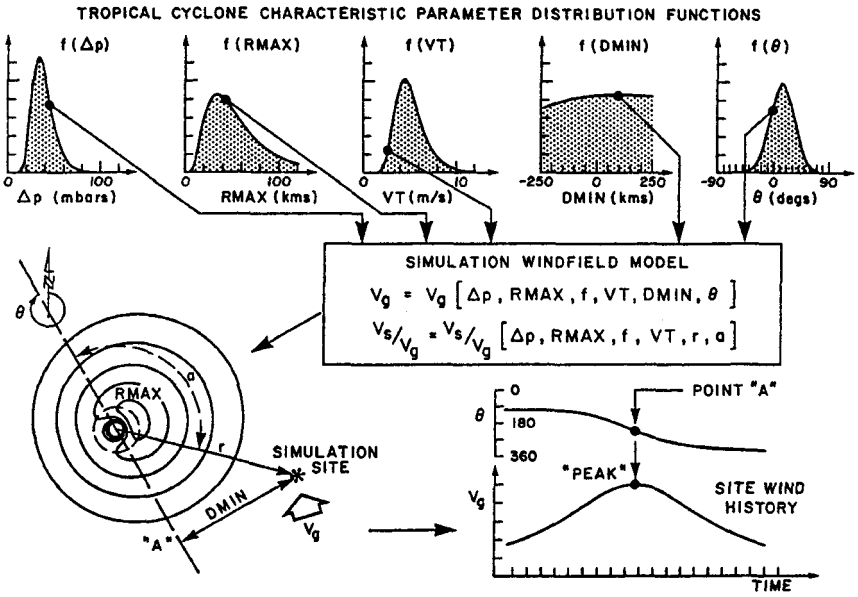

FIGURE C10.6. Hurricane Simulation Flow Diagram.

Source: Georgiou 1985.

by Gomes and Vickery (1976) and Tryggvason (1979b). Although the simulation methodologies used by these investigators are similar, there are significant differences in the statistical models, methods of data analysis, data sources, and critical hurricane windfield modeling used in each of these studies, and consequently produce wind speed predictions at a given location that may vary from study to study.

Once these synthesized wind speeds are produced, techniques similar to those discussed in Section C10.3 can be used to derive estimates of wind-induced response versus return period. For example, in each simulated storm the maximum value of the response of the structure is readily obtained using Eq. (C10.23) where $V_j(\theta)$ is the maximum simulated mean hourly wind speed for storm j for the direction $\theta_i \pm (\Delta\theta/2)$. Using this information the probability of exceeding a response level r, $P(r > R \mid x)$, given the occurrence of a storm is obtained. The annual probability of exceedance is then

$$P(r > R) = \lambda \cdot P(r > R|x) \tag{C10.26}$$

Alternately, simulated wind speeds produced on an hour-by-hour basis can be used to develop the parent probability distribution of hurricane wind speeds, for use in an upcrossing analysis, using the modified Davenport approach described in Georgiou (1985) or the approach developed by Lepage and Irwin (1985). If the Lepage and Irwin approach is used, Eq. (C10.14), then site-specific relationships between $|\dot{\bar{V}}|$ and V and $|\dot{\bar{\theta}}|$ and V must be developed in the simulation methodology, to replace the empirical expressions given in Irwin (1987).

Once the estimates of response versus return period associated with hurricanes are obtained, these estimates must then be combined with response versus return-period estimates produced by non-hurricane winds. Since the wind speeds produced by hurricanes and non-hurricanes are statistically independent, the combined distribution is

$$P(r > R) = 1 - P(r < R_H)P(r < R_N) \tag{C10.27}$$

where $P(r>R)$ is the probability that the response level R is exceeded, and $P(r<R_H)$ and $P(r<R_N)$ are the cumulative distributions for the hurricane and non-hurricane responses respectively.

This page intentionally left blank

GLOSSARY

Across-Wind Force: The aerodynamic force in a direction perpendicular to that of the mean wind velocity; sometimes referred to as lift.

Adiabatic Lapse Rate: Temperature variation with height of –1 °C/100 m that corresponds to temperature drop (without heat transfer) of a rising parcel of dry air.

Aerodynamic Damping: The force experienced by an object moving in an airstream that is proportional to the velocity of the body motion (body velocity).

Aerodynamic Derivatives: Non-dimensional parameters or coefficients that relate the aerodynamic forces acting on a moving body to its motion and the time derivatives of this motion. These derivatives are functions of the reduced frequency of the body motion.

Aerodynamic Forces: Flow-induced forces on a body (building or structure).

Aerodynamic Instability: Large oscillatory motions of a body in a moving airstream, typically a bridge deck, because of flutter or galloping. *Also see* Divergence.

Aerodynamic Interference: Changes in the aerodynamic forces, which result from the presence of another object (building or structure).

Aeroelastic Effect: The modification of the aerodynamic forces because of the wind-induced motion of a body (building or structure).

Approach Flow: Natural wind which approaches a particular building or structure and its surroundings and has properties that are determined by the topography and the roughness of the upstream terrain.

Atmospheric Boundary Layer: The lower part of the atmosphere, typically 600 to 1600 ft (200 to 500 m) thick, in which the properties of the flow are influenced by the earth's surface. In this layer, there is a pronounced increase in mean wind speed with height above ground and the flow is highly turbulent.

Atmospheric Surface-Layer: The lower portion of the atmospheric boundary layer, in which the shear stress remains approximately constant.

Autocorrelation: Normalized autocovariance of a random time-dependent variable evaluated at different time lags. The autocorrelation is unity at zero lag time, and for a random variable approaches zero as the lag time becomes large.

Balance: A device or transducer system used to measure wind-induced forces or moments, or both, on a model in the wind tunnel.

Barotropic Atmosphere: An atmosphere in which the density depends only on the atmospheric pressure (isobaric surfaces are also surfaces of constant density).

Blockage: The obstruction of the wind tunnel test section by the model and its surroundings. Corrections are appropriate if more than 5% of the cross-sectional area is blocked in this way.

Bulk Density: The density of a building or structure obtained by dividing its mass by its gross volume.

Cauchy Number (*Ca*): A non-dimensional parameter which represents the ratio of the elastic forces of a building or structure to the inertia forces of the flow. $Ca = E_{eff}/\rho V^2$, in which E_{eff} = effective elastic modulus of the structure, ρ = air density, and V = representative wind velocity.

Cladding: Components of the exterior skin or envelope of a building or structure, which keeps out the "weather" but does not contribute to the overall resistance to wind action. The cladding resists local wind loads and transfers them to the main structural system.

Critical Damping Ratio: The damping of a building or structure expressed as a ratio of the critical damping. The critical damping for a mode of vibration is the lowest value of the damping at which an initial motion decays without oscillation. Numerically the critical damping is equal to $2(MK)^{1/2}$, in which M and K are the generalized mass and stiffness, respectively.

Curtainwall: The exterior wall system of a building which keeps out the "weather" but does not contribute to the overall wind resistance of the building. The curtainwall resists local wind loads and transfers them to the structural frame.

Divergence: A form of aerodynamic instability that can occur when the deflection of a structure because of wind action results in larger forces, which in turn further increase the deflection. Instability occurs when the restoring forces of the structure are exceeded.

Drag Coefficient: A non-dimensional aerodynamic force in the direction of the mean velocity vector obtained by normalizing this force by its frontal area and $\frac{1}{2}\rho V^2$, the dynamic pressure of the flow. Here V is a representative or reference wind velocity.

Dynamic Magnification: The response of a structure to a dynamic load depends on the frequency or the time variation of the load. The response increases as the frequency of the load approaches resonance with a natural

mode of vibration of the structure. The magnitude of the response at and near resonance is controlled by damping. *Also see* Mechanical Admittance.

Dynamic Similitude: Consistent proportionality of the various forces acting on a model and prototype building or structure.

Extra-tropical Cyclone: A large-scale, low-pressure system, typically 500 to 800 miles (800 to 1300 km) in diameter. In the northern hemisphere, such systems tend to move from west to east and the flow within such systems moves in a counter-clockwise direction. This type of weather system is the main source of extreme winds in temperate regions.

Flow Visualization: The visualization of the flow around an object, in which streamlines and other characteristics of the flow are identified by adding smoke or some other visually seen tracer to the airstream.

Force Balance Model: A model of a building or structure that is used to measure the mean or dynamic wind forces, or both. Typically such measurements are made by mounting the model on an instrumented balance or force transducer system.

Frequency Response: The range of frequencies to which an instrument can respond without significant distortion of the measured quantity.

Froude Number (*Fr*): A non-dimensional parameter which represents the ratio of the inertia forces of the flow to the gravity forces acting on a building or structure. $Fr = V^2/(gL_b)$, in which V = representative wind velocity, g = acceleration of gravity, and L_b = a characteristic length of building or structure.

Galloping: An aerodynamic instability found with flexible structures with special cross-sectional shapes; typically square and rectangular sections, or D-sections characteristic of ice-coated cables. There is a potential for galloping if $(dC_L/d\alpha + C_D) < 0$ in which C_L and C_D are respectively the mean lift and drag coefficients, and α = angle of attack, in radians and $dC_L/d\alpha$ is the rate of change of the lift with angle of attack (Den Hartog criterion). The critical speed or the onset of galloping depends upon the magnitude of the structural damping.

Generalized Force: The wind-induced force effective in exciting a particular mode of vibration of a building or structure. Sometimes also referred to as the modal force. It corresponds to the integral of the force per unit length of the structure weighted by the mode shape and evaluated over the entire building or structure.

Generalized Mass: The effective mass associated with a particular mode of vibration. It corresponds to the integral of the mass per unit height, weighted by the square of the mode shape evaluated over the entire building or structure.

Generalized Stiffness: The effective stiffness of the structure associated with its response in a particular mode of vibration. The generalized stiffness = $(2\pi f_0)^2$ times the generalized mass, where f_0 = natural frequency of the particular mode.

Generalized Torque: The effective wind-induced torque associated with the torsional mode of vibration of a building or structure. Corresponds to the integral of the torque per unit height, weighted by the mode shape and evaluated over the entire building or structure.

Geostrophic Height: Height of the geostrophic wind above earth's surface. Geostrophic heights are in the range of 3000 to 6000 ft (1000 to 2000 m).

Geostrophic Wind: The velocity field when the Coriolis force balances the horizontal pressure gradient force.

Gradient Height: The height above ground at which the wind speed becomes approximately constant and effects of the surface shear stress become negligible. For wind engineering applications, this height is assumed to define the edge of the atmospheric boundary layer and is assumed to be about 250 to 500 m, depending on terrain roughness.

Gust Effect Factor: A factor by which the mean wind load must be multiplied to obtain the equivalent statically acting maximum or peak load. The gust effect factor allows for the turbulence present in the wind and the mechanical magnification of the dynamic loads by the structure or building.

Hot-Wire Anemometer: An instrument for measuring wind speed that is sufficiently responsive to detect velocity fluctuations because of turbulence. It consists of a small heated wire immersed into the flow. The cooling of the wire by the flow provides the measure of the wind speed.

Hurricane: A tropical cyclone with sustained (1 or 2 minute average) surface wind speed exceeding 74 mph (120 km/h). Tropical cyclones are storms which generally originate in latitudes between about 5° and 20° north and south of the equator, and which derive their energy from the latent heat release of the condensation of water vapor. Hurricanes are referred to as typhoons in the Far East, and as cyclones in the Southern Hemisphere.

Inertial Force: A force acting on a moving body equal to its mass multiplied by its acceleration.

Inertial Subrange: The range of wave numbers for which the spectrum of turbulence is independent of viscosity, ν. In this range, the power spectral densities of the components of turbulence vary as frequency raised to a power of $-5/3$.

Integral Scale: A characteristic length which represents a measure of the average size of turbulent eddies or gusts present in the atmospheric boundary layer. The integral scale of a particular component of turbulence corresponds to the product of the mean wind speed and the integral time scale of that component obtained from the integration of the autocorrelation function.

Internal Pressure: The wind-induced pressure within the interior of a building or structure. This internal pressure acts on the inside or back surfaces of the exterior envelope and must be considered in combination with exterior pressures.

Jensen Number (*Je*): A non-dimensional length scale parameter defined as the ratio of a characteristic building length L_b to the aerodynamic roughness length z_0. $Je = L_b/z_0$.

Lateral Component of Turbulence: The component velocity vector of turbulence in a horizontal direction normal to the direction of the mean flow.

Load Factor: A factor applied to the nominal design loads in order to allow for its inherent uncertainties.

Local Stationarity: A condition during which the statistical properties of a randomly varying process can be considered to remain invariant for a period of time significantly longer than the important time scale of the process. Turbulence, present in natural wind, can be considered to be locally stationary for periods on the order of 1 hour.

Local Wind Load: Wind load acting on a small area or part of the exterior of a building or structure over which the time-varying wind pressures are fully correlated.

Longitudinal Component of Turbulence: The component velocity vector of turbulence along the direction of the mean flow.

Lumped Parameter Systems: A discrete representation of a continuous structural system, in which the stiffness, mass, and damping characteristics are assumed to be concentrated at certain locations.

Mean Value: The average value of a random variable.

Mechanical Admittance: A function that describes the dynamic response of a structure to a sinusoidal excitation of constant amplitude at different frequencies. *Also see* Dynamic Magnification.

Micrometeorology: The meteorology of small areas within the atmospheric boundary layer, ranging from a few feet to a few miles in size.

Mode Shape: The characteristic shape or eigenvector which describes the dynamic equilibrium shape of a building or structure in a particular mode of vibration.

Mode of Vibration: A characteristic state of dynamic equilibrium in which all points on a building or structure move harmonically at a specific natural frequency (eigenvalue) characteristic of this mode, and in which the relative motions of these points follow a particular deflected configuration or mode shape (eigenvector). Also referred to as normal or principal modes of vibration.

Near Field: The flow field in the immediate vicinity of a particular building or structure, which reflects the aerodynamic influence of its surroundings.

Neutral Thermal Stratification: A stratification of the atmospheric boundary layer in which the vertical variation of the mean air temperature follows the adiabatic lapse rate. This is characteristic of strong winds during which buoyancy forces become negligible. Also referred to as neutral stability.

Overall Wind Forces: Wind forces that are effective over the entire building or structure and that determine the action of winds on the primary structural system.

Panel Wind Load: The wind load effective on an intermediate area of the exterior envelope and one that may be characteristic of the tributary area of a secondary structural member.

Planetary Boundary Layer: The region of atmospheric flow between the surface of earth and the geostrophic height. This region varies in depth from about 3000 to 6000 ft (1000 to 2000 m).

Pneumatic Averaging: The process of spatial averaging of pressures at a number of locations, achieved by connecting these pressures to a common manifold or pressure line. The resulting pressure corresponds to the spatial average for the area under consideration.

Pneumatic Damping: Damping forces that result from the flow within the cavity or internal volume of a building or structure because of the movements of the exterior envelope. This can be important for volume displacing modes of vibration of air-supported and other types of flexible roof systems.

Pneumatic Stiffness: The resistance to the deformation of a structure resulting from the compressibility of the air within the cavity or internal volume of a building or structure.

Poisson's Ratio: A characteristic elastic property of a material, which is defined as the negative of the ratio of the lateral strain to the axial strain in a uniaxial stress application. The modeling of the Poisson's ratio can be important for replica aeroelastic models of shells and membranes.

Power Spectrum: The Fourier transform of the autocorrelation of a particular stationary random process, and the measure which determines the contribution to the total variance of the process from various frequencies.

Pressure Tap: An opening in the surface of a building or a structure which allows the wind-induced pressure at that location to be communicated to a pressure transducer.

Proximity Model: A model of the immediate surroundings of a building or structure which must be included in order to representatively model its influence on the local or "near-field" flow conditions.

Quasi-Static: A condition in which the time-varying component of a process can be taken to depend on the same physical laws as its mean or static value.

Reduced Frequency: A frequency normalized by multiplying it by a characteristic length and dividing it by a characteristic velocity, fL/V.

Replica Model: An aeroelastic model in which the geometric as well as elastic prototype properties have been scaled exactly.

Resonant Vibrations: The oscillation of a building or structure at a natural frequency of vibration.

Return Period: The average time between the recurrence of an extreme event. The probability of exceeding the extreme event with a particular return period during any one year is equal to the inverse of the return period. Also called the recurrence interval.

Reynolds Number (*Re*): A non-dimensional parameter that represents the ratio of the inertia forces to the viscous forces acting on the flow. $Re = VL/\nu$ in which V = characteristic wind velocity, L = characteristic overall dimension, and ν = kinematic viscosity of the air. Various other forms of Reynolds are used including the roughness Re defined as $u_* z_0/\nu$, the stack Re_s defined as dW_s/ν_s, and the building Re_b defined as $L_b V/\nu$.

Richardson Number (*Ri*): A non-dimensional parameter that represents the ratio of buoyancy forces to inertia forces. The most common form of Ri is the bulk Richardson number $(Ri) = (\Delta T_0/T_0)L_0 g/V_0^2$, where the subscript o indicates a reference value.

Rossby Number (*Ro*): A non-dimensional parameter that represents the ratio of inertia forces to those resulting from the effect of the Coriolis accelerations. $Ro = V/(Lf_c)$ where V = characteristic wind velocity, L = characteristic length, and f_c is the Coriolis parameter; $f_c = 2\omega\sin\phi$, where ω is the rotational speed of the earth and ϕ is the latitude.

Roughness Length: A length denoted by z_o that characterizes the roughness of a surface. It is a parameter of the logarithmic mean velocity profile over an aerodynamically rough surface.

RMS Value: Root mean square value of the fluctuating component of a stationary variable. In wind engineering applications, it is taken as the square root of the average of the square of the deviations of the variable from its mean and is equivalent to the standard deviation. *See* variance.

Scruton Number (*Sc*): A non-dimensional parameter proportional to the product of the mass ratio and the critical damping ratio. $Sc = (4\pi m\zeta)/(\rho d^2)$.

Section Model: A rigid model of a part or section of a structure which is mounted in the wind tunnel to simulate the dynamic characteristics of the structure in particular modes of vibration and which is tested in two-dimensional flow conditions.

Sharp-Edged: Bluff aerodynamic shapes with sharp edges for which the flow separation and the aerodynamic forces tend to be relatively insensitive to variations in Reynolds number.

Spatial Averaging: The averaging of instantaneous wind-induced pressures over a particular tributary area. This can include arithmetic averaging or weighted averaging, as in the evaluation of the generalized force.

Spectra: *See* Power Spectrum.

Stick Aeroelastic Model: A type of aeroelastic model used to simulate the two fundamental sway modes of vibration of a vertical structure. The full-scale mode shapes are simulated by linearly varying modes above some selected pivot point.

Strouhal Number (*S*): The non-dimensional frequency of the shedding of vortices from a bluff object. $S = f_s d/V$, where f_s is the vortex shedding frequency, d is a characteristic width and V is a characteristic wind speed. *Also see* Vortex shedding.

Structural Damping: The damping inherent to the structure which represents the energy dissipation resulting from the inelastic action of the structural system, the foundations, and various nonstructural components. Sometimes also referred to as the mechanical damping or just damping.

Surface Wind Speed: Wind speed measured near the earth's surface, typically (but not always) at a height of 10 m above local ground or water surface.

Taut-Strip Model: A simplified version of a full bridge model which allows the evaluation of the wind-induced forces on the deck associated with particular modes of vibration. It consists of two parallel tensioned wires which support rigid sections of the bridge deck. The spacing of the wires and their tension are adjusted to achieve a particular frequency ratio for vertical and torsional modes of vibration.

Taut-Tube Model: Similar to a taut-strip model except that the wires are replaced by tubes to enable a wider range of ratios of torsional to vertical frequencies to be simulated.

Thermal Wind: Wind resulting from horizontal temperature gradients that cause the geostrophic wind to vary with height.

Topographic Model: A model that includes the topography and roughness of a particular terrain. Small-scale topographic models are used to study the structure of the atmospheric boundary layer over complicated terrain.

Tributary Area: Part of the exterior and/or interior surface of a structure which transfers its wind forces to a particular structural member.

Turbulence: Random fluctuations in the wind velocity or "gusts."

Turbulent Boundary Layer: *See* Atmospheric Boundary Layer.

Variance: The square of the RMS value or the average of the square of the deviation of a stationary variable from its mean.

Vertical Component of Turbulence: The component velocity vector of turbulence in the vertical direction normal to the direction of the mean flow.

Virtual Mass: A hypothetical mass of the fluid which, if assumed to move with the body, approximates additional inertial effects arising from the motion induced in the fluid.

Vortex Shedding: When the wind flows around and past a slender prismatic or cylindrical object, vortices are shed alternatively from one side and then the other giving rise to a fluctuating force acting at right angles to the wind direction. This shedding can be highly organized and can cause large amplitude motions when its frequency coincides with a natural frequency of the structure. *Also see* Strouhal number.

ACRONYMS

ABL: Atmospheric Boundary Layer
ANSI: American National Standards Institute
ASCE: American Society of Civil Engineers
ASHRAE: American Society of Heating, Refrigerating and Air-Conditioning Engineers
ASL: Atmospheric Surface Layer
ASME: American Society of Mechanical Engineers
BLWT: Boundary Layer Wind Tunnel
CAARC: Commonwealth Aeronautical Advisory Research Council
CIBC: Canadian Imperial Bank of Commerce Building, Toronto, Ontario, Canada
CSU: Colorado State University
EPA: Environmental Protection Agency
ESDU: Engineering Science Data Unit
FUR: Flat Uniformly Rough
MWT: Meteorological Wind Tunnel
NBCC: National Building Code of Canada
NSF: National Science Foundation
PBL: Planetary Boundary Layer
PLWs: Pedestrian Level Winds
TTU: Texas Tech University
UWO: University of Western Ontario

This page intentionally left blank

NOMENCLATURE

a	Height of pivot point of an aeroelastic stick model
$a(\theta)$	Direction dependent constant in structural response equation
a_a	Dispersion in Type I extreme value distribution for annual extremes
$a_a(\theta)$	Dispersion in Type I extreme value distribution for annual extremes within direction sector $\theta \pm \Delta\theta/2$
a_m	Dispersion in Type I extreme value distribution for monthly extremes
A	Cross-sectional area of structural member
$A(\theta)$	Fraction of time the wind approaches from within direction sector $\theta \pm \Delta\theta/2$
A_j	Coefficient for determining turbulence intensities; $= 0.4\ (\sigma_j/u_*)$; $j = 1$ for u; $j = 2$ for v; $j = 3$ for w
A_s	Stack exhaust area
$b(\theta)$	Directionality dependent exponent in wind-induced response equation
B	Characteristic length (i.e. bridge deck width)
c	Concentration of pollutant at point of interest
c_s	Concentration of pollutant at source or at exit from stack
C	Torsional moment of inertia constant, also the Weibull coefficient with units of wind speed
$C(\theta)$	Weibull coefficient for winds within directional sector $\theta \pm \Delta\theta/2$
C_1	Constant in crossing rate equation; $= \sqrt{2\pi}$ for Gaussian process
Ca	Cauchy number; $= E_{eff}/(\rho V^2)$
C_D	Drag coefficient of object; $= D/(qS)$
C_d	Surface drag coefficient; $= D/(gS)$
C_L	Lift coefficient of object; $= L/(qS)$
C_M	Coefficient of moment per unit length, used in bridge aerodynamics; $= M/(qB^2)$

C_p Pressure coefficient; $= (p - p_s)/q$

$C_p(\theta)$ Pressure coefficient measured in wind tunnel for wind from direction θ

d Diameter of stack, size of structural element, or depth of bridge

$d_{\min}$ Minimum distance of hurricane center from site

D Aerodynamic drag force on object or aerodynamic drag per unit length

E Modulus of elasticity of material

E_{eff} Effective modulus of elasticity for structure; $= EI/L^4$, EA/L^2, or $E\tau/L$ depending on the dominance of flexural, axial, or shear and membrane stresses respectively.

f Frequency in (Hz), also a reduced frequency defined $f = nL/V$ in descriptions of the ABL

f_c Coriolis force parameter; $= 2\omega\sin\phi$

f_m Value of f for which $nS_u(z,n)$ is a maximum

f_0 Frequency of fundamental mode of vibration of a structure

Fr Froude Number; $= V^2/(gL)$

f_s Frequency of vortex shedding

G Torsional modulus of elasticity of material, also gust factor relating wind speed averaged over one hour to that averaged over different time periods

G_{eff} Effective torsional modulus of elasticity of structure; $= GC/L^4$

g Acceleration of gravity. Also a peak factor used in forming peak quantities

h Height of top of aeroelastic stick model, building, structure, or roughness obstacles

$(\ )_i$ Subscript i

I Structural Moment of Inertia; second moment of area about some axis

$I_j(z)$ Turbulence intensity; $= \sigma_j(z)/U(z)$; $j = 1, u$; $j = 2, v$; $j = 3, w$

I_m Generalized mass moment of inertia

$(\ )_j$ Subscript j

k Exponent used in Weibull distribution formula

$k(\theta)$ Exponent used in Weibull distribution for winds within direction sector $\theta \pm \Delta\theta/2$

K_s Equivalent sand roughness diameter taken as $30\, z_o$

(K) Stiffness matrix for model or prototype

L Characteristic length or aerodynamic lift force or aerodynamic lift force per unit length

L_b Characteristic building length

L_f Upwind fetch

L_{mo} Monin–Obukhov Stability Length

L_t Length scale for longitudinal turbulence

${}^xL_u$ Length scale of longitudinal turbulence in x direction

$( )_m$ Subscript m implies model quantity
m Mass per unit length of building can be constant or can vary with position along the structure
M Generalized mass of building or model; or aerodynamic moment or aerodynamic moment per unit length
(M) Mass matrix for model or prototype
n Frequency component of gusting. Also distance normal to isobars; $= 1/t$
$N_v(v)$ Number of exceedances of v per unit time
$N_R(R)$ Number of crossings at response level R per unit time
p Pressure
Δp Hurricane central pressure difference
$p(v)$ Probability density of v
$p(\dot{v})$ Probability density of $\dot{v}$
$p(v,\dot{v})$ Joint Probability density of v and $\dot{v}$
$p_v(v_R,\theta)$ Probability density function of v_R within the direction sector $\theta \pm \Delta\theta/2$
$P(r<R_H)$ Cumulative probability of hurricane response
$P(r<R_N)$ Cumulative probability of nonhurricane response
$P(v>V_0)$ Probability that wind speed v exceeds V
$P(v(\theta)>V)$ Probability that wind speed $v(\theta)$ exceeds V, within the direction sector $\theta \pm \Delta\theta/2$
$P(v>V|x)$ Probability of v exceeding V during storm x
P_r Reference pressure
P_{RP} Pressure for return period RP
P_s Pressure in free stream far away from building or structure
$P_t(x)$ The probability of x storms occurring in one year
P_T Total pressure of wind stream (pressure obtained when wind is brought to rest)
P_x Pressure at pressure tap
$( )_p$ Subscript p implies full scale or prototype
q Dynamic or wind pressure; $= \frac{1}{2}\rho V^2$
q_r Reference dynamic pressure; $= \frac{1}{2}\rho V_r^2$
r Radius of curvature of the isobars. Also response of structure or building.
r_{1i} Random variable used in Simiu's (1983) method of predicting extreme loads
r_2 Random variable used in Simiu's (1983) method of predicting extreme loads
$R(v,\theta)$ Response of structure or component as a function of v and θ; $= a(\theta)V^{b(\theta)}$ for $v = V$
Re_b Building Reynolds number; $= V_h L_b/v$
$(Re_b)_{\min}$ Value of Re_b necessary to achieve minimal Reynolds number dependence

Re_f Fetch Reynolds number; $= V_g L_f/v$
Re_s Reynolds number of flow in stack; $= W_s d/v_s$
Ri Bulk Richardson number; $= (\Delta T_0/T_0)(L_0 g/V_0^2)$
R_H Response in hurricane winds
R_{max} Radius of maximum hurricane winds
R_N Response in non-hurricane winds
Ro Rossby number; $= V/Lf_c$ or $V_{geo}/z_0 f_c$
RP Return period
rms Root mean square value
$(\ )_s$ Subscript s to denote characteristics of source
S Characteristic area of structure or its component. Also the Strouhal number
$S_j(z,n)$ Power spectral density as function of height, z, and gust frequency; n; $j = 1, u$; $j = 2, v$; $j = 3, w$
$S_w(z,n)$ Power spectral density of longitudinal component of turbulence
$S_w(z,n)$ Power spectral density of vertical component of turbulence
t Time; $= 1/f$ or $1/n$
T Absolute temperature. Also averaging time
T_0 Absolute reference temperature
ΔT_0 Change in absolute reference temperature
u Fluctuating longitudinal component of wind speed
u_* Friction velocity
U Mean velocity component in longitudinal direction
$U(z)$ Mean u-component at height, z
U_a Mode in Type I extreme value distribution of annual extreme wind speeds
$U_a(\theta)$ Mode in Type I extreme value distribution of annual extreme wind speeds within direction sector $\theta \pm \Delta\theta/2$
U_m Mode of monthly extreme wind speeds
v Instantaneous lateral component of wind speed, $j = 2$. Also a wind speed.
V Mean wind speed, normally for an averaging time of 1 hour
V_a Mean wind speed at anemometer. Also referred to as surface wind speed
V_{eff} Effective gust wind speed (accounts for turbulence in equivalent average); $= \overline{U} + g \times \sigma$; where g is a constant equal to 1.5
V_{fm} Fastest-mile wind speed
V_g Wind speed at gradient height
V_{geo} Wind speed at geostropic height
V_h Wind speed at top of building or structure
V_0 Reference wind speed
V_r Reference wind speed
$V_R(\theta)$ Wind speed from direction sector $\theta \pm \Delta\theta/2$ required to generate a response that exceeds response R

V_{RP} Wind speed for return period RP
V_{10} Wind speed at 10 m
$V(z)$ Mean wind speed at height z
$V_R(\theta)$ Wind velocity within the direction sector $\theta \pm \Delta\theta/2$ required to exceed a specified response level R
VT Translation speed of hurricane
w Instantaneous vertical component of wind speed, $j = 3$
W_s Exhaust gas wind speed at stack exit
x Distance in longitudinal direction, $j = 1$ non-dimensional frequency in Davenport's spectrum $= 1200\, n/V_{10}$; V_{10} in m/s
x' Average spacing of obstacles
y Distance in lateral direction, $j = 2$
z Distance in vertical direction, $j = 3$
z_a Height of anemometer above ground
z_g Height at which the gradient wind is obtained; in the model this is taken as the top of the boundary layer
z_{geo} Height of geostropic boundary layer
z_0 Aerodynamic roughness length
z_{inv} Height to an inversion layer
z_r Reference height used for the power law boundary layer approximation
z_r Depth of atmospheric surface-layer

GLOSSARY OF GREEK SYMBOLS USED

α Angle of attack
$1/\alpha$ Exponent in power law approximation boundary layer
δ Boundary layer thickness in wind tunnels
ζ Damping expressed as a ratio of the critical damping
θ Wind direction angle
$\Delta\theta$ Sector of wind direction
κ Von Karman constant; $= 0.4$
λ Average cycling rate of process $V(t)$; also mean rate of storm occurrence
λ_f Frequency scaling factor
λ_{Im} Rotational moment of inertia factor for aeroelastic stick model
λ_{IM} Torsional mass moment of inertia scaling factor
λ_K Stiffness scaling factor
λ_L Geometric scale of model
λ_M Mass scaling factor
λ_{ps} Scaling factor for density of structure
λ_t Time scaling factor
λ_V Wind speed scaling factor

λ_{vol} Pneumatic stiffness scaling factor
μ Viscosity of air
$\mu_z(z)$ Fundamental mode shape of building or structure
ν Kinematic viscosity of air; $= \mu/\rho$
ν_0 A reference kinematic air viscosity
ρ Density of air
ρ_s Structural bulk density of structure or density of stack exhaust
σ Root mean square value of longitudinal component of velocity (rms)
σ_j rms of; $u, j = 1$; $v, j = 2$; or $w, j = 3$
σ_v Long term standard deviation of wind speed
τ Wall thickness of shell-like structure
τ_0 Mean surface shear stress
ϕ Latitude. Also source strength distortion factor
Φ Source distortion factor in pollution dispersion
ω Rotational speed of earth; $= 7.27 \times 10^{-5}$ rad/sec
$\bar{(\ )}$ Bar over symbol indicates time average or mean fluctuating values
$\dot{(\ )}$ Dot over symbol indicates time derivative
$|\ |$ Absolute value

DERIVATIVES

$\partial p/\partial x$ Partial derivative of the pressure with respect to distance in longitudinal distance. Also referred to as the longitudinal pressure gradient
$\partial p/\partial n$ Partial derivative of atmospheric pressure with respect to distance normal to the isobars in a weather system
$\partial V_R/\partial\theta$ Partial derivative of the wind speed needed to achieve response R with wind direction
$dC_L/d\alpha$ Rate of change of the mean lift coefficient with angle of attack

REFERENCES

American Society of Mechanical Engineers (ASME). (1996) "Quality Assurance Program Requirements for Nuclear Facilities," ANSI/ASME NQA-1-1986 Edition.

Auer, A.H., Veal, D.L., and Marwitz, J.D. (1969) "Updraft Deterioration below Cloud Base," In *Proc. Sixth Conf. on Severe Local Storms.* American Meteorological Society, Boston, 16–19.

Batts, M.E., Cordes, M.R., Russell, C.R., Shaver, J.R., and Simiu, E. (1980) *Hurricane Windspeeds in the United States,* Report Number BSS-124, National Bureau of Standards, U.S. Department of Commerce.

Bedard, A.J., and LeFebvre, T.J. (1986) *Surface Measurements of Gust Fronts and Microbursts during the JAWS Project: Statistical Results and Implications for Wind Shear Detection, Prediction, and Modeling,* National Oceanic and Atmospheric Administration, Environmental Research Laboratories, Wave Propagation Laboratory, Boulder, CO.

Bendat, J.S., and Piersol, A.G. (1986) *Random Data Analysis and Measurement Procedures,* 2nd Ed., John Wiley & Sons, New York.

Beranek, W.J. (1984) "Wind Environment around a Single Building of Rectangular Shape and Wind Environment around Building Configurations," *Heron,* 29(1), 3–70.

Bienkiewicz, B., Cermak, J.E., and Peterka, J.A. (1983) "Active Modeling of Large Scale Turbulence," *J. Wind Eng. Ind. Aero.* 13, 465–475.

Blumen, W., ed. (1990) *Atmospheric Processes over Complex Terrain,* American Meteorological Society, Boston.

Boggs, D.W., and Peterka, J.A. (1989) "Aerodynamic Model Tests on Tall Buildings," *J. Eng. Mech.,* 115(3), 618–635.

Bottema, M. (1992) "Wind Climate and Urban Geometry," Doctoral Thesis, Technische Universiteit Eindhoven, Faculteit Bouwkunde, Vakgroep Fago, Raport nr,92.63,k.

Bottema, M., Leene, J.A., and Wisse, J.A. (1992) "Toward Forecasting of Wind Comfort," In *Progress in Wind Engineering,* Proc. of the 8th Int'l Conf. on Wind Engineering, Elsevier, New York, 2365–2376.

Bradbury, L.S.J. (1976) "Measurements with a Pulsed-Wire and Hot Wire Anemometer in the Highly Turbulent Wake of a Normal Flat Plate," *J. Fluid Mech,* 177, 473–497.

Britter, R. (1982) "Modeling Flow over Complex Terrain and Implications for Determining the Extent of Adjacent Terrain to be Modeled," In *Proc. Int'l Workshop on Wind Tunnel Modeling Criteria and Techniques in Civil Engineering Application* (T.A. Reinhold, ed.), National Bureau of Standards, Gaithersburg, MD, and Cambridge University Press, Cambridge, UK, 186–196.

Browning, K.A. (1964) "Airflow and Precipitation Trajectories within Severe Local Storm Which Travel to the Right of the Winds," *J. Atmos. Sci.*, 21, 634–39.

Busch, N.E. (1973) "On the Mechanics of Atmospheric Turbulence," In *Workshop on Micrometeorology*, American Meteorological Society, Boston.

Canadian Standards Association (CSA). (1991) "Quality Assurance Program—Category 1," CAN3-Z299.1-85, Reaffirmed.

Carpenter, P. (1990) "Wind Speeds in City Streets—Full-Scale Measurements and Comparison with Wind Tunnel Results," In *Recent Advances in Wind Engineering*, Proc. 2nd Asia Pacific Symp. on Wind Engineering, Pergamon Press, New York.

Castro, I.P., and Robins, A.G. (1977) "The Flow around a Surface-Mounted Cube in Uniform and Turbulent Streams," *J. Fluid Mech.*, 79, 307–35.

Cermak, J.E. (1958) "Wind Tunnel for the Study of Turbulence in the Atmospheric Surface Layer," Tech. Rept. CER58JEC42, Fluid Dynamics and Diffusion Laboratory, Colorado State University, Fort Collins, CO.

Cermak, J.E. (1975) "Applications of Fluid Mechanics to Wind Engineering," *J. Fluids Eng.*, American Society of Mechanical Engineers, 97(1), 9–38.

Cermak, J.E. (1981) "Wind Tunnel Design for Physical Modeling of Atmospheric Boundary Layers," *J. Eng. Mech.*, 107(3), 523–642.

Cermak, J.E. (1982) "Physical Modeling of the Atmospheric Boundary Layer (ABL) in Long Boundary-Layer Wind Tunnels (BLWT)," In *Proc. Int'l Workshop on Wind Tunnel Modeling Criteria and Techniques in Civil Engineering Application* (T.A. Reinhold, ed.), National Bureau of Standards, Gaithersburg, MD, and Cambridge University Press, Cambridge, UK, 97–137.

Cermak, J.E. (1984) "Physical Modeling of Flow and Dispersion over Complex Terrain," *Boundary Layer Meteorol.*, 30, 261–292.

Cermak, J.E., Cochran, L.S., and Leffler, R.D. (1993) "Wind-Tunnel Modeling of the Atmospheric Surface Layer," *J. Wind Eng. Ind. Aero.*, 54/55, 505–513.

Cermak, J.E. (1995) "Development of Wind Tunnels for Physical Modeling of the Atmospheric Boundary Layer." In *A State of the Art in Wind Engineering*, Davenport Sixtieth Birth Anniversary Volume, Wiley Eastern Limited, 1–25.

Chok, C.V. (1988) "Wind Parameters of Texas Tech University Field Site," Master of Science Thesis, Civil Engineering Department, Texas Tech University.

Chuang H., and Cermak, J.E. (1966) "Similarity of Thermally Stratified Shear Flows in the Laboratory and Atmosphere," *Phys. Fluids Supp.*, 10, II, S255–S258.

Cochran, L.S. (1992) "Wind Tunnel Modeling of Low-Rise Structures," Ph.D. Dissertation, Civil Engineering Department, Colorado State University, Fort Collins, CO.

Cook, N.J. (1973) "On Simulating the Lower Third of the Urban Adiabatic Boundary Layer in a Wind Tunnel," *Atmos. Environ.*, 7, 691–705.

Cook, N.J. (1978) "Wind-Tunnel Simulation of the Adiabatic Atmospheric Boundary Layer by Roughness, Barrier and Mixing-Device Methods," *J. Ind. Aero.*, 3, 157–176.

Cook, N.J. (1982) "Towards Better Estimation of Extreme Winds," *J. Wind Eng. Ind. Aero.*, 9, 295–323.

Cook, N.J. (1985) *The Designer's Guide to Wind Loading of Building Structures, Part 1: Background, Damage Survey, Wind Data, and Structural Classification*, Butterworths, London.

Cook, N.J. (1990) *The Designer's Guide to Wind Loading of Building Structures, Part 2: Static Structures*, Butterworths, London.

Counihan, J. (1969) "An Improved Method of Simulating an Atmospheric Boundary Layer in a Wind Tunnel," *Atmos. Environ.*, 3, 197–214.

Counihan, J. (1975) "Adiabatic Atmospheric Boundary Layers: A Review and Analysis of Data from the Period 1880–1972," *Atmos. Environ.*, 9, 871–905.

Dalgliesh, W.A. (1975) "Comparison of Model/Full-Scale Wind Pressures on a High Rise Building," *J. Wind Eng. Ind. Aero.*, 1, 55–66.

Davenport, A.G. (1960) "Rationale for Determining Design Wind Velocities," *J. Struct. Eng.*, 86, 39–68.

Davenport, A.G. (1961a) "The Spectrum and Horizontal Gustiness near the Ground in High Winds," *Q.J. Royal Meteorol. Soc.*, 87, 194–221.

Davenport, A.G. (1961b) "The Application of Statistical Concepts to the Wind Loading of Structures," In. *Proc. Institute of Civil Engineers*, 19, 449–472.

Davenport, A.G., and Isyumov, N. (1967) "The Application of the Boundary Layer Wind Tunnel to the Prediction of Wind Loading," In *Proc. Int'l Res. Seminar Wind Effects on Buildings and Structures, Second Int'l Conf. on Wind Engineering*, Ottawa, Canada, 201–230.

Davenport, A.G. (1968) "The Dependence of Wind Loading on Meteorological Parameters," In *Proc. Int'l Res. Seminar on Wind Effects on Buildings and Structures*, University of Toronto Press.

Davenport, A.G. (1972) "An Approach to Human Comfort Criteria for Environmental Wind Conditions," In *Proc. Colloquium on Building Climatology*, Stockholm, Sweden.

Davenport, A.G. (1975) "Tall Buildings—An Anatomy of Wind Risk," *Const. South Africa*, Dec.

Davenport, A.G. (1977) "The Prediction of Risk under Wind Loading," In *Proc. 2nd Int'l Conf. on Structural Safety and Reliability*, Munich.

Davenport, A.G. (1982) "Considerations in Relating Wind Tunnel Results to Design for a Specific Site," In *Wind Tunnel Modeling for Civil Engineering Applications* (T.A. Reinhold, ed.), National Bureau of Standards, Gaithersburg, MD, and Cambridge University Press, Cambridge, U.K.

Davenport, A.G. (1983) "The Relationship of Reliability to Wind Loading," *J. Wind Eng. Ind. Aero.*, 13, 3–27.

Davenport, A.G., and King, J.P.C. (1984) "Dynamic Wind Forces on Long Span Bridges," 12th IABSE Congress, Vancouver.

Davenport, A.G., Isyumov, N., King. J.P.C., Novak, M., Surry, D., and Vickery, B.J. (1985) "BLWT II: The Design and Performance of a New Boundary Layer Wind Tunnel," In *Proc. Fifth U.S. National Conf. on Wind Engineering*, Texas Tech University, Lubbock, TX.

Davenport, A.G., King, J.P.C., and Larose, G.L. (1992) "Taut Strip Model Tests," In *Proc. Aerodynamics of Large Bridges*, Balkema, Rotterdam.

Durgin, F. (1982) "Instrumentation Requirements or Aerodynamic Pressure and Force Measurements on Buildings and Structures," In *Wind Tunnel Modeling for Civil Engineering Applications* (T.A. Reinhold, ed.), National Bureau of Standards, Gaithersburg, MD, and Cambridge University Press, Cambridge, U.K., 329–348.

Durgin, F.H. (1985) "Proposed Standards and a New Criteria for Pedestrian Level Wind Studies for Boston Massachusetts," In *Proc. 5th U.S. National Conf. on Wind Engineering*, Wind Engineering Council, Lubbock, Texas; also Massachusetts Institute of Technology, Department of Aeronautics and Astronautics, Wright Brothers Facility Report WBWT-TR-1214, Cambridge, Massachusetts.

Durgin, F.H. (1989) "Proposed Guidelines for Pedestrian Level Wind Studies in Boston: Comparison of Results from 12 Studies," *Build. Environ.*, 24(4), 314–315.

Durgin, F.H. (1992) "Pedestrian Level Wind Studies at the Wright Brothers Facility," In *Progress in Wind Engineering*, Proc. 8th Int'l Conf. on Wind Engineering, Elsevier, Amsterdam, and *J. Wind Eng. Ind. Aero.*, 412–44, 2253–2264.

Durgin, F.H. (1995) "Equivalent Average Pedestrian Wind Comfort Criteria," In *Restructuring: America and Beyond*, Proc. Structures Congress XIII, ASCE, 112–115.

Durst, C. (1960) "Wind Speeds over Short Periods of Time," *Meteorol. Mag.*, 89:1056, 181–187.

ESDU International. (1991) *Wind Engineering Data Sheet: 86010 Revision D—Characteristics of Atmospheric Turbulence near the Ground*, London.

ESDU International. (1993a) *Wind Engineering Data Sheets: 84011 Revision D—Wind Speed Profiles over Terrain with Roughness Changes; 84030 Revision C—Longitudinal Turbulence Intensities over Terrain with Roughness Changes;* and *86035 Revision E—Integral Length Scales of Turbulence over Flat Terrain with Roughness Changes*, London.

ESDU International. (1993b) *Wind Engineering Data Sheet: 91043 Revision B—Mean Wind Speeds over Hills and Other Topography*, London.

Estoque, M.A. (1973) "Numerical Modeling of the Planetary Boundary Layer," In *Workshop on Micrometeorology*, American Meteorological Society, Boston, 217–268.

Fanger, P.O., Melikov, A.K., Hanzawa, H., and Ring, J. (1988) "Air Turbulence and Sensation of Draught," *Energy Build.* 12(1), 21–39.

Fujita, T.T. (1976) "Spearhead Echo and Downburst near the Approach End of a John F. Kennedy Airport Runway, New York City," Satellite and Mesometeorological Research Project Research Paper 137, Department of Geophysical Sciences, University of Chicago.

Fujita, T.T. (1985) "The Downburst: Microburst and Macroburst," Satellite and Mesometeorological Research Project, Department of Geophysical Sciences, University of Chicago.

Gandemer, J. (1978) "Aerodynamic Studies of Built-Up Areas Made by C.S.T.B. at Nantes, France," *J. Ind. Aero.*, 3, 227–240.

Georgiou, P.N., Davenport, A.G., and Vickery, B.J. (1983) "Design Wind Speeds in Regions Dominated by Tropical Cyclones," In *Proc. 6th Int'l Conf. on Wind Engineering*, Auckland, New Zealand.

Georgiou, P.N. (1985) "Design Windspeeds in Tropical Cyclone-Prone Regions," Ph.D. Thesis, Faculty of Engineering Science, University of Western Ontario.

Gerhardt, H.J., and Kramer, C. (1992) "Wind Comfort and Pollutant Transport in a Satellite City," In *Progress in Wind Engineering*, Proc. 8th Int'l Conf. on Wind Engineering, Elsevier, New York, 2343–2351.

Gerstoft, P., and Hansen, S.O. (1987) "A New Tubing System for the Measurement of Fluctuating Pressures," *J. Wind Eng. Ind. Aero.*, 25, 335–354.

Golden, J.H. (1961) "Scale Model Techniques," M.S. Thesis, New York University, College of Engineering.

Golden, J.H., and Snow, J.T. (1991) "Mitigation against Extreme Windstorms," *Rev. Geophys.*, 29, 477–504.

Gomes, L., and Vickery, B.J. (1976) "On the Prediction of Tropical Cyclone Gust Speeds along the Northern Australian Coast," *Inst. Eng. Aust.*, 18(2), 40–49.

Gomes, L., and Vickery, B.J. (1977) "On the Prediction of Extreme Wind Speeds from the Parent Distribution," *J. Ind. Aero.*, 2(1).

Gomes, L., and Vickery, B.J. (1978) "Extreme Windspeeds in Mixed Wind Climates," *J. Ind. Aero.*, 2(4), 331–344.

Grip, R.E. (1982) "An Investigation of the Erosion Technique for the Evaluation of Pedestrian Level Winds," Master's Thesis, Department of Civil Engineering, Massachusetts Institute of Technology, Cambridge, MA.

Hansen, R.J., Reed, J.W., and VanMarcke, E.H. (1973) "Human Response to Wind-Induced Motion of Buildings," *J. Struct. Eng.*, 99, 1589–1605.

Harris, R.I., and Deaves, D.M. (1981) "The Structure of Strong Winds," Paper 4 of CIRA Conf. on Wind Engineering in the Eighties, Construction Industry Research and Information Association, London.

Harris, R.I. (1986) "Longer Turbulence Length Scales," *J. Wind Eng. Ind. Aero.*, 24, 61–68.

Hellman, G. (1916) "Über Die Bewegung der Luft in Den Untersten Schichten der Atmosphäre," *Meteorol. Z.*, 34, 273.

Hjorth-Hansen, E. (1992) "Section Model Tests," In *Proc. Aerodynamics of Large Bridges*, Balkema, Rotterdam.

Holmes, J.D. (1986) "The Application of Probability Theory to the Directional Effects of Wind," 10th Australian Conf. on the Mechanics of Structures and Materials, University of Adelaide.

Holmes, J.D. (1987) "Mode Shape Corrections for Dynamic Response to Wind," *Eng. Struct.*, 9, 210–212.

Holton, J.R. (1971) *An Introduction to Dynamic Meteorology*, Academic Press, New York.

Hosker, R.P. (1984) "Flow and Diffusion near Obstacles," In *Atmospheric Science and Power Production* (D. Randerson, ed.).

Hosker, R.P. (1985) "Flow around Isolated Structures and Building Clusters: A Review," *ASHRAE Trans.* 91(2B), 1672–1692.

Hunt, J.C.R., Poulton, E.C., and Mumfort, J.C. (1976) "The Effects of Wind on People: New Criteria Based on Wind Tunnel Experiments," *Build. Environ.*, 11, 15–38.

Irwin, P.A, Cooper, K.R., and Girard, R. (1979) "Correction of Distortion Effects Caused by Tubing Systems in Measurements of Fluctuating Pressures," *J. Wind Eng. Ind. Aero.*, 5, 93–107.

Irwin, P.A. (1979) "Cross-Spectra of Turbulence Velocities in Isotropic Turbulence," *Boundary Layer Meteorol.*, 16, 237–243.

Irwin, P.A. (1981a) "The Design of Spires for Wind Simulation," *J. Wind Eng. Ind. Aero.*, 7, 361–366.

Irwin, P.A. (1981b) "A Simple Omni-Directional Sensor for Wind Tunnel Studies of Pedestrian-Level Winds," *J. Wind Eng. Ind. Aero.*, 7, 219–239.

Irwin, P.A. (1987) "Pressure Model Techniques for Cladding Loads," In *Proc. 7th Int'l Conf. on Wind Engineering*, Aachen, Germany.

Irwin, P.A. (1988) "Pressure Model Techniques for Cladding Wind Loads," *J. Wind Eng. Ind. Aero.*, 29, 69–78.

Irwin, P.A. (1992) "Full Aeroelastic Model Tests," In *Proc. Aerodynamics of Large Bridges*, Balkema, Rotterdam.

Irwin, P.A., and Xie, J. (1993) "Wind Loading and Serviceability of Tall Buildings in Tropical Cyclone Regions," Third Asia Pacific Symp. on Wind Engineering, Dept. Civil Eng.

Irwin, P.A., and Kochanski, W.W. (1995) "Measurement of Structural Wind Loads using the High Frequency Pressure Integration Method." In *Restructuring: America and Beyond;* Proc. of Structures Congress XIII, ASCE, 1631–1634.

Isyumov, N. (1972) "Wind Tunnel Methods for Evaluating Wind Effects on Buildings and Structures," Int'l Symp. on Exp. Mech., University of Waterloo, Ontario.

Isyumov, N., and Davenport, A.G. (1975a) "Comparison of Full-Scale and Wind Tunnel Wind Speed Measurements in the Commerce Court Plaza," *J. Ind. Aero.*, 1, 201–212.

Isyumov, N., and Davenport, A.G. (1975b) "Ground Level Wind Environment in Built-Up Areas," In *Proc. 4th Int'l Conf. on Wind Effects on Buildings and Structures,* Heathrow, U.K., 403–422.

Isyumov, N. (1981) "The Role of Physical Models in Design against Wind," In *3rd Canadian Workshop on Wind Engineering,* Vancouver & Toronto.

Isyumov, N. (1982) "The Aeroelastic Modeling of Tall Buildings," In *Wind Tunnel Modeling for Civil Engineering Applications* (T.A. Reinhold, ed.), National Bureau of Standards, Gaithersburg, MD, and Cambridge University Press, Cambridge, U.K.

Isyumov, N., Davenport, A.G., and Monbaliu, J. (1984) "CN-Tower, Toronto: Model and Full-Scale Response to Wind," 12th Congress IABSE, Vancouver, B.C.

Isyumov, N., and Halvorson, R. (1984) "Dynamic Response of Allied Bank Plaza during Alicia," In *Proc. ASCE Specialty Conf. Alicia One Year Later,* Galveston, TX.

Isyumov, N., and Ramsay, S. (1993) "Physical Modeling of Atmospheric Dispersion in Complex Settings," In *Proc. NATO Advanced Study Institute, Wind Climate in Cities,* Waldbronn, Germany.

Isyumov, N. (1995) "Full-Scale Studies of Pedestrian Winds: Comparison with Wind Tunnel and Evaluation of Human Comfort," In *Restructuring: America and Beyond;* Proc. of Structures Congress XIII, ASCE, 104–107.

Izumi, Y. (ed.) (1971) "Kansas 1968 Field Progress Report," Environmental Research Paper No. 79, AFCRL-72-0041, Air Force Cambridge Research Laboratories, L.G. Hanscom Field, Bedford, MA.

Jackson, P.S. (1978) "The Evaluation of Windy Environments," *Build. Environ.*, 13, 251–260.

Jensen, M. (1958) "The Model Law for Phenomena in Natural Wind," *Ingeniøren,* Int'l Edition, 2, 121–128.

Kaimal, J.C., Wyngaard, J.C., Izumi, Y., and Coté, O.R. (1972) "Spectral Characteristics of Surface-Layer Turbulence," *Q. J. Royal Meteorol. Soc.*, 98, 563–589.

Kaimal, J.C., and Finnigan, J.J. (1994) *Atmospheric Boundary Layer Flows: Their Structure and Measurement,* Oxford University Press, New York.

Krayer, W.R., and Marshall, R.D. (1992) "Gust Factors Applied to Hurricane Winds," *Bull. Am. Meteorol. Soc.*, 63, 613–617.

Lawson, T.V. (1978) "The Wind Content of the Built Environment," *J. Ind. Aero.*, 3, 93–105.

Lawson, T.V., and Penwarden, A.D. (1975) "Effect of Wind on People in the Vicinity of Buildings," In *Proc. 4th Int'l Conf. on Wind Effects on Buildings and Structures,* Heathrow, U.K., 605–622.

Lemelin, D.R., Surry, D., and Davenport, A.G. (1988) "Simple Approximations for Wind Speed-Up over Hills," *J. Wind Eng. Ind. Aero.*, 28, 117–127.

Lepage, M.F., and Irwin, P.A. (1985) "A Technique for Combining Historical Wind Data with Wind Tunnel Tests to Predict Extreme Wind Loads," In *Proc. Fifth U.S. National Conf. on Wind Engineering*, Lubbock, TX, 2B-71–2B-78.

Lettau, H.H. (1962) "Theoretical Wind Spirals in the Boundary Layer of a Barotropic Atmosphere," *Beitr. Phys. Atmos.*, 35, 195–212.

Lieblein, J. (1974) "Efficient Methods of Extreme-Value Methodology," COM-75-10048, United States Government Printing Office.

Livesey, F., Inculet, D., Isyumov, N., and Davenport, A.G. (1990) "A Scour Technique for the Evaluation of Pedestrian Winds," *J. Wind Eng. Ind. Aero.*, 3, 779–789.

Marshall, R.D. (1984) "Wind Tunnels Applied to Wind Engineering in Japan," *J. Struct. Eng.*, 110, 1203–1221.

Melbourne, W.H., and Joubert, P.N. (1971) "Problems of Wind Flow at the Base of Tall Buildings," In *Proc. 3rd Int'l Conf. on Wind Effects on Buildings and Structures*, Tokyo, Japan, 105–114.

Meroney, R.N. (1980) "Wind-Tunnel Simulation of the Flow over Hills and Complex Terrain," *J. Ind. Aero.*, 5, 297–321.

Meroney, R.N. (1982) "Turbulent Diffusion Near Buildings," In *Engineering Meteorology*, (E. Plate, ed.), Elsevier, Amsterdam.

Meroney, R.N. (1987) "Guidelines for Fluid Modeling of Dense Gas Cloud Dispersion," *J. Haz. Mat.*, 17, 23–46.

Meroney, R.N., Rafailidis, S., and Pavageau, M. (1995a) "Dispersion in Idealized Urban Street Canyons," Tech. Rept. CEP95-96-RNM-SR-MP, Fluid Mechanics and Wind Engineering Program, Colorado State University, Fort Collins, CO.

Meroney, R.N., Neff, D.E., and Birdsall, J.B. (1995b) "Wind-Tunnel Simulation of Infiltration across Permeable Building Envelopes: Energy and Air Pollution Exchange Rates," 7th Int'l Symp. on Measurement and Modeling of Environmental Flows, Int'l Mech. Engineers Conf., San Francisco, CA.

Miyata, T., Yokoyama, K., Yasuda, M., and Hikami, Y. (1992) "Akashi Kaikyo Bridge: Wind Effects and Full Model Wind Tunnel Tests," In *Proc. Aerodynamics of Large Bridges*, Balkema, Rotterdam.

Murakami, S., Uehara, K., and Deguchi, K. (1979a) "Wind Effect on Pedestrians: New Criteria Based on Outdoor Observation of over 2000 Persons," In *Wind Engineering* (J.E. Cermak ed.), 277–288.

Murakami, S., Uehara, K., and Komine, H. (1979b) "Amplification of Wind Speed at Ground Level Due to Construction of High Rise Building in Urban Area," *J. Ind. Aero.*, 4, 343–370.

Murakami, S., Iwasa, Y., and Morikawa, Y. (1986) "Study on Acceptable Criteria for Assessing Wind Environment on Ground Level Based on Residents Diaries," *J. Wind Eng. Ind. Aero.*, 24, 1–18.

National Building Code of Canada (NBCC). (1995) *Commentary B Wind Loads.* Issued by the Canadian Commission on Building and Fire Codes, National Research Council of Canada.

Neff, D.E., and Meroney, R.N. (1995) "Reynolds Number Independence of the Wind-Tunnel Simulation of Transport and Dispersion About Buildings," Technical Report, Fluid Mechanics and Wind Engineering Program, Colorado State University, Fort Collins, CA.

Olesen, H.R., Larsen, S.E., and Hjstrup, J. (1984) "Modeling Velocity Spectra in the Lower Part of the Planetary Boundary Layer," *Boundary Layer Meteorol.*, 29, 285–312.

Panofsky, H.A., and Dutton, J.A. (1983) *Atmospheric Turbulence: Models and Methods for Engineering Applications*, Wiley, New York.

Penwarden, A.D. (1973) "Acceptable Wind Speeds in Towns," *Build. Sci.* 8, 259–267.

Penwarden, A.D., and Wise, A.F.E. (1975) "Wind Environment around Buildings," Building Research Establishment Digest.

Peterka, J.A. (1983) "Selection of Local Peak Pressure Coefficients for Wind-Tunnel Studies of Buildings," *J. Wind Eng. Ind. Aero.*, 13, 477–488.

Peterka, J.A. (1992) "Improved Extreme Wind Predictions in the United States," *J. Wind Eng. Ind. Aero.*, 41, 533–541.

Rae, W.H., Jr., and Pope, A. (1984) *Low-Speed Wind Tunnel Testing*," John Wiley & Sons, New York.

Ratcliff, M.A., and Peterka, J.A. (1990) "Comparison of Pedestrian Wind Acceptability Criteria," *J. Wind Eng. Ind. Aero.*, 36, 791–800.

Reinhold, T.A., and Vickery, P.J. (1990) "Variable Mode Shape High-Frequency Force Balance," NSF Contract ISI 8660406, National Science Foundation, Washington, DC.

Reinhold, T.A., Brinch, M., and Damsgaard, A. (1992) "Wind Tunnel Tests for the Great Belt Link," In *Proc. Aerodynamics of Large Bridges*, Balkema, Rotterdam.

Reinhold, T.A., and Brinch, M. (1992) "Documentation of Winds in DMI's Very Large Boundary-Layer Wind Tunnel," Report 91032.30.01, Danish Maritime Institute, Copenhagen, Denmark.

Rice, S.O. (1945) "Mathematical Analysis of Random Noise," *Bell Tech. J.*, 18, 19.

Russell, L.R. (1971) "Probability Distributions for Hurricane Effects," *J. Waterways, Harbors, Coastal Eng. Div.*, ASCE, 97(WW1), 139–154.

Russell, L.R., and Schueller, G.F. (1974) "Probabilistic Models for Texas Gulf Coast Hurricane Occurrences," *J. Petrol. Technol.*

Sarkar, P.P., Jones, N.P., and Scanlan, R.H. (1992) "System Identification for Estimation of Flutter Derivatives," In *Progress in Wind Engineering*, Proc. 8th Int'l Conf. on Wind Engineering (A.G. Davenport, et al., Eds.), and *J. Wind Eng. Ind. Aero.*, 42, 1243–1254.

Sarkar, P.P. (1996) Personal Communication.

Saunders, J.W., and Melbourne, W.H. (1975) "Tall Rectangular Building Response to Cross-Wind Excitation," In *Proc. 4th Int'l Conf. on Wind Effects on Buildings and Structures*, Cambridge University Press, London, 369–379.

Scanlan, R.H. (1982) "Aeroelastic Modeling of Bridges," In *Wind Tunnel Modeling for Civil Engineering Applications*, (T.A. Reinhold, ed.) Cambridge University Press, New York, 440–456.

Scanlan, R.H. (1992) "Wind Dynamics of Long Span Bridges," In *Proc. Aerodynamics of Large Bridges*, Balkema, Rotterdam.

Scruton, C. (1963) "On the Wind-Excited Oscillations of Stacks, Towers, and Masts," In *Proc. Conf. on Wind Effects on Buildings and Structures*, NPL, Teddington, U.K..

Simiu, E. (1974) "Wind Spectra and Dynamic Alongwind Response," *J. Struct. Eng.*, 100, 1877–1910.

Simiu, E., Changery, M.J., and Filliben, J.J. (1979) "Extreme Windspeeds of 129 Stations in the Contiguous United States," NBS Building Science Series 118, U.S. Dept. of Commerce.

Simiu, E., and Filliben, J.J. (1981) "Wind Direction Effects on Cladding and Structural Loads," *Eng. Struct.*, 3, 181–186.

Simiu, E., Filliben, J.J., and Shaver, J.R. (1982) "Short-Term Records and Extreme Wind Speeds," *J. Struct. Eng.*, 108(11), 2571–2577.

Simiu, E. (1983) "Aerodynamic Coefficients and Risk Consistent Design," *J. Struct. Eng.*, 109(5), 1278–1289.

Simiu, E., and Scanlan, R.H. (1986) *Wind Effects on Structures: An Introduction to Wind Engineering*, 2nd Ed., John Wiley & Sons, New York.

Soligo, M.J., Irwin, P.A., Williams, C.J., and Schuyler, G.D. (1995) "Pedestrian Comfort: A Discussion of the Components to Conduct a Comprehensive Assessment," In *Restructuring: America and Beyond*, Proc. of Structures Congress XIII, ASCE, 108–111.

Snyder, W.H. (1981) "Guideline for Fluid Modeling of Atmospheric Diffusion," Report No. EPA600/8-81-009, Environmental Sciences Research Laboratory, Office of Research and Development, Research Triangle Park, NC 27711.

Snyder, W.H. (1994) "Some Observations of the Influence of Stratification on Diffusion in Building Wakes." In *Stably Stratified Flows: Flow and Dispersion over Topography*, (Castro, I.P., and Rockliff, N.J., eds.), Clarendon Press, Oxford, 301–324.

Standen, N.M. (1972) "A Spire Array for Generating Thick Turbulent Shear Layers for Natural Wind Simulation in Wind Tunnels," Tech. Rept. LTR-LA-94, National Aeronautical Establishment, Ottawa, Canada.

Stathopoulos, T. (1975) "Technique of Pneumatically Averaging Pressures," Report BLWT-2-75, University of Western Ontario, Faculty of Engineering Science, London, Ontario.

Stathopoulos, T., Wu, H., and Bedard, C. (1992) "Wind Environment around Buildings: A Knowledge-Based Approach," In *Progress in Wind Engineering*, Proc. 8th Int'l Conf. on Wind Engineering, Elsevier, New York, 2377–2388.

Stathopoulos, T., and Basharan, A. (1996) "Computer Simulation of Wind Environmental Conditions around Buildings," *Engineering Structures* 18(11), 876–885.

Steckley, A.C. (1989) "Motion-Induced Wind Forces on Chimneys and Tall Buildings," Ph.D. Thesis, University of Western Ontario, London, Ontario.

Steckley, A., Vickery, B.J., and Isyumov, N. (1992) "The Use of Integrated Pressures To Determine Overall Wind-Induced Responses," *J. Wind Eng. Ind. Aero.*, 41–44, 1023–1034.

Surry, D., and Stathopoulos, T. (1978) "An Experimental Approach to the Economical Measurement of Spatially-Averaged Wind Loads," *J. Wind Eng. Ind. Aero.*, 2, 385–397.

Surry, D., and Davenport, A.G. (1979) "Modeling the Wind Climate: An Overview," In *Proc. Workshop on Wind Climate*, Asheville, NC, 141–168.

Teunissen, H.W. (1983) "Wind-Tunnel and Full-Scale Comparisons of Mean Wind Flow over an Isolated Low Hill," *J. Wind Eng. Ind. Aero.*, 15, 271–286.

Thomas, G., Cochran, L.S., Cermak, J.E., and Mehta, K. (1993) "Comparison of Field and Wind-Tunnel Measured Spectra," In *Proc. 7th U.S. National Conf. on Wind Engineering*, University of California, Los Angeles, 793–802.

Tieleman, H.W. (1992a) "Universality of Velocity Spectra," Presented at the 11th Australasian Fluid Mechanics Conf., Hobart, Tasmania, Australia.

Tieleman, H.W. (1992b) "Wind Characteristics in the Surface Layer over Heterogeneous Terrain," *J. Wind Eng. Ind. Aero.*, 41, 329–340.

Tryggvason, B.V., Surry, D., and Davenport, A.G. (1976) "Predicting Wind-Induced Response in Hurricane Zones," *J. Struct. Eng.*, 102(12).

Tryggvason, B.V., and Isyumov, N. (1977) "A Study of the Wind-Induced Response of the Air-Supported Roof of the Dalhousie University Sports Complex," Boundary Layer Wind Tunnel Laboratory Report SS7-1977, University of Western Ontario.

Tryggvason, B.V. (1979) "Aeroelastic Modeling of Pneumatic and Tensioned Fabric Structures," In *Proc. 5th Int'l Conf. on Wind Engineering*, Fort Collins, CO, 1061–1072.

Tryggvason, B.V. (1979) "Computer Simulation of Tropical Cyclone Wind Effects for Australia," Wind Engineering Report 2/79, Department of Civil and Systems Engingeering, James Cook University, Townsville, Australia.

Tschanz, T. (1982) "The Base Balance Measurement Technique and Applications to Dynamic Wind Loading of Structures," Ph.D. Thesis, University of Western Ontario, Faculty of Engineering Science, London, Ontario.

Twisdale, L.A. (1978) "Tornado Data Characterization and Wind Speed Risk," *J. Struct. Eng.*, 104(ST10), 1611–1630.

Twisdale, L.A., and Vickery, P.J. (1992) "Research on Thunderstorm Wind Design Parameters," *J. Wind Eng. Ind. Aero.*, 41, 545–556.

Twisdale, L.A., and Vickery, P.J. (1993) "Analysis of Thunderstorm Occurrences and Wind Speed Statistics," In *Proc. 7th U.S. National Conf. on Wind Engineering*, Irvine, CA.

Van Der Hoven. (1967) "Power Spectrum of Horizontal Wind Speed in the Frequency Range from 0.0007 to 900 Cycles per Hour," *J. Meteorol.*, 14.

Vickery, B.J. (1973) "On the Use of Balloon Data to Define Wind Speeds for Tall Structures," Research Report R226, School of Civil Engineering, University of Sydney, Australia.

Vickery, B.J. (1982) "The Aeroelastic Modeling of Chimneys and Towers," In *Proc. Int'l Workshop on Wind Tunnel Modeling Criteria and Techniques in Civil Engineering Applications*, Cambridge University Press, London.

Vickery, P.J., Steckley, A.C., Isyumov, N., and Vickery, B.J. (1985) "The Effect of Mode Shape on the Wind-Induced Response of Tall Buildings," 5th U.S. National Conf. on Wind Engineering, Texas Tech University, Lubbock, TX.

Vickery, P.J., and Twisdale, L.A. (1995a) "Wind-Field and Filling Models for Hurricane Wind-Speed Predictions," *J. Struct. Eng.* 121(11), 1700–1709.

Vickery, P.J., and Twisdale, L.A. (1995b) "Prediction of Hurricane Wind Speeds in the United States," *J. Struct. Eng.* 121(11), 1691–1699.

Visser, G. Th. (1980) "Windhindercriteria: Een Literatuuronderzoek Naar en Voorstellen voor het Hanteren Van Uniforme TNO-Windhindercriteria" (in Dutch), Report 80-02746, IMET-TNO, Apeldoorn, Netherlands.

von Kármán, T. (1948) "Progress in the Statistical Theory of Turbulence," In *Proc. National Academy of Sciences*, Washington, DC, 530–539.

Wedding, J.B., Lombardi, D.J., and Cermak, J.E. (1977) "A Wind Tunnel Study of Gaseous Pollutants in City Street Canyons," *APAC J.*, 27(6).

Whitbread, R.E. (1975) "The Measurement of Non-Steady Wind Forces on Small-Scale Building Models," In *Proc. 4th Int'l Conf. on Wind Effects on Buildings and Structures*, Heathrow, England, Cambridge University Press, London, 369–379.

Wieringa, J. (1992) "Updating the Davenport Roughness Classification," *J. Wind Eng. Ind. Aero.*, 41–44, 357–368.

Wieringa, J. (1993) "Representative Roughness Parameters for Homogeneous Terrain," *Boundary Layer Meteorol.*, 63, 323–363.

Williams, C.D., and Wardlaw, R.L. (1992) "Determination of the Pedestrian Wind Environment in the City of Ottawa Using Wind Tunnel and Field Measure-

ments," In *Progress in Wind Engineering,* Proc. 8th Int'l Conf. on Wind Engineering, Elsevier, New York, and *J. Wind Eng. Ind. Aero.*, 41–44, 2253–2264.

Williams, C.J., and Soligo, M.J. (1992) "A Discussion of the Components for a Comprehensive Pedestrian Level Comfort Criteria," In *Progress in Wind Engineering,* Proc. 8th Int'l Conf. on Wind Engineering, Elsevier, New York, 2389–2390.

Wise, A.F.E., Sexton, D.E., and Lillywhite, M.S. (1965) "Air Flow around Buildings," In *Proc. Urban Planning Research Symposium, Building Research Station,* London, 71–91.

Wu, H., and Stathopoulos, T. (1993) "Wind-Tunnel Techniques for the Assessment of Pedestrian-level Winds," *J. Eng. Mech.*, 110(10).

Wu, H., and Stathopoulos, T. (1997) "Application of Infrared Thermography for Pedestrian Wind Evaluation," *J. Eng. Mech.* 123(10).

This page intentionally left blank

INDEX